DISSERTATION

On

Accuracy of Components during Single Point Incremental Forming

Submitted in partial fulfilment of the requirement for the award of degree

of

Master of Engineering

IN

CAD/CAM Engineering

Submitted by

Dharminder singh

Roll No.: 801481008

Under the Supervisions of

Dr. Anirban Bhattacharya

Assistant Professor

Department of Mechanical Engineering

IIT, Patna

Dr. Tarun Kumar Bera

Associate Professor

Department of Mechanical Engineering

Thapar University, Patiala

DEPARTMENT OF MECHANICAL ENGINEERING

THAPAR UNIVERSITY

PATIALA-147004, INDIA

JULY-2016

DECLARATION

I hereby declare that work done in this seminar report entitled, "**Accuracy of Components during Single Point Incremental Forming**" submitted towards partial fulfilment of requirement for award of Master of Engineering degree in CAD/CAM Engineering in Mechanical Engineering Department of Thapar University, Patiala, is an authentic record of work carried out by me under the supervision and guidance of Dr. Tarun Kumar Bera, Associate Professor of Mechanical Engineering Department, Thapar University, Patiala and Dr. Anirban Bhattacharya, Assistant Professor, Department of Mechanical Engineering, IIT, Patna .

This matter embodied in this report has not been submitted in part or full to any other university or institute for the award of any degree.

Dharminder Singh

Dharminder Singh

This is to certify that above declaration made by the student concerned is correct to the best of my knowledge and belief.

Anirban Bhattacharya 12/07/16

Dr. Anirban Bhattacharya

Assistant Professor

Department of Mechanical Engineering

IIT, Patna

Tarun Kumar Bera 14/7/16

Dr. Tarun Kumar Bera

Associate Professor

Department of Mechanical Engineering

Thapar University, Patiala

Countersigned by:

Head of ME Department,

Thapar University, Patiala.

Dean of Academic Affairs,

Thapar University, Patiala.

DECLARATION

I hereby declare that work done in this seminar report entitled, "**Accuracy of Components during Single Point Incremental Forming**" submitted towards partial fulfilment of requirement for award of Master of Engineering degree in CAD/CAM Engineering in Mechanical Engineering Department of Thapar University, Patiala, is an authentic record of work carried out by me under the supervision and guidance of Dr. Tarun Kumar Bera, Associate Professor of Mechanical Engineering Department, Thapar University, Patiala and Dr. Anirban Bhattacharya, Assistant Professor, Department of Mechanical Engineering, IIT, Patna .

This matter embodied in this report has not been submitted in part or full to any other university or institute for the award of any degree.

Dharminder Singh

This is to certify that above declaration made by the student concerned is correct to the best of my knowledge and belief.

Dr. Anirban Bhattacharya	**Dr. Tarun Kumar Bera**
Assistant Professor	***Associate Professor***
Department of Mechanical Engineering	***Department of Mechanical Engineering***
IIT, Patna	***Thapar University, Patiala***

Countersigned by:

Head of ME Department,	**Dean of Academic Affairs,**
Thapar University, Patiala.	**Thapar University, Patiala.**

ACKNOWLEDGEMENT

Words often fall short to reveal one's deepest regards. Understanding that a work like this can never be accompanied by the efforts of a single person, I would be obliged to express my profound gratitude and respect to all the people who helped me throughout the duration of this work.

I would like to thank my supervisor, Dr. Tarun Kumar Bera, Associate Professor, Mechanical Engineering Department, Thapar University, Patiala and and Dr. Anirban Bhattacharya, Assistant Professor, Department of Mechanical Engineering, IIT, Patna for their unreserved guidance, constructive suggestions, thought provoking discussions and unabashed inspiration in the nurturing work. They also provided the help in technical writing and presentation style and I found their guidance to be extremely valuable.

I am also Dr. S. K. Mohapatra, Sr. Professor and Head, Mechanical Engineering Department for providing the facilities for the completion of work.

Finally, I am grateful to my family and friends, without their encouragement, patience and moral support, it would not have been possible for me to complete my thesis.

Dharminder Singh

Reg. No. 801481008

ACKNOWLEDGEMENT

Words often fall short to reveal one's deepest regards. Understanding that a work like this can never be accompanied by the efforts of a single person, I would be obliged to express my profound gratitude and respect to all the people who helped me throughout the duration of this work.

I would like to thank my supervisor, Dr. Tarun Kumar Bera, Associate Professor, Mechanical Engineering Department, Thapar University, Patiala and and Dr. Anirban Bhattacharya, Assistant Professor, Department of Mechanical Engineering, IIT, Patna for their unreserved guidance, constructive suggestions, thought provoking discussions and unabashed inspiration in the nurturing work. They also provided the help in technical writing and presentation style and I found their guidance to be extremely valuable.

I am also Dr. S. K. Mohapatra, Sr. Professor and Head, Mechanical Engineering Department for providing the facilities for the completion of work.

Finally, I am grateful to my family and friends, without their encouragement, patience and moral support, it would not have been possible for me to complete my thesis.

Dharminder Singh

Reg. No. 801481008

ABSTRACT

The use of computers in manufacturing has enabled the development of several new sheet metal forming processes, which are based upon older technologies. This report describes the literature survey of SPIF and conclusion of literature. In sheet forming inaccuracies occur due to the spring back of sheet and the residual stresses in the sheet that deforms the component shape after the process is complete. The effect of variations of process parameters on the final accuracy of components is studied by varying the incremental depth and radius of tool in three stages. To make SPIF feasible for large scale production, multiple features are formed on single plate. Two types of measurements of components were done to study the component accuracy on Coordinate Measuring Machine (CMM). First measurement is done when the sheet is clamped between the flanges and the second one when sheet is not clamped in the flanges. One more innovative idea of measurement of component at the end of program is also successfully implemented with the help of casting the component shape on the Plaster of Paris. To validate the experiment results modeling of SPIF in done in the symbol Shakti software with the bond graph approach and successfully validated the process SPIF. The thickness variation is also studied during the forming at various heights. The deformation occurs due to the localized heat of sheet. Recent advances have enabled this localized deformation to be accurately controlled and studied. Current developments have been focused on forming parts using CNC technology, without the need for costly dies. Single point Incremental Forming has the potential to revolutionize sheet metal forming, making it accessible to all levels of manufacturing.

Key words: Forming, SPIF, Sheet Metal, Process Parameters, Accuracy, Thickness Variation, Bond Graph

LIST OF ACRONYMS

ISF	≡	Incremental Sheet Forming
SPIF	≡	Single Point Incremental Forming
TPIF	≡	Two Point Incremental Forming
CNC	≡	Computer Numeric Control
CMM	≡	Coordinate Measuring Machine
CAD	≡	Computer Aided Design

NOMENCLATURE

R	Opening radius of the Cone shape component to be formed
H	Height of the Cone
α	Wall angle of the Cone or also called as draw angle
α_{min}	Minimum wall angle of the funnel near the major base of funnel
α_{max}	Maximum wall angle of funnel near the minor base of funnel
R_{uf}	Radius of upper fillet near the major base
R_{lf}	Radius of lower fillet near the minor base
Δ_z	Incremental depth (along height of component) between each contour
Δ_r	Incremental reduction in radius after each contour (along radius)

SYMBOLS

α	Wall angle of the cone or also called as draw angle
α_{min}	Minimum wall angle of the funnel near the major base of funnel
α_{max}	Maximum wall angle of funnel near the minor base of funnel
Δ_z	Incremental depth (along height of component) between each contour
Δ_r	Incremental reduction in radius after each contour (along radius)

LIST OF FIGURES

LIST OF TABLES

TABLE OF CONTENTS

Chapter 1 Introduction

1.1 Introduction

In today's era, many industrial organizations are using outdated forming processes like deep drawing, stamping processes of forming to form components from metal sheets using dies and punches. The dimensional variations of these processes depend upon the dimensions of the component. It also require long span of time for preparation of die due to the need of large initial financial funds. These processes require large initial financial investments and long span of time for preparation of die; due to these reasons this method is considered as feasible only for large scale production. Advanced sheet metal forming methods are being proposed in the last few years for small scale customized production. Incremental forming may become a suitable technique, specifically if one or few customized parts are to be produced with a very simple and low-cost methodology. These types of processes are generally carried out on 3-axes CNC vertical milling machines where it is possible generate the controlled motion of punch [1].

In 1991 Schmoeckel found that with developments related to automation of metal forming tools would develop extra flexible. Leszak patented dieless forming called ISF. Today, new processes in ISF enabling the really flexible construction of intricate sheet metal parts. This process can be valuable in both small batch size having short lead times, and in case of rapid prototypes of complex part in less overall cost [3]. Jeswiet in 2005 stated about Spinning that, it is achieved over and done with a successions of comprehensive hits with a forming tool as shown in Fig. 1.1 which is showing the movement of material in various stages from the original blank (that fixed on machine) to the final required conical shape. In forming (spinning), a roller ball end tool is used which follows continuous programmed path Based on the dies and punches sheet, metal industry also using different techniques to deform the sheets, normally for mass production. For short series of production this is not feasible. Flexibility of the process incremental sheet forming made this process acceptable for small volume production for the purpose of reducing the high cost and large processing time needed with former engineering processes such as stamping and Punching. For this reason, scientific work is demanded for the objective to optimize the process, and to resolve the current limitations of this process to make it useful for small scale industry [6]

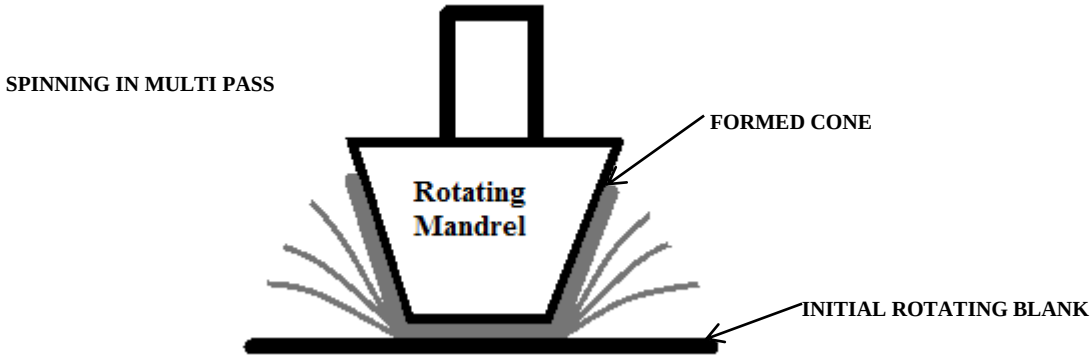

Fig. 1.1 Spinning of rotating blank to generate final shape

1.2 Background and motivation

Now a day's Sheet metal forming process is widely used in many industrial sectors. From last few decades, technology is changing and allows creating the extremely intricate shapes of parts. This is why shorter production cycles have weighty reduction in process time. Let's discuss an example, in the automobile industries there is requirement to produce about 40-50 critical profiles per a car model as shown in Fig. 1.2. This is only possible by use of at least 100-120 dies for stamping process of sheet [7]. Thus, a large volume of work is required to create these dies. On the other hand, if there is a demand of customized car in industry, it becomes tougher to generate die for small production. In this case, the die cost affects the overall cost of product up to greater extent.

Fig. 1.2 Metal sheet parts in major panels of car body [3]

The foremost stage at which ISF technology is considered having advantage over all other conventional process when to manufacture parts from sheet of material both metal and polymer complex job for conventional process without any use of costlier dies and large

setup times. A significant and technologically appropriate research line is related to the fabrication of intricate parts. Though the method of forming is slower than traditional processes, the incremental sheet metal forming process for sheet materials is suitable way to manufacture the prototypes and intricate components produced in small scale lots for is applications in various fields.

1.3 Incremental forming technology

The incremental sheet metal forming technology is technique in which numerically controlled (NC) machine is used to create part from the sheet blank. This technology has ability to make part from CAD tool-path. Working cycle of this process is shown in Fig. 1.3.

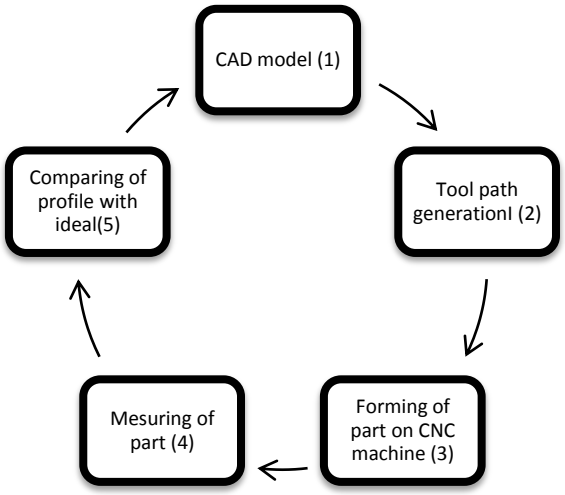

Fig. 1.3 Steps of incremental forming process

1.4 Types of forming processes

The sheet metal forming process further classified in below categories.

1.4.1 Spinning

Spinning is the oldest method of shape changing in history and is treated as the forerunner of ISF for sheet materials [12]. This process is accomplished by rotating a work piece (blank) which is clamped against the mandrel of lathe spinner parallel to this the spinning tool progressively deformed the blank to the desired shape with respect to the profile incorporated on mandrel. Figure 1.4 clearly shows the forming parts with use of spinning technique. There is need of two workers to perform spinning; first worker forces the sheet onto a mandrel that

has an imperfection of final product. The second worker operates machine to rotate mandrel at the desire speed.

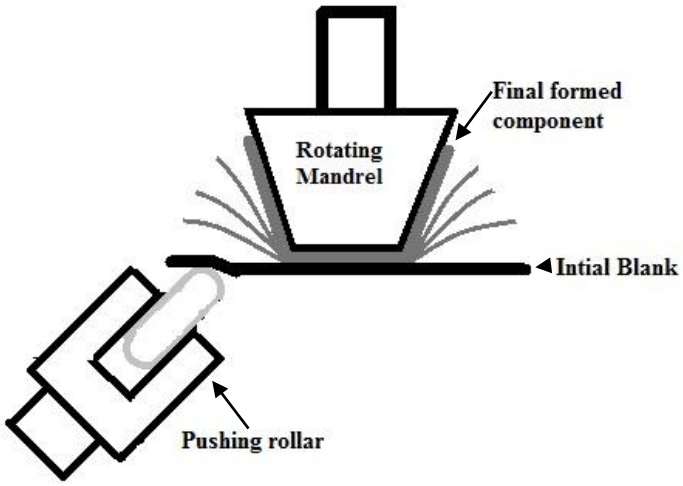

Fig. 1.4 Spinning a hollow body using roller

1.4.2 Single point incremental forming (SPIF)

Single Point sheet metal Incremental Forming is a relatively new, dieless sheet metal process for forming of sheet. Jeswiet, Leach and Fratini have discovered the SPIF method by performing on a standard three-axis CNC milling machine. The tool path is planned either with the CAD software or with the use of Matlab programming. It is full die-less forming. The first patent is registered on SPIF in 1968; this process was developed to enhance the output of industry. Figure 1.5 describes the basic component of the process which includes metal blank (sheet), fixture to hold blank, backing plate to increase accuracy, single point hemispherical ended forming tool.

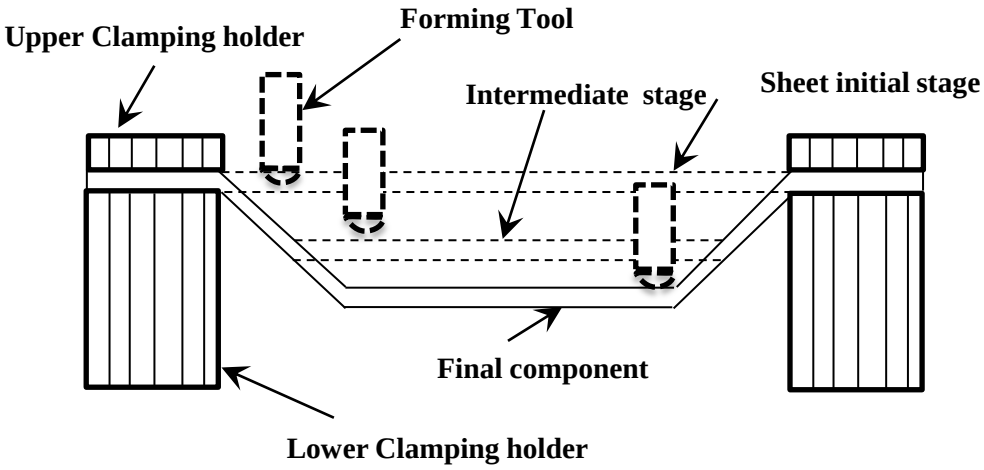

Fig. 1.5 Single points incremental forming

The flanges (blank holder) are used for clamping the sheet during ISF. Backing plate used between the flanges below blank is to reduce bending of plate. The hemispherical ball ended tool is utilized to progressively create the desire shape of the sheet following continuous spiral path. Basic process variables in SPIF are tool radius, sheet thickness, drawing angle ψ, and the downwards steps size per revolution.

1.4.3 Two points incremental forming (TPIF)

In the TPIF process, Fig. 1.6 blank of metal sheet (workpiece) moves vertically on bearings, which move on sheet holder posts along with sheet, along the z-axis of setup, as the tool pushes into the metal sheet. Due to presence of two contact points between the sheet and tool this process is called as TPIF [6]. The point of application of load is plastically deformed the second point is the point having contact point between a static post and the blank creating when the tool is got pushed into the blank. Either two point incremental sheet metal forming process is using the partial dies to create shapes, it is often called as dieless forming [4,5].

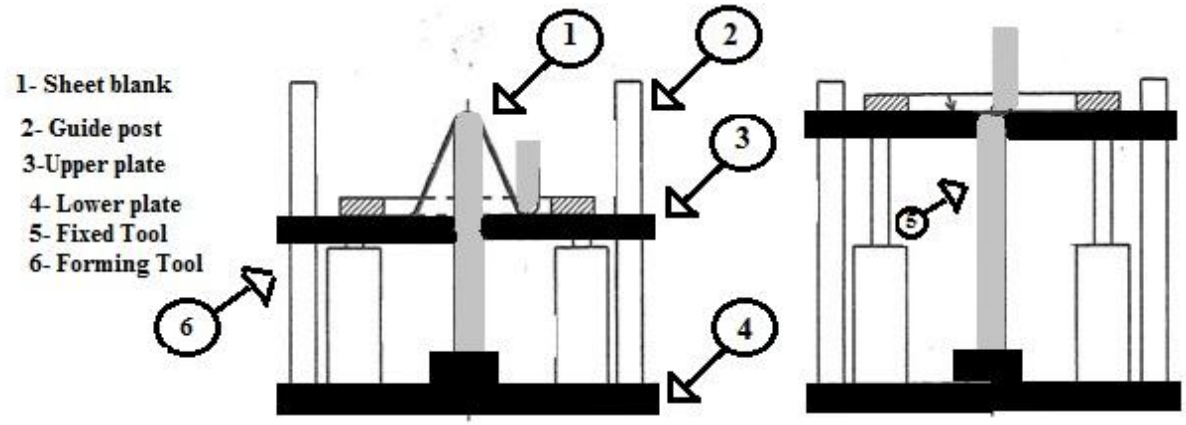

Fig. 1.6 (a) Beginning and (b) the finishing stage of two points incremental forming

1.5 Principles of SPIF

Layer by layer manufacturing technique is the basic principle of ISF. The sheet blank is deformed in the form of horizontal slices. The locus of points that are followed by forming tool is called as tool-path to construct finished part by the use of NC technology. The tool-path is created with the help of Matlab programming or directly generating from CAD model. The forming tool is hemispherical ended ball tool which follows the spiral tool-path while keeping the sheet clamped rigidly between flanges. All of main steps in ISF process presented in Fig. 1.7 are i) clamped sheet in frame, ii) forming tool pushing sheet down at

first point of contact, iii) tool motion while following first contour of tool-path and iv) So forth, the tool repeats these operations until it obtains the end of tool-path.

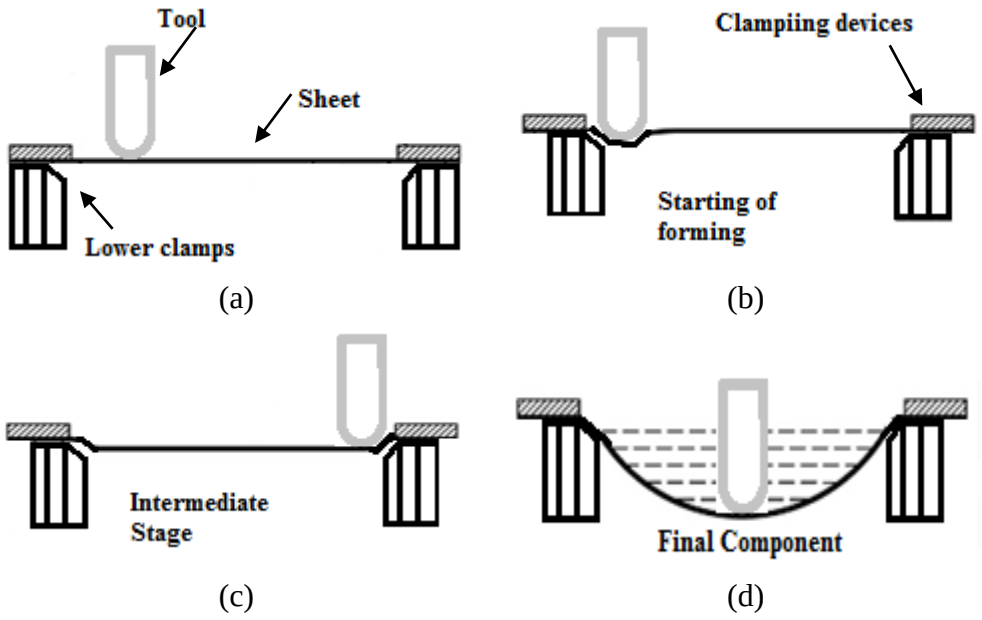

Fig. 1.7 Schematic diagram of the incremental sheet metal forming process

1.6 Important parameters for SPIF

The technique SPIF is greatly influenced by each process variables listed as sheet material, radius of tool tip, wall angle, incremental step size, feed rate of forming, spindle rotation speed, sheet blank thickness; these all have their own effect on the process in different ways such as accuracy of part, formability of sheet material, maximum possible wall angle, final thickness of part after forming etc. Hence, parameter study is important aspect to study the part accuracy.

1.6.1 Sheet material

Sheet material properties affect the formability of forming components regarding to study of Frantini et al. [6]. Strength and strain hardening coefficient (*n*) have prominent influence on formability as compared to other parameters as shown in Table 1.1.

Table 1.1 Effects of different parameters on formability [3]

Properties Parameters	Conventional stamping	Incremental forming
n	no	high
K	high	moderate
σ_{uts}	no	low
A	no	moderate
R_n	high	low

1.6.2 Step size

Incremental depth or step down distance or pitch of tool refers to the deformation of material in each revolution of tool path. Real effect of this parameter is not well understood till date that does it really affect the formability or it affects the surface roughness. Though, Ham et al. [1] after various experiment proved that step size did not had any influence on formability. Only step size affect the manufacturing time. .

1.6.3 Forming speed

Two basic speed of forming i.e. feed rate of tool (mm/min) and spindle speed (rpm) are important parameters in the study of forming method because these cause the heat generation. As speed increases the heat effects can arise to increase formability [7]. Surface finish decreases as the speed increases [2]. Formability of sheet is reduced as tool feed rate increases and as it slows down the localize heating of sheet [3]. However, both Ham and Jeswiet and Ambrogio et al. proved that formability of sheet increases by increasing spindle speed.

1.6.4 Sheet thickness

However, wall thickness after forming product can be calculated by sine law prediction [5, 6] but it can be noticed after forming component that the wall thinning may not be following sine law. Researcher Hussain et al. has proven that resultant thickness not following sine law in case of conical shape component. Ham and Jeswiet determined that more the thickness more will be material for drawing and more will the formability.

1.6.5 Lubrication

Importance of lubrication in SPIF is for minimizing tool wear and to decrease heat generated on sheet surface from friction. Referring Brimley's work, lubricant type is not important in case of SPIF not a major factor but necessary for obtaining good surface finish. Other, Kim

and Park [49] studied that formability increased with ball ended tool used without lubricant that causes more heat but if too much friction can leads to fast failure in sheet.

1.6.6 Part geometry

Complexity in the part shape has significant effect on forming force and preparation time. To form the components with large angle for example right wall angle, multi-stage is required which consume more time. So many methods are already developed to obtain good surface quality and uniform thickness.

1.7 Limitations and applications

1.7.1 Limitation

The thickness of formed sheet is calculated by sin formulae. The theoretical work done for calculation of sheet thickness proves that the thickness is zero when the wall is vertical. Therefore the SPIF process is able to deform the wall having angle less than 90 degrees. Researchers also studied that the geometrical accuracy of formed part and roughness of formed part in SPIF process and shown that accuracy is an important problem and is lower than conventional forming. Quality of surface of formed part is mainly affected by incremental depth feed-rate [12].

To overcome these limitations different types of techniques are have been developed which provide potential to SPIF process to make use in industrial applications. Multistage forming is one the good strategies to enhance the overall accuracy.

1.7.2 Application of ISF

The main area where the incremental forming is showing its great applications are

- Automobile industry
- Architectural part of decorative panels
- Customized products
- Medicals: prostheses, dental covers
- Aeronautical and space parts industry
- Ship hull building industry

Fig. 1.8 Various application of ISF [10]

1.8 Bond graph approach

Now-a-days, this theory of Bond Graph is greatly expanded to vast fields such as modeling of hydraulic systems, also of mechatronic systems, also in the field of thermodynamic processes. Now, bond graph of electronic system can also be developed to model electronic circuits. Any physical existing system can be modeled with help of bond graph by use of some symbols and some line with known power direction. Elements like resistance, capacitance and inertance may be connected with the use of bonds with results in a network of bonds called structure of physical system [32–34].

1.8 Structure of thesis

The thesis is presented in six chapters with their contents summarized as follows:

Chapter 1 explains the ISF process in detail and also refers the motivating points of the study and objectives. It focuses on the methods to improve the accuracy of SPIF process and various types of strategies developed to model the ISF process for validation of experimental results. It also explains the limitations and advantages of ISF in industrial application.

Chapter 2 provides literature survey in ISF technique for metal. In SPIF process with metallic material, investigated material is Aluminum alloy in series of 6110. How the research on ISF is going on in the world can be clearly understood from literature. What are the different types of techniques developed for improving the accuracy of incremental forming? The literature on bond graph modeling is also discussed in this chapter.

Chapter 3 defines the methodology of process. It explains equipment's used and developed out, procedures followed for forming the components, and strategies of experiments carried out for SPIF process for aluminum material. The experimental caring equipment's include forming tool, jig and fixture, CNC machine. To study the effect of process parameters on the formability of material, the parameters are varied in three stages. Understanding the effect of these parameters is a fundament for selecting the optimal processing parameters to achieve high formability.

Chapter 4 explains all the experimental procedure followed for successfully completion of objective. Effects of variation in parameters value and shape at the end of program are studied. Component is measure in clamped and unclamped position to compare the profile with idea profile. Multiple feature on single sheet is also studied. The component thickness after forming is also studied. Results after the validation of ISF are also discussed.

Chapter 5 describes the results generated and made a conclusion of all the experiments.

The scope of future work on single point incremental forming is also discussed in this chapter.

Chapter 2 Literature Survey

2.1 Introduction

The history analysis done for SPIF is basically moving in the direction to identify the influence of various process parameters on the accuracy of component. The effects of parameters variable can be eliminated to enhance the final accuracy of desired component. What are the various techniques developed to reduce the errors in the profile of final product? Later on what are the types of forces encounter in the SPIF during forming? How these forces can be calculated and which force is most prominent cause of failure of sheet? What are the different modeling techniques can be implemented to validate the experiment results? How bond graph technique can be used to model forces and to find the final spring-back in the sheet? Literature survey consists of basically three sections.

- Background of incremental sheet metal forming technique
- Accuracy related literature survey
- Literature survey for forces calculation and its modeling technique
- Bond graph approach related literature survey

2.2 Background of incremental sheet metal forming

The process and term incremental sheet forming (ISF) was first time introduced by Leszak in 1967 under his patent (US 3342051), in this patent he developed cup shape component by pushing the rotating blank with help of roller punch [2]. During same time, Berghahn made an enhancement in the process with the use of a roller pushing circular blank along the radial line [2]. On the other hand, these two patents were the modified spinning process. Mason's bachelor thesis work is considered as start of incremental sheet forming process [2]. ISF was defined as process in which a small punch or roller follows the contours of the final shape to form that shape which now studied as of ISF.

The revolution about ISF was started in Japan by Appleton in 1984 [4] and later this revolution of was on peak in late 20^{th} century. Inventor researchers like Iseki initiated to publish results on ISF by implementation of CNC milling machines to form component of clamped blank. Now the growth has been made from conventional xyz operation to computer controlled motions using CNC milling machine for ISF.

In the last stage of 20^{th} century, ISF was being developed to greater extant. Another variants of Incremental Sheet Forming has been invented, Two-Point Incremental Forming (TPIF) is one of the development of ISF which was patented by Matsubara in 1994 [6]. In

this type of forming with two tools are performed. One moving tool and one fixed tool are simultaneously performing work to generate complex components. From that time the methodology of ISF has been emerging speedily and motivating to other parts of world by Japanese companies and organizations. Number of types of ISF has been developed till now like SPIF, TPIF, Robot forming, Water forming, etc.

2.3 Accuracy related literatures for SPIF

The former strategies used for forming Incremental forming comprises the forming in single stage, in which tool follows series of path lines having small pitch depth between each contour layer. The plastic deformation zone in ISF is very lesser and strictly limited to the contact area between tool and workpiece. As a consequence, the following drawbacks are noticed in ISF [7].

a. The maximum possible wall angle is resisting the scope of process.
b. Components having complex state of geometry show variable thickness after forming.
c. Stability of process is the issue

The toolpath generated with Cad model also arise the process limits. While following this path, the tool tries to make the preferred shape on the work piece sheet. This type of technique used for developing the toolpath will be successful for the plastic deformation of component. The elasticity of sheet material generates the local spring back on the component. In addition to this, by cyclic loading and unloading in plastic region significant residual stresses developed in component. This can cause to significant eccentricities in the profile of component formed, basically while forming the complex parts.

The flexible rolling process forces are used with predefined thickness or with variable thickness which is called tailor rolled blank. TRB principle can be used as a substitute to the limitations of multistage forming technique. More homogeneous thickness of formed part is achieved by this blank. This set up has been adopted on the basis of the cosine law by calculating the achievable thickness to be got produced to generate homogeneous wall thickness throughout the profile of component. An effort was made to develop a general correction algorithm based on tool path optimization [8].

Later Ambrogio et al. studied the spring-back phenomenon [10]. First of all a complete set of experiments were performed on aluminum sheet samples, by varying the two significant process input parameters. These two parameters were the tool tip ball radius and the incremental depth (pitch). In specific, the accuracy of the finally formed component impressively depends upon the selected pitch of toolpath and tool tip radius. It is noticed with

the increase of incremental pitch enormous thinning and enormous stretching in the sheet are obtained along with the more surface roughness [9]. Since, tool is not in contact with the whole surface staircase effect can be seen on the surface. For smaller tool diameter small localized heat is generated and the localized deformation occurs. Two types of approaches are use in order to simulate forming using the FEM, which are the implicit and explicit model. 3-D analysis of forming to do numerical analysis is required. Because there is no any homogenous conditions which can be assumed during the forming [10]. To model the progressive contact continuous attention is paid to the contact of tool and work piece. Although explicit dynamic model is used to model continuous contact with low time increments but small increments will increase computational time.

Several considerations may be pointed out as

1. Error between the desired profile and actual one correspond to the interaction between the wall
2. Elastic spring-back in the profile causes errors which show lesser effect at edges having higher stiffness.
3. Replication of geometry is not able to formed same accuracy.
4. If the errors of bending the sheet near the major base are neglected, then the average can be noticed in the profile of component is about 1 mm.

During this work good it was noticed that FEM results were validating the experimental performed results. This validation was clearing that the numerical simulation of forming may be used as a design tool.

CNC-three-axis machines are used to achieve ASIF. High RPM of spindle and high feed rate, large bed area are favorable to ISF. A list of the types of machines available to do incremental forming is [11]

- CNC milling machines
- Purpose built machines
- Robots
- Stewart platforms and Hexapods

Robotic forming has Proving their usefulness in the forming field. They have large working volume, fine movements, fast drives. Several industries are using the robots for doing forming. Biaxial strains are measureable in the sheets on in the particular condition.

Draw angle of the sheet is the formability index of the sheet. Much higher level of strains is only possible due to the small localized pressure under the tool. Maximum draw angle φ_{max} [32°, 33°, 60°, 61°, 62°] is the formability benchmark for the sheet.

To measure the forces generated in ISF KU Leuven and Queen's University have designed special sensors definitely to measure the forces [11]. Force sensor is based on the friction between the tool and workpiece. Tool in this sensor supposed as the cantilever beam. Strain gauges with the Wheatstone bridge are attached on the sensor. Two bending force and on axial force is measure with this sensor. Two bending forces are the Radial 'F_r' and the Tangential force 'F_t', and one axial direction, 'F_a'. Spring-back in the material and the geometric distortion due to stress propagation and over-spinning effects that result in unwanted bulging of sheet from the desired location create inaccuracy in the profile. The sheet thinning can be the cause of the errors in the profile of components. Ambrogio et al. reported the major effect of smaller tool diameters and pitch size on the geometric inaccuracies between the workpiece and the target geometry. Duflou concluded that double pass processing with an upward contour finishing pass provided the best overall accuracy [13]. Hirt et al. [11] measured the complete part as a reverse engineering exercise, providing data for an adjusted tool path generation. The proposed method is based on mirroring the measured points around the desire geometry with a scale factor, and using these points o generate new path.

The process ISF still needs more optimization to prove the consistency required for industrial applications. Modeling of the ISF process in FEM has been carried out with the use of the ABAQUS software (explicit), which is very useful for solving highly non-linear problems Material parameters were selected from the work by Shim and Park. Tool is taken as rigid element. Spiral trajectory is used to model ISF. Advancing speed of 3000 mm/min was considered.. Experimental testing was being carried out on CNC milling machine with a FANUC numeric control. Also, a 75° wall angle square based pyramid was formed and force measurement [14].

Strain hardening effects appears when the deformation of sheet takes place, which result changing the mechanical properties of the material and it also effect the deformation ability of the blank. As the deformation increase the strain hardening also gets increased. This is a very important aspect of making part with ISF. The fracture takes place when component formed in one pass and three pass, but if we try to make component with seven pass fracture not occurred.

The main goal of this work was achieving the desired part profile when the punch removal, unclamping and trimming. In this research the accuracy just after when punch is removed from sheet. The bending of sheet is resolved by use of backing plate. The backing plate increase rigidity of the plate [15]. 3-D motion of the tool that follows a continuous spiral or contour trajectory, while designing the toolpath with cad minor base is not considered in toolpath.

Two profiles measured along two sections perpendicular to each other passing through center. These measured profiles help to calculate errors along these two planes. Third measurement was done along the diagonal also. Geometrical error is calculated as the distance between the actual and desired. The optimized selection of process variable is necessary to have minimum erroneousness in the geometrical error at wall. To compensate these errors over depth of component is applied to the profile so that after springback it becomes possible to achieve desired height [15].

The dimensional assurance of the formed part is a still a challenge for the use of ISF in industry. Numerical simulation is not providing significant results to the designers, due to the complexity in shape and the very long simulation time. Many methods to simulate spring-back have been recently recommended. Narasimhan et al. used explicit and implicit techniques for the forecasting of spring-back. Elasticity of component during the process of spring-back helps in the convergence of simulation results in reasonable time [16]. LS-Dyna used commercial code that was based on the code is based on an explicit formulation, it considered the spring-back phenomena by following mixed technique based on the explicit loading and implicit unloading analysis of the process. In this way modeling was able to study the final shape of part after punch removal.

For making a model to study the dimensional accuracy of component while experimentally making of component and after the trimming process a careful attention was paid on the shape definition and on the adopted material. Previously researchers have proven that convex and concave curvatures are mostly affected by the elastic behavior of sheet which results formed surface different from the desired one.

Each experiment is performed to measure the accuracy at the time of making and after unflagging and after trimming test was executed. The results generated by measuring points with the help of laser based system then was compared with the numerical modeling of the process analyze the deviation between the results of experimental formed component and the virtual environment mathematical model.

The dimensional correctness of the formed component is basic problem of SPIF. As sheet can bend near the clamped edges and its spring-back at base are the noticeable errors in the profile [18]. To eliminate this error, various strategies are being developed such as backing plate of toll path compensations etc. There are other errors also that can be prediction upon unflagging or trimming. Finally, some strategies for error minimisation are presented and discussed in this research.

Sheet bending at the major base can be controller with the use of backing plate. When punch is lifted up convex shaped surface formed at the minor base that is called as the pillow effect. Two different methodologies can be used for detecting the errors; each of one has some advantages and drawbacks also.

a) Out of machine control

- Laser scanners: Works on generation of cloud of point
- Probe systems: Able to measure point in space
- CMM systems: Very fast measurement and very accurate readings

b) On-machine control

Hybrid milling-CMM machine is developed to measure online errors in tool wear compensation. Error measured with the help of CMM is again the fed as input to system to correct the inaccuracies in the profile.

Accuracy of component can be improved by using following method at the time of forming the components.

a) Using Backing Plate
b) Multi stage incremental forming
c) Use of counter pressure
d) Back drawing of incremental forming

An experiment is executed in order to study the effect of tool rotation with aluminum grade sheet. Keeping the same speed of rotation in both directions of rotation clockwise and counter clockwise, pyramid is formed to do some analysis. When the tool rotation is there is reduction in peak of forces. This difference effects the formability and friction component also effects. For clockwise rotation of tool forming forces are lesser as compared to the anticlockwise direction, this change in value of peak forces not negligible. Different speeds

and different direction of rotation change the temperatures measurement at the contact point. Surface quality depends also on tool rotation that tool is in motion or not. Speed of tool and direction of rotation do not have any effect. This study becomes stable to predict the results for following statements.

- Friction coefficient
- Forming forces
- Temperature measurements
- Surface roughness

After using the multistage forming technique for axi-symmetric components, now it is being used for non-axi-symmetric parts to create complex shaped profile through incremental forming [20].

Steps to perform multi stage forming includes

1. With the use of a partial die first 'performing stage' is excused having large wall angle.
2. Forming tool achieve number of stages from upward to downwards.
3. To form a wall angle of 80° 10 to 12 stages were used by making 3 to 4° wall step in each stage.

Multivariate Adaptive Regression Splines (MARS) is used in this research to predict final formed profile of component without forming the component in real world [21]. Prediction of profile depends upon the complexity in the shape to be achieved. Finding the feature on the surface is the most prominent step in this method. Complexity of shape is detected with the help of *.stl* file generated from CAD model by the use of the MARS method. Different types of mathematical models are being developed to generate surface for planer and curved profile or the combination of both. These mathematical models depend on part profile and process parameters. Collaboration of different features on the geometry arise extra problem during the prediction of input parameters for complex geometry. It became needs to improve an algorithm which governs joining of the feature normal with the feature boundaries. It becomes possible to develop compensated tool paths with over depths using MARS forecasts by conversion of the corner points of *.stl* model of the part. Factor of +1 is most important in general studies, and thus it delivers good application of this. Moreover, MARS Process for generation of tool paths of profile of component can do offsetting which improve the accuracy of profile. Offsetting of profile can leads to the failure of component when wall

angle is critical. This can be overcome by clubbing the multi stage forming technique with the MARS technique. However, this process needs further developments which offer possibility for additional refining tool paths. Thickness and geometric accuracy are an important issue regarding this forming technology. The techniques used to improve the thickness and geometric accuracy of product guessed to remain flexible and die-less characteristic of SPIF. Ambrogio [23] has developed ankle support with accuracy of less than 1 mm in his experiment. Leach [22] found out that an accuracy of asymmetric component less than 2 mm. Duflou [24] reported accuracy from -1.8 - 5.4 mm while making a solar oven cavity with ISF. The main concept behind the improvement of accuracy of component is just the correction of toolpath with compensative toolpath programming. Hirt [25] generated an algorithm in which CMM based error compensation system is used. Ambrogio [23] also reported DOE approach for compensating toolpath. Micari [26] suggested the different approaches to improve the geometric accuracy such as back-drawing ISF, flexible support, counter pressure, multipoint tools. However, these approaches compromised the flexibility of the process.

2.4 Literature survey for forces calculation and its modeling technique

The physics behind the fracture point among the end point of inclined wall and start point of the lower fillet of the sheet is having great significance in SPIF [27]. Stress and strain are two concepts that can be used to explain the formability sheet forming. It helps to improve the robustness of process. Smaller tools diameter is able to focus the strain on the sheet at localized portion whereas, larger radius have more strains. The state of stress and strain plays effective role in to increase formability of component.

Membrane analysis

The physics behind the crack formation is understood by the detail study of forces considered and resolving the force acting on small element equilibrium along the circumferential direction, meridional direction, and thickness direction and upon neglecting higher order terms one obtains. The value of principle stresses after resolving force and assuming assumptions comes out to be.

$$\sigma_{\emptyset} = \sigma_1 = \frac{\sigma_y}{\left(1+\frac{t}{r_{tool}}\right)} > 0 \tag{2.1}$$

$$\sigma_{\theta} = \sigma_2 = \frac{1}{2}(\sigma_1 + \sigma_3) \tag{2.2}$$

$$\sigma_t = \sigma_3 = \frac{t}{(r_{tool}+t)}\left(-\sigma_y\right) < 0 \tag{2.3}$$

Results show that with the increase in tool diameter formability in incremental forming decreases [28]. On the other hand, as with increase in incremental depth wall slope that can be achieved first rise and then decreases. With the rise in pitch of tool surface roughness first rises up to certain angle and then suddenly decreases. Hagan and Jeswiet formed conical parts using contour tool path to forecast maximum value of roughness R_t in forming. Ham et al. also develop model to enhance quality of surface by reducing effect of tool size and pitch. In this research, a simple examination is completed by generating mathematical model related to the model that created by Silva et al. to forecast the stresses during the deformation. The circumferential stress (σ_Φ), meridional stress (σ_θ) and thickness stress (σ_t) are considered to be principal stresses. The bending of plate occurs near the major base is neglected. Stress components obtained are according to below equations [28].

$$\sigma_t = -\frac{2\sigma_{eq}}{\sqrt{3}}\left(\frac{t}{R_{tool}+t}\right) \tag{2.4}$$

$$\sigma_\emptyset = \frac{2\sigma_{eq}}{\sqrt{3}}\left(\frac{R_{tool}}{R_{tool}+t}\right) \tag{2.5}$$

$$\sigma_\theta = \frac{\sigma_{eq}}{\sqrt{3}}\left(\frac{R_{tool}-t}{R_{tool}+t}\right) \tag{2.6}$$

Final thickness can be obtained by sin law. Due to repeated deformation at some points the thickness is not constant for constant wall angle. Contact area between tool and workpiece at each instant is calculated with this system bearing in mind incremental depth, tool radius. The normal vector drawn to the any contact point always passes through the center of the tool. As tool pushes down intended areas also shifted downward. The tool pushes the sheet along normal direction along height while moving from one layer of path to other. After calculating the contact area, strain and stress components is calculated with the use of equivalent stress which can be is calculated as

$$\sigma_{eq} = 385.7 * \left(\varepsilon_{eq} + 0.009\right)^{0.148} \tag{2.7}$$

It is concluded from all experiments that maximum wall angle possible rise with downfall in tool diameter and rise in sheet thickness. Work material contact area rises as the tool radius rises which increases friction that causes stretching. With the increase in depth Surface roughness increases up to certain angle and then decreases.

This research has motive to diminish the dimensional eccentricity in the wall and base regions of formed components [30]. Axial force cause sheet deflection and radial force causes tool deflection is noticed practically. Ambrogio et al. generated out the enhanced tool

path later on forming a component with having smaller opening radius and higher tilting of wall than the desired up to some depth later on forming the component upto full depth with the desired wall slope. Conical shape component is formed with this technique and it reduces the bending near opening part of formed component. This create model of compensated tool path. In case to apply compensation methodology the forming forces are to be predict in axial, tangential and radial directions. Mathematical model develop by Bhattacharya et al [28] is replicated in this work as base of work. While measuring the thickness it is observed that some part of sheet is repeatedly under load and gets deformed each time of loading. The stress components calculated with model are assumed to be acting over the contact area uniformly. To determine the corresponding forces i.e. tangential F_t, circumferential F_θ, meridional F_Φ forces are resolved to calculate the components of forces along axial (F_z), radial (F_r) and tangential (F_{tg}) directions [30]. To calculate deflection for sheet [29], the formula is given by

$$\delta_{sheet} = \frac{F_z}{8\pi D}\left[-(r^2+b^2)ln\left(\frac{a}{b}\right)+(r^2-b^2)+\frac{1}{2}\left(1+\frac{b^2}{a^2}\right)(a^2-r^2)\right] \quad (2.8)$$

where a is the linear distance from component center to the clamped edges, F_z is the axial forces in z direction, b is opening radius of the component and D is the flexural rigidity of sheet material calculated as [29]

$$D = \frac{Et^3}{12(1-\vartheta^2)} \quad (2.9)$$

The sheet deflection calculated by this method can be added to tool path to enhance the accuracy of workpiece. This deflection compare with the FEA modeling of the SPIF and small errors are noticed as compared to the ideal profile of formed component.

In another technique to study the forces with the help of bond graph of the end milling process is reviewed. In this method end milling considered at cantilever beam which is having fixed end at the collect side and free end towards workpiece was modeled with the help of Rayleigh beam modeling technique which is further dependent upon the castigliano's theorem of strain energy . This is used to find out the deflections due to forces acting on component i.e. radial, tangential, and axial cutting forces. The results obtained from rayleigh modeling is compares with finite element analysis (FEA) modeling to force calculation verification and consequent cutter deflection. Tool-workpiece contact region is discretized into small elements. The forces calculated while experimentation for end milling operation is

used as input for the calculation of deflection. The bending of tool due to stored elastic energy and errors or deflection can be calculated out using Castigliano's theorem [31].

$$\delta_t = \frac{\partial U}{\partial F_a} = \frac{F_a L}{AL} \tag{2.10}$$

$$\delta_r = \frac{\partial U}{\partial F_r} = \frac{F_r L}{AG} + \frac{F_r L^3}{3EI} \tag{2.11}$$

$$\delta_t = \frac{\partial U}{\partial F_t} = \frac{F_t L}{AG} + \frac{F_t L^3}{3EI} + \frac{F_t L^3}{3GJ} \tag{2.12}$$

Tool is under the influence of both shear force and the radial force. The stiffness matrix(C-field) and resistive matrix (R-field) for beam model is represented as [32]

$$[K]_i = \frac{EI}{{L_i}^3} * \begin{bmatrix} 12 & 6L_i & -12 & 6L_i \\ 6L_i & 4{L_i}^2 & 6L_i & 2{L_i}^2 \\ -12 & -6L_i & 12 & 6L_i \\ 6L_i & 2{L_i}^2 & -6L_i & 4{L_i}^2 \end{bmatrix}; \; [R]_i = \frac{EIR}{{L_i}^3} * \begin{bmatrix} 12 & 6L_i & -12 & 6L_i \\ 6L_i & 4{L_i}^2 & -6L_i & 2{L_i}^2 \\ -12 & -6L_i & 12 & -6L_i \\ 6L_i & 2{L_i}^2 & -6L_i & 4{L_i}^2 \end{bmatrix} \tag{2.13}$$

The stiffness matrix relates the both generalized force and generalized displacement. This stiffness matrix can be represented as 4 port C-field elements connected to four 1 elements. Similarly the damping matrix modeled as R-field is shown above. The lumped linear inertia is represented as

$$m = \frac{\rho A(L_i + L_{i+1})}{2} \tag{2.14}$$

Lumped rotary inertia is represented as

$$J = \frac{\rho I(L_i + L_{i+1})}{2} \tag{2.15}$$

Flute part is loaded with radial force (F_r) no moment on cutter represents Se=0 shank also represents the zero loaded effort Se=0. The flow sensor (D_f) measures the radial deflection (dr_1). Summation of both dr_1 and dr_2 provides the total radial deformation on the tool. Bond graph for tangential force is similar as the axial force.

The impreciseness of the cutter forecast by the FEA modeling and bond graph modeling methodology are narrowly relating the experimental results. The error in the profile cutter is showing the most prominent affect by the radial and tangential forces. The depth of cut has the major effect on profile error.

2.5 Literature survey related to bond graph approach.

During era of 1959, H. M. Paynter generated an idea to represent system in form of some bonds that are called power bond, joining the physics behind the system to the junction of structures on basis of some limitations. This process of exchanging power in the picture of bonds is called bond graph. Now-a-days, this theory of bond graph is greatly expanded to vast fields such as modeling of hydraulic systems, also of mechatronic systems, also in the field of thermodynamic processes. Now bond graph of electronic system can also be developed to model electronic circuits. Any physical existing system can be modeled with help of bond graph by use of some symbols and some line with known power direction. Elements are resistance, capacitance and inertance and may be connected with the use of bonds with results in a network of bonds called structure of physical system [32–34].

Bond Graphs power variables

The power factors are effort variable and flow variable and have different definitions in different working areas. By considering the power as a generalized parameter, then could be used as a method to connect systems from several domains shown in Table 2.1.

Table 2.1 Flow and effort variables in some areas [32]

Systems	Effort (e)	Flow (f)
Mechanical	Force (F)	Velocity (v)
	Torque (τ)	Angular velocity (ω)
Electrical	Voltage (V)	Current (i)
Hydraulic	Pressure (P)	Volume flow rate ($\mathrm{d}Q/\mathrm{d}t$)
Chemical	Chemical potential (μ)	Mole flow rate ($\mathrm{d}N/\mathrm{d}t$)
	Enthalpy (h)	Mass flow rate ($\mathrm{d}m/\mathrm{d}t$)
Magnetic	Magneto-motive force (e_{m})	Magnetic flux (Φ)

Basic elements of this technique

There are three types of active and three types of passive elements and two types of basic active elements, two types of double port elements and two types of junctions.

R-Elements

The dependency of 1-port resistor (resistance) element on effort and flow variables is static. Resistor dissipates energy of system. Resistors are electrical resistors and mechanical dampers.

The bond between two elements is represented by a half arrow symbol arrow describes power flow direction, the symbol *e* donates force (effort) and symbol *f* represents velocity (flow).

C-Elements

C element in bond graph is also a static for correlation between effort and displacement. This type energy storing device connected to system. Capacitors in electrical and springs in mechanical domain are energy storing elements.

I-Elements

Inertial element is another type of one port element. This is used when the momentum (*P*) is to be correlated to the flow (*f*). Inductance in electrical field and mass or Inertia in mechanical domain is inertial elements.

Effort and flow sources

Elements which provide reaction on the action of source are called as the active elements. Let us considered the example in which a force is acting on body in that case force will be considered as effort source to the system and the surface of a body act as velocity source of system.

Basic 2-Port elements

Gyrator and transformer are the two types of basic two port elements.

Transformer: The transformer is the element in bond graph that does not generated or store or consumes any type of energy of system. It just has ability to scale up and scale down the conserves power by transformer modulus. The transformer element magnifies the flow from input side to provide us with the flow on the output side of the element. The relation generated by effort and flow when a transformer is used in network as

$$f_2 = \mu f_1 \tag{2.16}$$

$$e_1 f_1 = e_2 f_2 \quad (2.17)$$

$$e_2 = 1/\mu\, e_1 \quad (2.18)$$

From Eq. 2.16–2.18, it is observed that as power in always conserved, there is also a relation between the input and output effort. As the transformer converts flow to flow and effort to effort the causal direction is not changed when the power flows through a transformer.

Gyrator: Gyrator does not create nor destroys energy. It redistributes the amount of flow and effort information. The gyrator element magnifies the flow from input side to provide us with the effort on the output side of the element. The relation generated by effort and flow when a gyrator is used in network as

$$e_2 = \mu f_1 \quad (2.19)$$

$$e_1 f_1 = e_2 f_2 \quad (2.20)$$

$$e_1 = \mu f_2 \quad (2.21)$$

From Eq. 2.19– 2.21, it is observed that as power in always conserved, there is also a relation between the input effort and output flow.

The 3-Port junction elements

There are two kinds of junctions in bond graph that are the 1 and the 0 junction. These junctions help to conserves power and are reversible in nature. The 1 junction has equality of flows i.e. flows are equal in all direction and effort sum of efforts coming to the junction and leaving the junction is equal to zero. It can designated by the letter S or letter 1. The conserved power at junction may be written as

$$e_1 f_1 + e_2 f_2 + e_3 f_3 + e_4 f_4 = 0 \quad (2.22)$$

As 1 junction is a flow equalizing junction,

$$f_1 = f_2 = f_3 = f_4 \quad (2.23)$$

This leads to

$$e_1 + e_2 + e_3 + e_4 = 0 \quad (2.24)$$

For zero junction: 0 junctions have equality of efforts i.e efforts coming to junction and leaving the junction are equal and flows sum at junction is up to zero, In earlier time the

junction can be represented as letter P or letter 0. In case of model with same power direction, the constitutive relation becomes

$$e_1 f_1 + e_2 f_2 + e_3 f_3 + e_4 f_4 = 0 \quad (2.25)$$

As 0 junction is an effort equalizing junction,

$$e_1 = e_2 = e_3 = e_4 \quad (2.26)$$

This leads to

$$f_1 + f_2 + f_3 + f_4 = 0 \quad (2.27)$$

Causality of junction

In bond graph scheme the input bond to junction and the output bonds are analyzed by the causal stroke. The causal stroke defines the effort moving direction. Other end of bond without a causal stroke defines flow moving direction. Sources to the junction impose either effort or flow to the system.

Modeling of Rayleigh beam

Rayleigh beam model is innovative replacement of the Euler-Bernoulli model as it considers rotary inertia. Shear deformation is not taken into account and element to be observed is generally modelled as beams. Beam is a structural member which is having various forces. A beam element under the influence of shear forces and moments is shown in Fig. 2.1.

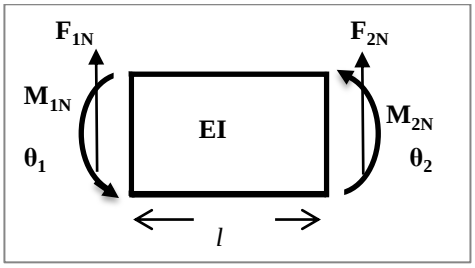

Fig. 2.1 Beam element under influence of shear force and moments

The stiffness of beam is related to Newtonian force and displacements at the ends of the beam as given by equation.

$$\begin{bmatrix} F_{1N} \\ M_{1N} \\ F_{2N} \\ M_{2N} \end{bmatrix} = \begin{bmatrix} y_1 \\ \theta_1 \\ y2 \\ \theta_2 \end{bmatrix} \quad (2.28)$$

The stiffness matrix [K] in bond graph can be denoted as a 4-port C-field for storing energy by the reason of four displacements at the beam as

$$[K]_i = \frac{EI}{{L_i}^3} * \begin{bmatrix} 12 & 6L_i & -12 & 6L_i \\ 6L_i & 4{L_i}^2 & 6L_i & 2{L_i}^2 \\ -12 & -6L_i & 12 & 6L_i \\ 6L_i & 2{L_i}^2 & -6L_i & 4{L_i}^2 \end{bmatrix} \quad (2.29)$$

A cantilever beam is considered with reticulation and lumping of inertia [34]. Fixed end inertias are differential causalled in the bond graph because the flows depend upon boundary condition. So, these are neglected in order to obtain the integrally causalled bond graph. Lumped linear inertia may be calculated as

$$m = \frac{\rho A(L_i + L_{i+1})}{2} \quad (2.30)$$

Where *ρ represents the* density of the material and *A* represents the area of cross sectional area and *i* varies from 1 to 4.

2.6 Literature gap for SPIF

After doing the detail literature survey on incremental forming, it is found that much type of parameter variations has been done to enhance the accuracy of incremental forming. Errors noted at major base due to bending major cause of inaccuracy. There is need of proper study of bending of plate in upper fillet region. Inaccuracy due to tool wear can be studied. The more literature work is necessary for validation of incremental forming with the help of bond graph. More study can be done on forming of steel materials. Effect of heating environment on accuracy during in forming can be studied. Literature gap can be noticed on effect of tool design and tool wear on formability. Bidirectional tool path approach can be studied to greater extent. The more work can be done on to study of profile component at the end component forming and what is the change of profile when the tool detaches from the minor base.

2.7 Objectives of the thesis

The objectives of this thesis are the study of ISF technique for metallic materials. For metallic material aluminum alloy sheet with series of 6110 T_4 tempered were selected for this study. The main difference with previous studies is to measure the profile at the end of program and to form multiple components on single sheet and moreover, also to develop the model of ISF with help of bond graph. The thickness variation study in incremental forming is also done using technique of multi stage forming. To achieve the objectives, a series of tasks are performed as listed below:

- Consider the applicability of SPIF process and its types.
- Design the fixture for clamping the sheet on CNC milling machine bed.
- Perform the series of experiments of SPIF with three stage variation of incremental depth and radius of tool.
- Review on modeling of ISF and to methods to find forces acting on blank during work
- Model the ISF process with the help of bond graph.
- Validate the experimental results with the bond graph results

Chapter 3 Methodology

3.1 Introduction

The accuracy of components generated by the process of single point incremental forming is the basic concerns to wide its applications in the industry. So, as to study the accuracy of single point incremental forming, the series of experiments are carried out on the 3-axis BFW's CNC milling machine model Chandra +, Bangalore, India as shown in Fig. 3.1. The cutter assembly in the adaptor (type BT-40, no. CHE = BT40 = ER32-070, make Robin Precision Products Pvt. Ltd., India) using an appropriate size collet (ER32, size 9–10 mm) is shown in Fig. 3.1. The maximum speed achievable on machine is up to the range of 35 000 rpm. The sheet bending taking place on the major bottom is not considered while studying the accuracy of component. The inaccuracy at the minor base due to springback is the main goal of this work. Aluminum AL-6061 alloy sheet is used for the forming of components with sheet thickness of 0.902 mm, Young's modulus (E) =70 GPa, Poisson's ratio (μ) = 0.33. Sheet bending occurring in the major base can be resolved by the use of backing plate. Cone and funnel shaped two type of components is developed to study the inaccuracy of the shape of components. Tool follows continues spiral tool path to form the part. Reverse engineering is done to compare the accuracy with the help of co-ordinate measuring machine (CMM, make-Accurate Gaging, India, model-Spectra 5.6.4, least-count = 0.1 µm, accuracy = 3.5 +L_m/350 µm, L_m being the length of measurement, stylus and probe system model-MH20i, make-Renishaw, Gloucestershire, (UK) as shown in Fig. 3.12 and to compare the formed path with the desires one.

As per the literature, only one component on single sheet is formed to check the accuracy of components. In this work, study of the multiple components on a single sheet is performed. This process of making multiple components on single sheet is can be refer as multi feature on single plate. Benefit of making the multiple components on the single sheet will help to reduce the setup time. As, the incremental sheet metal forming is feasible for small scale production only, the multiple components is formed on the single sheet for making it useable for the large scale production. While making the multiple components on single sheet, it is noticed that how the making of new one the sheet components affects the components that are already being formed. Various types of results are obtained while doing this work. The effect of changes in process parameters of the single point incremental forming is also studied by varying the tool radius and the incremental depth of component.

The validation of spring back length is also done by the bond graph approach using Rayleigh beam modeling.

(a)

(b)

Fig. 3.1 (a) Three-axes BFW (Chandra +) CNC milling machine and (b) adapter assembly

3.2 Setup making

Firstly, to study the all types of analysis the blank size chosen for making the components is 340 mm × 340 mm. According to this blank size, the fixture for holding the sheet on 3-axes CNC milling machine bed is designed and fabricated. The setup made is highly rigid to withstand the high force. The first step for making the fixture is to do the modeling of setup through software Creo 5.0. The CAD modeling of setup is shown in Fig. 3.2.

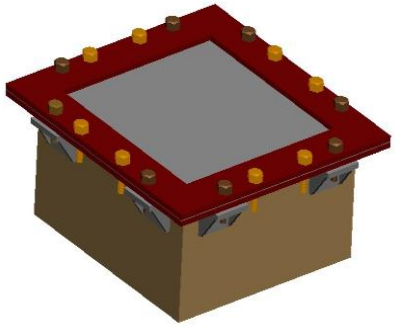

(a)

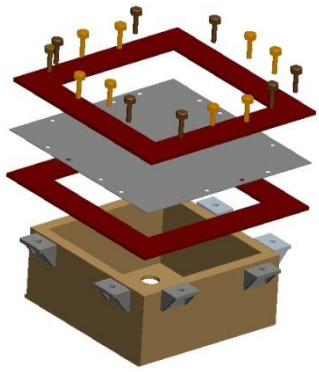

(b)

Fig. 3.2 (a) Assembled and (b) exploded view of the setup in CAD modeling

The setup is made up of mild steel material and approximate mass of setup is 22 kg after the complete fabrication of setup. Two types of arrangements are possible in this setup. First, sheet in clamped position can be removed from the setup to measure the sheet in clamped position. Second, sheet can be unclamped to measure the sheet in unclamped position. After clamping the sheet the useable area for working on sheet is 240 mm × 240 mm. The detail drawings for the setup are shown in Fig. 3.3.

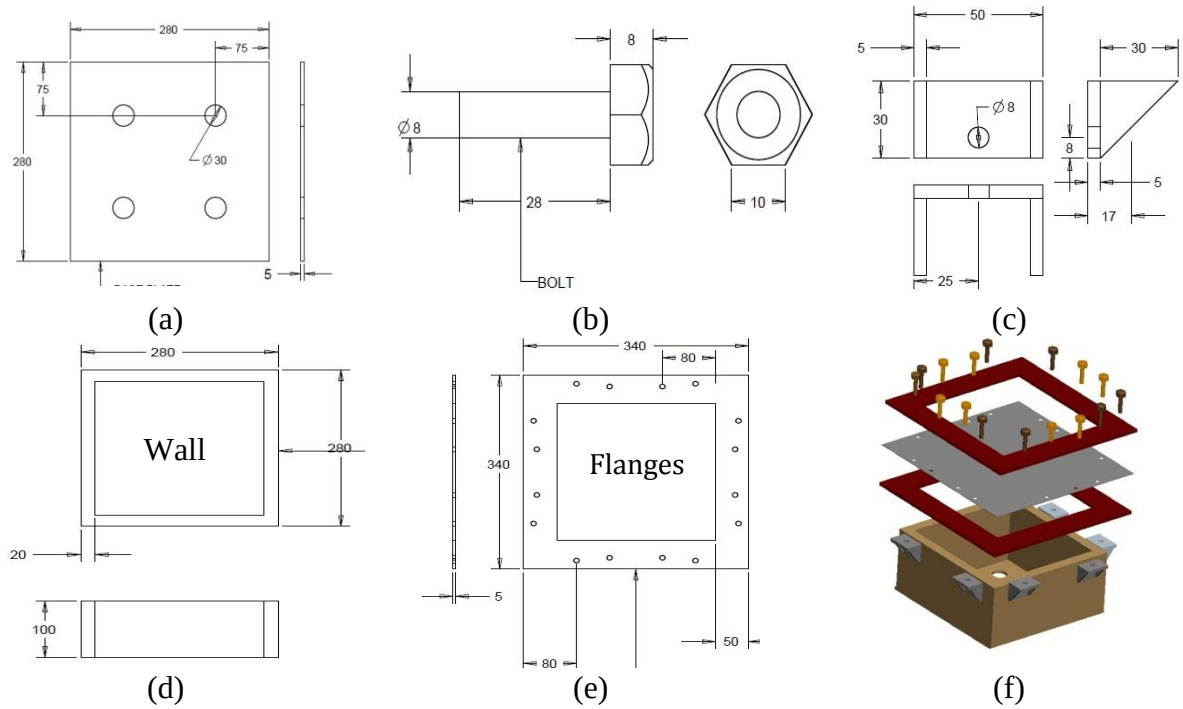

Fig. 3.3 Detail drawing of setup parts (a) base plate, (b) nut bolt, (c) sides hinges to fix flanges with base, (d) wall of setup, (e) flanges used to clamp sheet and (f) CAD model of setup

After modeling the setup in CAD software, the setup is fabricated in the real world. The whole setup is fabricated in the workshops of Mechanical Engineering Department, Thapar University. During the fabrication, the guidance from workshop technician played important role in the fabrication. The most of joining process used during making of setup is welding. The views of setup after fabrication are shown in Fig. 3.4. Two types of settings are possible in this setup. After making the part (forming the part) on the sheet (Blank) of desired profile the sheet can be removed from base in the clamped condition between the flanges and can be measured in clamped condition and then sheet can be unclamped from flanges to measure in unclamped condition so that the two types of measurements can be made possible to analyze the accuracy of components by comparing the produced shape with the desired one.

(a) (b)

Fig. 3.4 Setup fabricated (a) detail parts of setup and (b) isometric view of setup

First measurement is done when the sheet is in the clamped position and the second when the sheet removed from the flanges so that it can be compared how the shape variation occurs after the component unclamped.

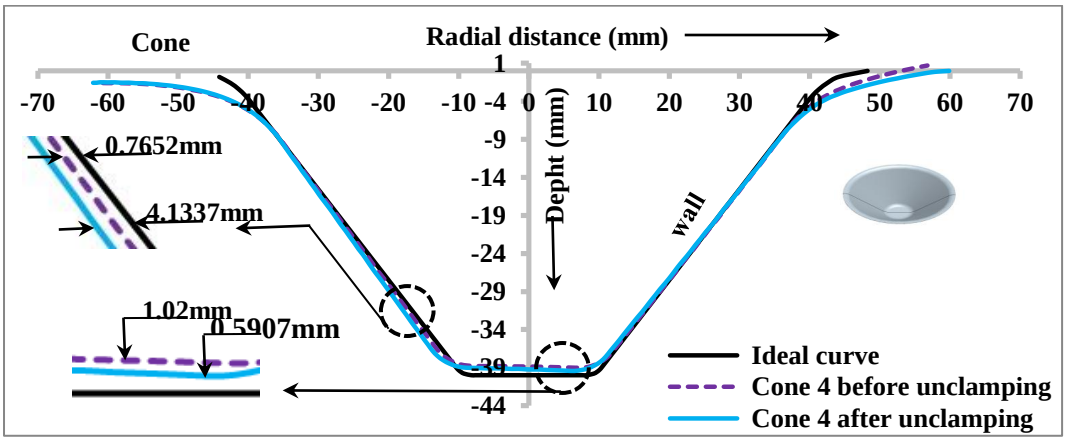

Fig. 3.5 Variation of profile in clamped and in unclamped condition

The Fig. 3.5 is clearly shows the variation of component from its ideal profile when the cone is in clamped and unclamped position. The black line [——] represents the ideal profile or desired profile of the component. The dotted line in purple color [— —] represents the profile of cone before unclamping from the flanges and the sky-blue line [— —] represents the profile of the cone in unclamped position. The error between the profile before and after unclamping represents the spring-back error due to residual stresses produced while making the part. Experimentation is performed just to check accuracy along the both clamped edges of the plate. The results are plotted in excel sheet and it is noticed that, the accuracy of component is comparable along both the clamped edges of sheet. With this experiment, it can be concluded that in further experiments, the component can be measured only along one side of edge to compare the accuracy. In Fig. 3.6 it is clearly visible when the component is measured along both the clamped edges of the profile, component overlaps along both the sides. Red [——] line represents when the component is measured along the X-axis, and Brown dotted line [— —] represent the profile when the component is measured along the Y-axis of component. The Fig 3.6 shows the co-ordinate system of machine with respect to the work piece. All the objects in all experiments are measured only along x- axes of system.

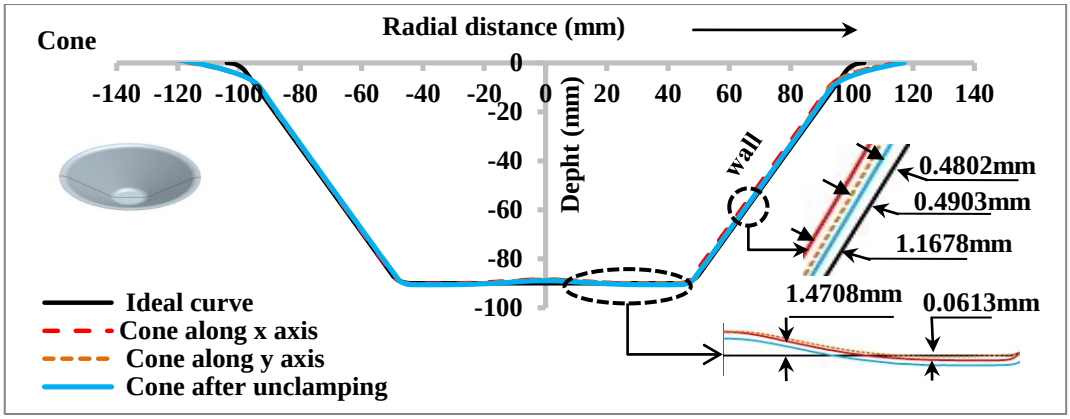

Fig. 3.6 Variation of profile of cone along x-axis and y-axis of plane

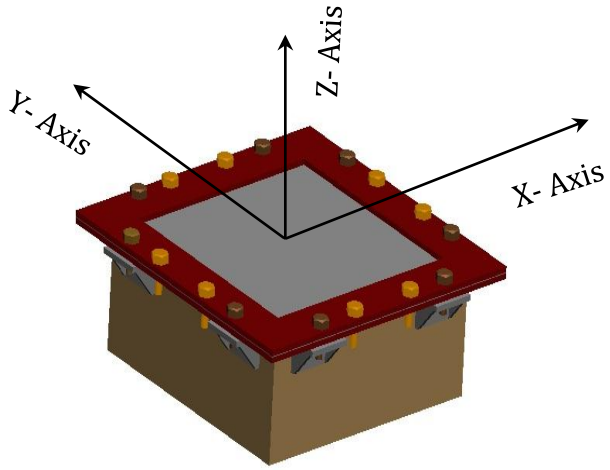

Fig. 3.7 Co-ordinate system of machine with respect to workpiece

3.3 Tool path generation

There are two types of tool path strategies possible to make the part; first is contour shaped profile and the second is of the spiral shaped path. In case of contour shape profile, the tool after following the every contour, tool is shifted down by some fixed incremental depth. The force applied and power used is maximum values while shifting from one contour to the other contour. The drawback of this contour shaped path is that it leaves marks on the sheet where the shifting takes place from one contour to another. On the other hand, in case of spiral profile the tool moves in continuous path while shifting along Z-axis by some incremental depth which is called as pitch of tool.

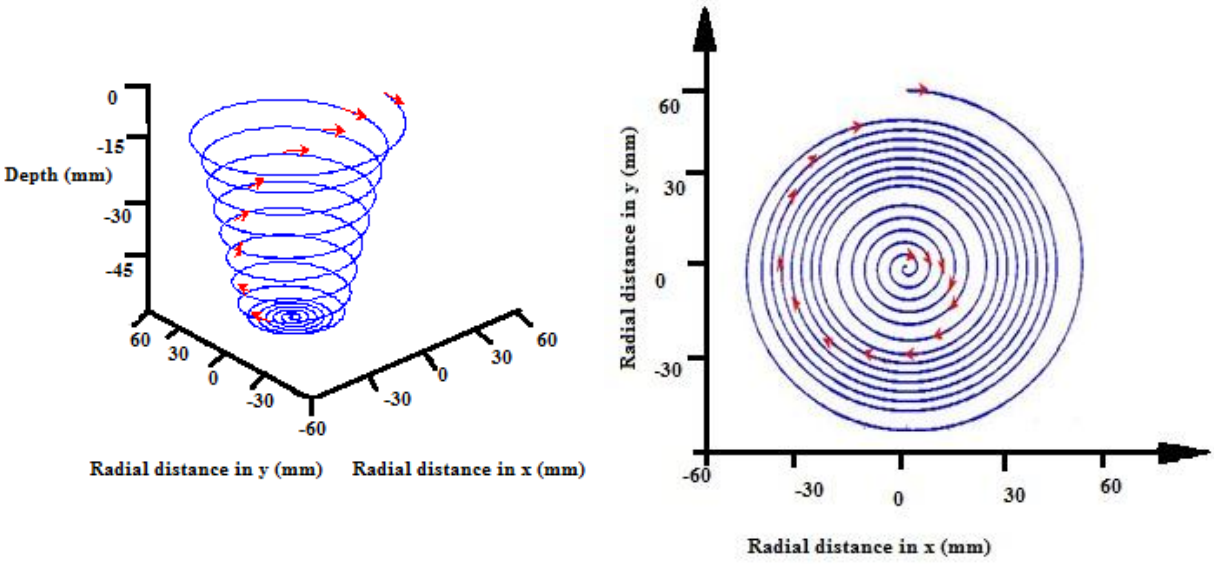

(a) (b)

Fig. 3.8 The spiral tool path strategies (a) isometric view of toolpath and (b) Top view shows the spiral shape toolpath

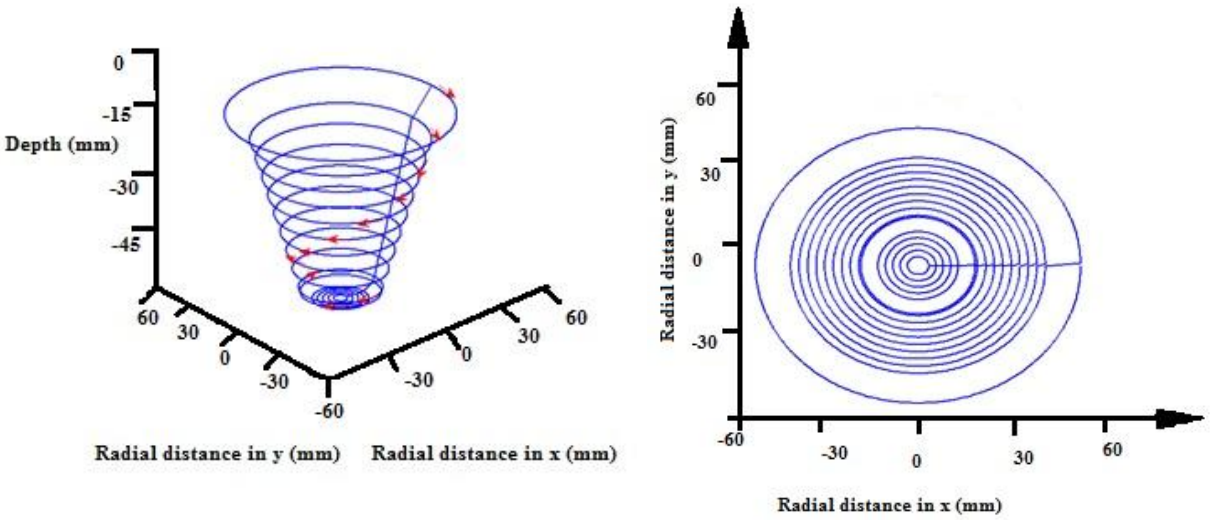

(a) (b)

Fig. 3.9 The contour tool path strategies (a) isometric view of toolpath and (b) Top view shows the spiral shape toolpath

Figures 3.8 and 3.9 show the contour and spiral shaped of toolpath strategies used to from the part, respectively. In this work of checking accuracy, spiral shaped tool path profile is used so that it provides better surface finish and consumes the less power as compare to the contour one. The spiral shaped contour path is generated for two types of components i.e., cone and funnel shaped component. In this work, the entire work for tool path is done in Matlab rather than previous used techniques to generate the tool path from the CAD model.

With the use of Matlab, it becomes possible to provide the tool radius compensation in tool path.

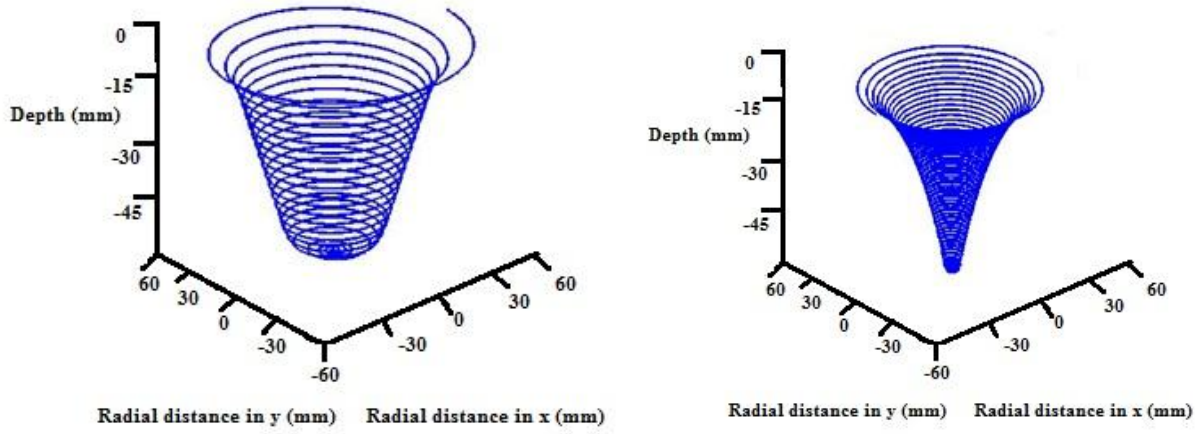

(a) (b)

Fig. 3.10 (a) Tool path for cone shaped object and (b) tool path for funnel shaped object

There is no any role of CAD software in generating the tool path of geometry. CNC programming (G-code and M-code) is generated directly as Matlab output in notepad (.txt) file format. Then this text files is transferred to compact flash card to make it useable on CNC milling machine. The feed rate selected for running of the machine is 2000 mm/min for all the experiments. The minimum possible spindle speed selected for all the experiments is 50 rpm as below this spindle speed, the milling machine does not work. So, as to make milling machine workable, minimum speed is selected to perform experiments.

3.4 Tool making process

After doing the tool path planning for the component, the tool is fabricated. The tool chosen for making the component is the ball ended hemispherical top shaped tool for performing *incremental sheet forming* (ISF). Generally the tool radius can vary from 2 mm to 50 mm as per the requirement of profile to be generated. In this work, three variation of tool radius is selected to study the effect of change in radius on the accuracy obtained for producing component i.e., error in the desired profile and produced one. This error is measured with *coordinate measuring machin*e (CMM) machine. Tool is formed on the CNC lathe machine by programming the entire profile of tool with the hemispherical head and also with the process of turning. The shank radius is made less than that of ball radius so that shank portion would not touch the workpiece. Material selected for tool making is *high speed stainless steel* (HSS). Finishing of hemispherical ended portion requires very high accuracy so as to have

better surface finish on the workpiece obtained. Tool radius highly affects the formability of workpiece; higher tool radius has high friction between the workpiece and the tool. High friction reduces the formability of sheet whereas, the smaller radius produces localized plastic zone to increase formability.

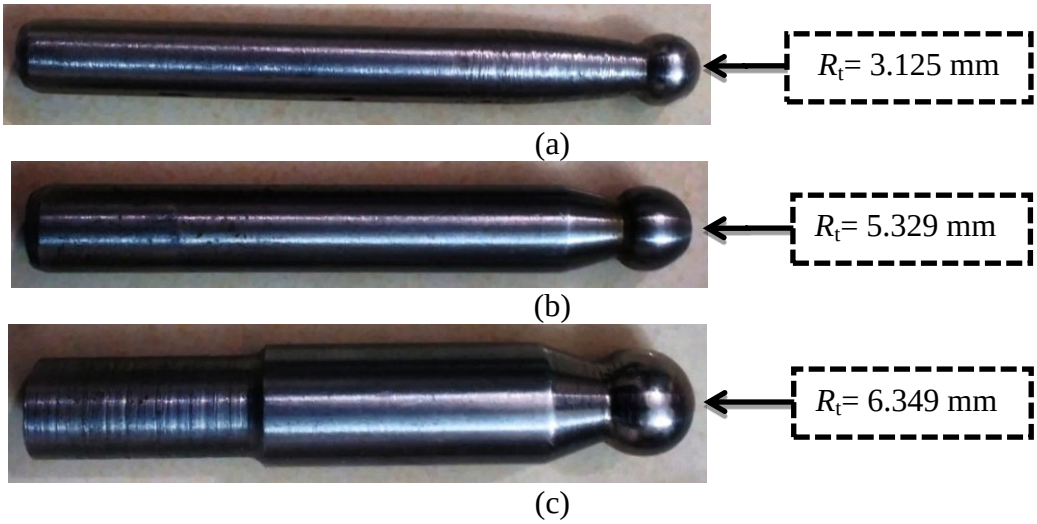

Fig. 3.11 Ball end tool with (a) R_t = 3.125 mm, (b) R_t = 5.329 mm and (c) R_t = 6.349 mm

3.5 Final work plan

Finally, to measure the impreciseness in the profile of formed component, the reverse engineering of formed component is done with the help of CMM in Advance measurement laboratory, Thapar University. The CMM used is of probe type as shown in Fig. 3.12. This machine has a least count of 0.01 µm. The outputs from this machine is directly generated from it in the form of excel file (.xls) format. The manufacturer of CMM is Accurate Gaging, India, model Spectra 5.6.3.

Fig. 3.12 CMM used for the reverse engineering

3.6 Selection of parameters

Three stages variation of two parameters is selected to examine the effect of this variation on the final geometry. Table 3.1 shows the variation of parameters in three stages.

Table 3.1 Parameter variation in three stages

Tool radius R_t (mm)	Tool pitch Δ_z (mm)
3.125	0.25
5.329	0.50
6.349	0.75

Two types of shape variations are also made possible (cone, funnel) to study the effect of this parametric variation on the shapes. The experimental variation of shape and all parameters is chosen as shown in Fig. 3.13. In this figure, the symbol represents as C = Cone shaped component, F = Funnel shaped component, R= Opening radius of component, Δ_z = Incremental depth (Pitch of tool), R_t = Radius of hemispherical end tool. In first three experiments, the component cone is manufactured only by varying incremental depth; rest of all other parameters remains same. This variation results the accuracy affected by the change in incremental depth. In fourth and the fifth turn, the radius of tool (R_t) is varied to see the change in shape due to tool radius variation. By this combination, we are able to get the results for the incremental depth variation and the tool radius variations in single component which is of cone shaped. On the other hand, this same sequence of experiments is repeated for the funnel type component and same results are observed for funnel also.Multiple components on a single blank results faster process by reducing the setup time for creating multiple components of same shape. Multiple features on single plate also helps to make the ISF process feasible for large scale production. Sequence of pattern variation in making the multiple components can also be studied for the stability of the multiple features on single plate. The table 3.2, 3.3, 3.4 shows the parametric variations for all the experiments to be performed to analyze the results. The Table 3.2 shows the parameter variations to study the effect variation in parameters for cone shaped component. Similarly, Table 3.3 shows the parameter variations to study the effect variation in parameters for funnel shaped component. Table 3.4 shows the variation in parameters for multi-point incremental forming.

Table 3.2 Parameter variation for cone shaped components

Opening radius (R mm)	Incremental depth (Δ_z mm)	Tool radius (R_t mm)
R_1	z_1	r_1
R_1	z_2	r_2
R_1	z_3	r_3

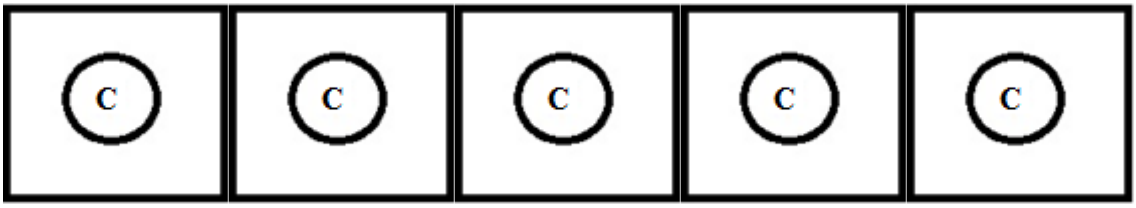

Table 3.3 Parameter variation for funnel shaped components

Opening radius (R mm)	Incremental depth (Δ_z mm)	Tool radius (R_t mm)
R_1	z_1	r_1
R_1	z_2	r_2
R_1	z_3	r_3

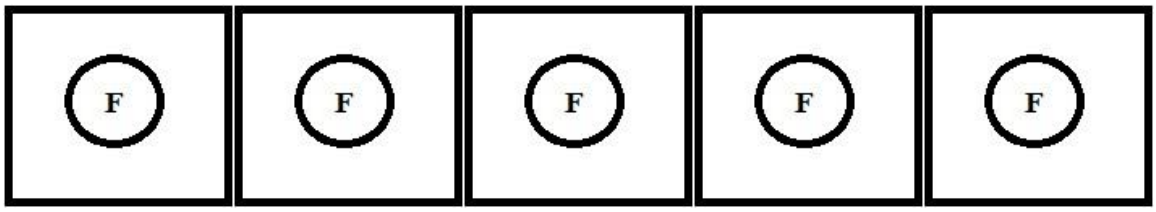

Table 3.4 Parameter variation for multi feature on single sheet point forming

Opening radius (R mm)	Incremental depth (Δ_z mm)	Tool radius (R_t mm)
R_1	Z_2	r_1
R_1	Z_2	r_1
R_1	Z_2	r_1

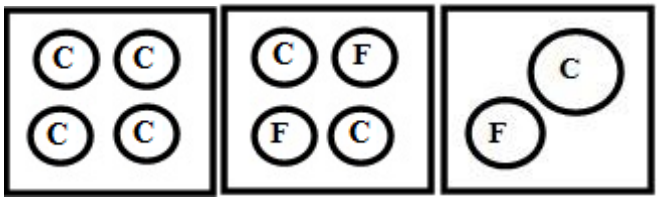

To study the accuracy of multistage incremental forming, the single component is made in four stages. The total height of component is selected as 30 mm height. The stage of forming are: In first stage, the component is only made up to the end of upper fillet; In second stage, the component is made up to the 10 mm height; In third stage, up to 20 mm height and in final fourth stage, the component with full depth 40 mm is formed. The benefit of multistage incremental forming is that we can make the components with greater wall angle which is not possible with single stage forming.

3.7 Input parameters

The input parameters play very important role in defining the tool path planning for the geometry to be obtained. In case of cone and funnel, the input parameters are listed in Table 3.2 and also shown in Fig 3.14. These are the input parameters which we can control to obtain the desired dimensions of the cone and funnel. It can be noticed that in case of cone, the wall angle is constant throughout the height of component and only the variation in wall angle occurs near the upper fillet and lower fillet. The wall angle of funnel is continuously varying from some minimum slope value to some maximum value.

Table 3.5 Input parameters

Symbols	Descriptions
R	Opening radius of the cone shape component to be formed
H	Height of the cone
α	Wall angle of the cone or also called as draw angle
α_{min}	Minimum wall angle of the funnel near the major base of funnel
α_{max}	Maximum wall angle of funnel near the minor base of funnel
R_{uf}	Radius of upper fillet near the major base
R_{lf}	Radius of lower fillet near the minor base
Δ_z	Incremental depth (along height of component) between each contour
Δ_r	Incremental reduction in radius after each contour (along radius)

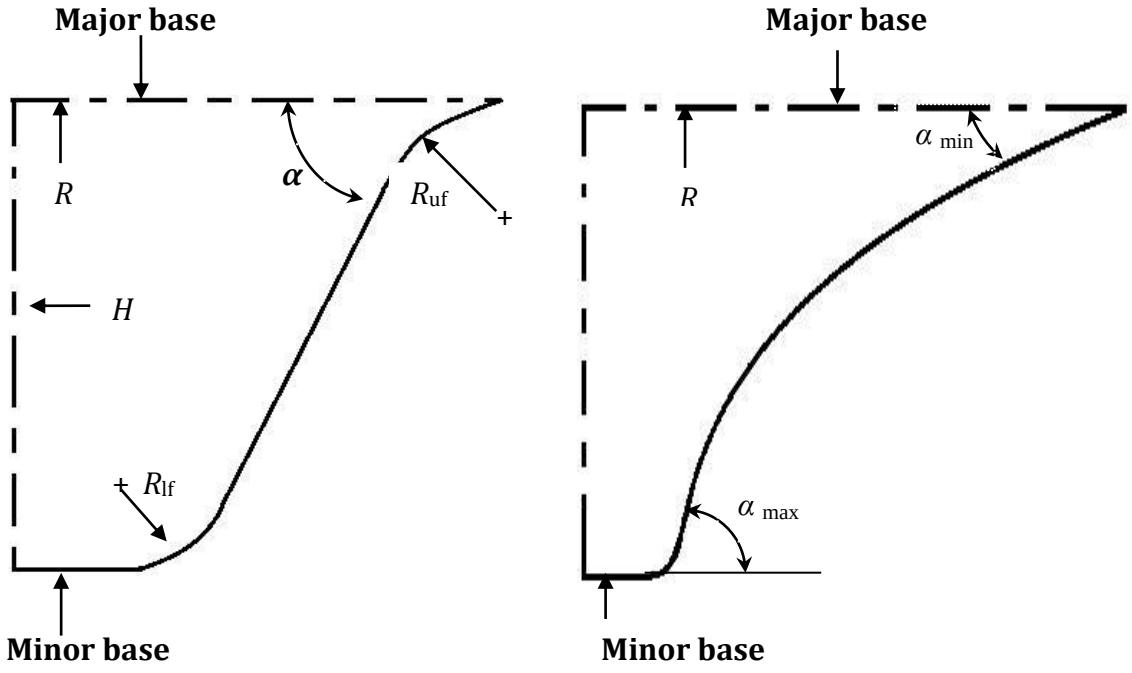

Fig. 3.14 Nomenclature of input parameters for cone and funnel

In this work, the wall angle varies from 5° to 60°. Benefit of varying the wall angle is that in funnel rather than measuring the component from two places of the wall and the upper fillet as in case of cone we can measure the funnel from only one location to obtain same results. In funnel, height is not an input as in cone. The height depends upon the maximum wall angle, opening radius of the funnel.

3.8 Bond Graph Modeling on Bending of Concentrically Loaded Clamped Plate

The bond graph approach is used for modeling on bending of concentrically loaded clamped plate required for single point incremental forming. As, all the sides of sheet in SPIF are clamped, the sheet is assumed as the 2-D clamped beam having end conditions of edges as clamped. The slope and deflection at the clamped portion is taken as zero. By using bond graph approach, beam is modeled with Rayleigh beam modeling technique. The beam is discretized in a number of small Rayleigh elements (reticules). From the experiments done (discussed in Chapter 4) it can be clearly noticed that the maximum spring-back occurs between 4 mm to 5 mm. In case of Rayleigh beam modeling, the deflection of beam relates to the spring-back of components. It is noticed from the literature [5] that the load acting in the upper fillet region only is responsible for the spring-back action. The load acting in the other region of cone is not responsible for the reasonable spring-back in the component. The total beam is discretized into 116 (58×2) Rayleigh elements as shown in Fig. 3.15. Top view of plate is shown in Fig. 3.16. The component is formed at center with opening radius (R) = 100 mm, the base (minor base) part of cone is having radius (R) = 50 mm. Upper fillet region (6.062 mm) is only loaded. The rest of the component that includes wall and the lower fillet region has a length of 43.928 mm. After forming the component, the distance of component from the edges is 20 mm from all sides of edges. One side of the beam (58 reticules) is the mirror image of the other and this side is discretized into four zones $(58 = 5 + 7 + 11 + 35)$. No load part of sheet (20 mm from both the sides) is discretized into 5 Rayleigh reticules. The upper fillet region of distance 6.062 mm is discretized into 7 reticules. The other part of component that includes wall and lower fillet region having distance 43.928 mm on both side of component is discretized into 11 reticules and the lower minor base region component is discretized into 35 reticules.

The incremental depth has the major effect on profile error. The detail diagram of discretization is shown in Fig. 3.15. This diagram showed all the reticules at each part of

component throughout the beam span. The bond graph of SPIF for deflection calculation is shown in Fig. 3.17.

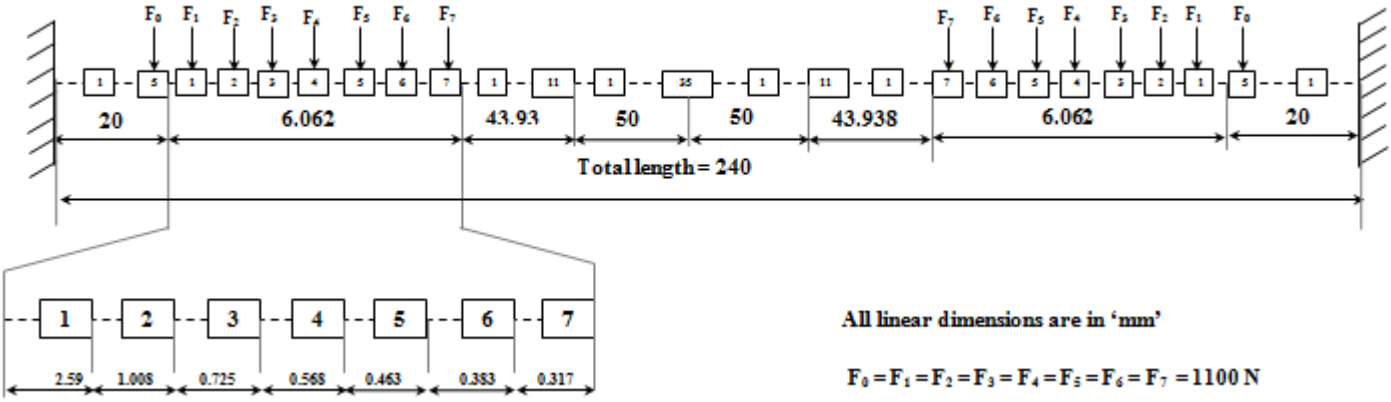

Fig 3.15 Detail view of discretization of whole length of beam

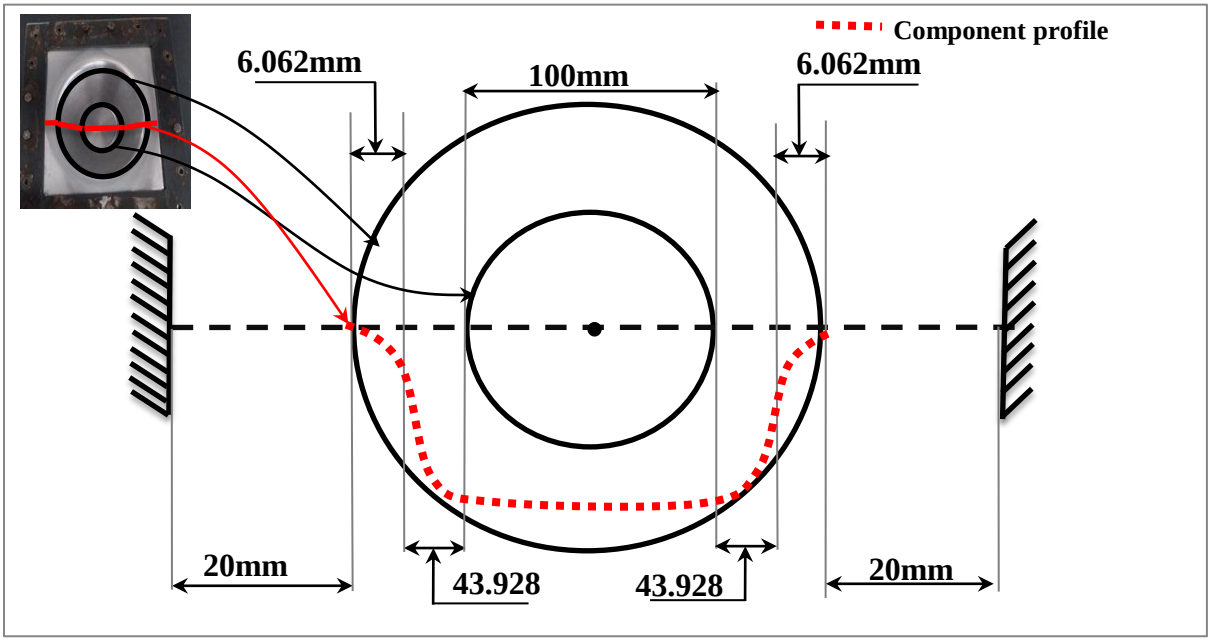

Fig. 3.16 Top view of sheet specifying all dimensions for discretization of beam

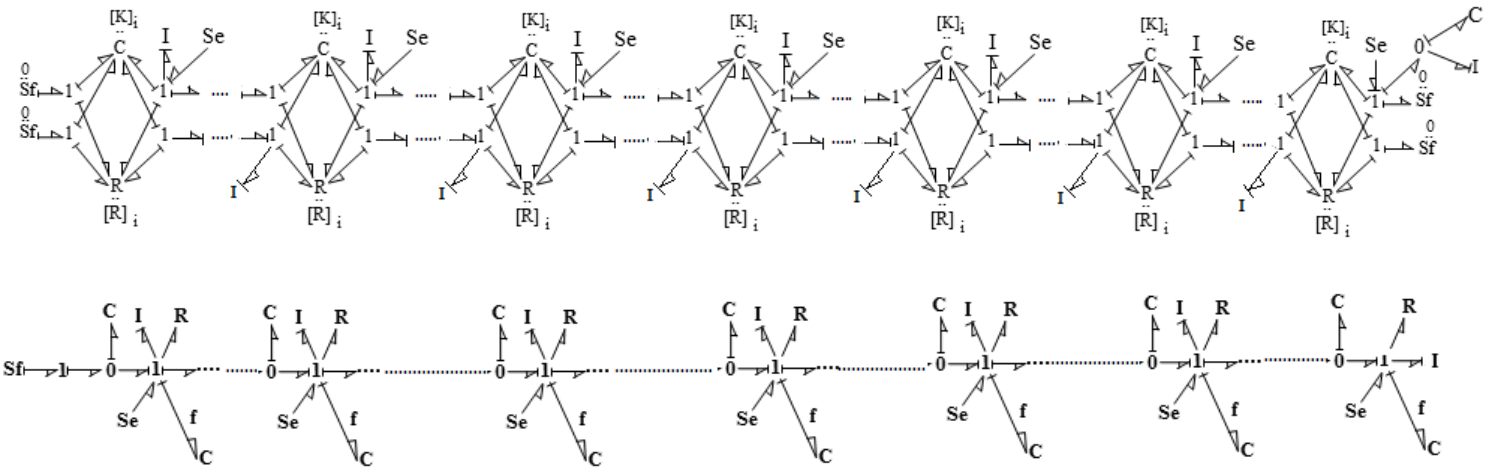

Fig. 3.17 Bond graph model of (a) transverse deflection using the Rayleigh beam model and (b) axial deflection of the sheet

Considering the sheet as a simply supported beam clamped from all sides is modeled. To model shear force effect, Rayleigh beam model is used for modeling and Castigliano's theorem of strain energy is used to predict the deflections due to transverse forces. To exactly forecast the deflection of sheet, sheet is discretized into smaller elements. The force acting transverse direction on sheet is considered from literature and used for deflection prediction. During the forming, energy is stored into the sheet. The sheet bends due to this elastic energy and this deformation can be found out using Castigliano's theorem [32].

$$\delta_t = \frac{\partial U}{\partial F_a} = \frac{F_a L}{AL} \tag{3.1}$$

$$\delta_r = \frac{\partial U}{\partial F_r} = \frac{F_r L}{AG} + \frac{F_r L^3}{3EI} \tag{3.2}$$

Figure 3.17 shows that zero source flow is taken at the fixed end of the sheet connected at the 0-junction i.e., Sf=0. The detailed bond graph of a single space reticule of the sheet as shown in Fig. 3.17(b) in the extreme left would be discussed now. The stiffness value (AE/L_i) of the element with length (L_i) is denoted by the compliance element C connected at the same 0-junction. The mass (AL_i) of the element is represented by I element. R represents the damping of element. The Se element represents the axial force (F_a), connected at the 1-junction. The shear deformation (F_r/AE) is considered, by modifying the bond graph. The Fig. 3.17(b) is the model for shear deformation additionally added to Rayleigh beam model. The upper part of bond graph represents the Rayleigh beam model to with Sf=0 on left and right for fixed end. The stiffness matrix (C-field) and resistive matrix (R-field) for beam model is represented as

$$[K]_i = \frac{EI}{{L_i}^3} * \begin{bmatrix} 12 & 6L_i & -12 & 6L_i \\ 6L_i & 4{L_i}^2 & 6L_i & 2{L_i}^2 \\ -12 & -6L_i & 12 & 6L_i \\ 6L_i & 2{L_i}^2 & -6L_i & 4{L_i}^2 \end{bmatrix}; \; [R]_i = \frac{EIR}{{L_i}^3} * \begin{bmatrix} 12 & 6L_i & -12 & 6L_i \\ 6L_i & 4{L_i}^2 & -6L_i & 2{L_i}^2 \\ -12 & -6L_i & 12 & -6L_i \\ 6L_i & 2{L_i}^2 & -6L_i & 4{L_i}^2 \end{bmatrix} \quad (3.3)$$

The stiffness matrix relates the both generalized force and generalized displacement. This stiffness matrix can be modeled as 4 port C-field elements connected to four 1 elements. Similarly the damping matrix modeled as R-field is shown above. Sheet part is loaded with transverse force (F_r) which is represented by Se element. The lumped linear inertia is represented as

$$M = \frac{\rho A(L_i + L_{i+1})}{2} \quad (3.4)$$

Chapter 4 Results and Discussion

4.1 Introduction

In this section, the discussion on the results generated after the experimental testing of part to study the effect of various parameters on the accuracy of the component is done. All the experiments are performed on 3-axis CNC milling machine. Only *Single Point Incremental Forming* (SPIF) is studied in which contact between the tool and the workpiece is a single point. Inaccuracies in SPIF due to the residual stresses and the spring-back in the sheet are studied. Spring-back is an elastic phenomenon which depends on the elasticity of material. Spring-back at the bottom of component is nothing else just represents the difference in height or error in height from the desired height or magnitude by which the height of formed component is smaller than the desired height of ideal component.

Elasticity of material varies from material to material. Stress concentration is generated or residual stresses in the component due to continuous application of load while the component is being formed. Various types of the variations of parameters made possible to notice the effect of these changes on the final part being formed. Radius of hemispherical ended tool and the incremental depth (Pitch) changed in three stages. At the very first stage of experiments the effect of variation in incremental depth (Δ_z) on the component is studied on the part (Cone). The parameter variation for studying the Δ_z variation is as shown in Table 4.1.

Table 4.1 Parameter variation to study effect of Δ_z variation on cone

Exp no.	Tool radius R_t (mm)	Tool pitch Δ_z (mm)
1	4.125	0.25
2	4.125	0.5
3	4.125	0.75

4.2 Experiments performed to study the effect of change in process parameters

4.2.1 Cone with $\Delta_z = z_1$, $R_t = r_1$

The input parameters for this study in first experiment for the shape of cone were as opening radius(R) =100 mm, wall angle (α) = 60°, height of component (H) = 90 mm, radius of upper fillet (R_{uf}) =7 mm, radius of lower fillet (R_{lf}) =7 mm, radial increment (Δ_r)= 0.3 mm, incremental depth (Δ_z) = 0.25 mm, tool radius (R_t) = 4.125 mm.

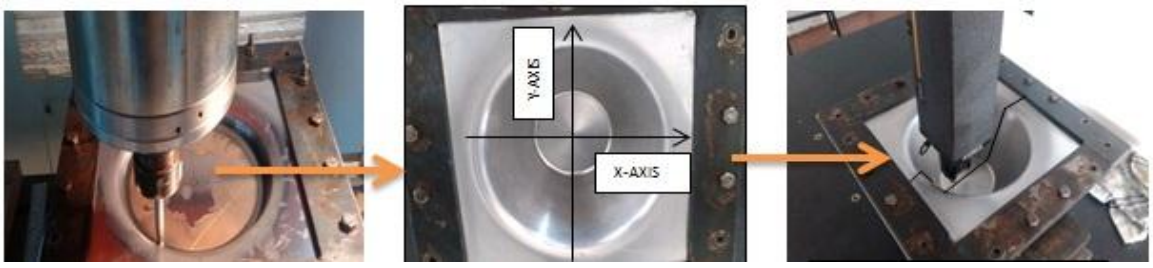

(a) (b) (c)

Fig. 4.1 Steps followed to formed the parts (a) forming of cone, (b) formed cone in clamped position and (c) measurement of cup using CMM

The Fig. 4.1 is showing the various steps to make the components. These three steps of making component will remain common in all the experiments and variation in shape would occur only. In these experiments, pillow effect can be seen at the minor base of the cone as shown in Fig. 4.4. To check the profile of formed cone in the clamped condition, component is measured along both the x-axis and y-axis of cone. Due to the symmetrical shape of component (cone) about its central axis, it becomes easy to compare the shape of component along x-axis and y-axis. It can be seen from the plot of measurements shown in Fig. 4.2 that profile of cone along the both the axis is approximately overlapping with each other. It results that for future work it is possible to measure the component only along one axis due to symmetrical in shape to compare profile. Height of component achieved is approximately equal to the desired one the minor base edges. At the center of the minor base, sheet is distorted from the desired path towards the major base. This distortion is called as the pillow effect.

Each component is measured three times. First, when the component is got formed and in clamped position along x-axis and it is represented by the red color line [——]. Second, when the component measured along the y-axis, it is represented by the brown color dotted line [— —]. Third, when the components is unclamped (in unclamped position) from the flanges the distortion occurred is measured after unclamping, it is denoted by sky blue color continuous line as [— —].Spring-back is the residual stresses in the sheet due to continuous loading. Due to spring-back, the component becomes unable to achieve desired height and desired profile at the walls of the components. In this experiment, it is clearly visible from the Fig. 4.2 that the cone minor base is distorted from its minor base by 1.4708 mm but, at the edges, height is same as desired one. This causes pillow effect at the minor base. Height

continuously varies from the edge of minor base to the center of minor base. Center has minimum height and edges of minor base have max height.

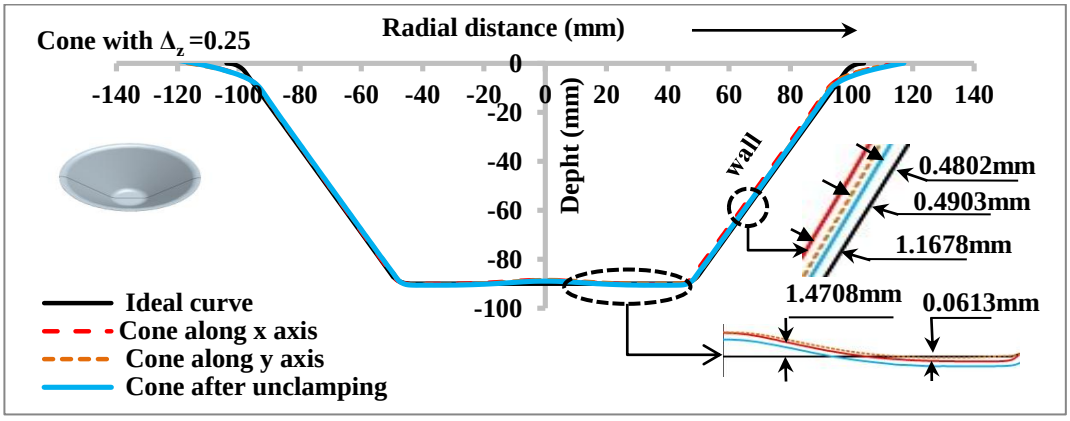

Fig. 4.2 Plot of cone with Δ_z = 0.25 mm

The walls of the cone are distorted from the ideal desired profile also. When measured along x-axis, it is noticed that the walls are deviated from profile by 0.5902 mm, along y it is 0.4903 mm and after unclamping, the difference remain as of 0.4802 mm. Walls are not overlapping with the desired profile which shows the inaccuracy of the profile but, the profile at the time of measuring along x-axes and y-axes are approximately overlapping with each other which shows that it is possible to measure the component only along one side to predict the results about other axis.

4.2.2 Cone with $\Delta_z = z_2$, $R_t = r_1$

Next, in the 2nd experiment again the Cone is formed with variable incremental height rest all other parameter is same. The incremental depth is changing from 0.25 mm to 0.5 mm rest all other parameters kept constant. The component making scheme is same as used in previous one. Again the results from CMM plotted in the excel sheet. In this experiment the component is measured only along the x-axis and the results generated compared with the last experiment. This time the incremental depth varied to its second stage. The plot generated after generation all the points is shown in Fig. 4.4.

To study the shape of component at the end of program, when after following the each layer of spiral path at last tool is at last point and in touch with the center of sheet minor base. To make it possible, the shape of cone at last of program is casted on the plaster of Paris (POP). When the POP got soaked and attained the shape of cone and when tool is in touch with sheet only the tool is detached from the sheet. Casting of POP is only the way to measure the component at end of program. As the tool detaches the sheet the spring-back in the sheet due to residual stresses distort the shape of component from the shape of component

at last of program. This distortion is measured by doing the reverse engineering of the casted piece POP of the cone. Figure 4.3 shows the casting of POP and the measurements of casting. In this experiment, cone is measured three times and one time casted shape on POP is measured. Two types of analysis can be predicted after this experiment:

- What is the effect of change in incremental depth on the accuracy of the cone?
- What is the shape of cone when tool is in touch with the minor base at the end of program?

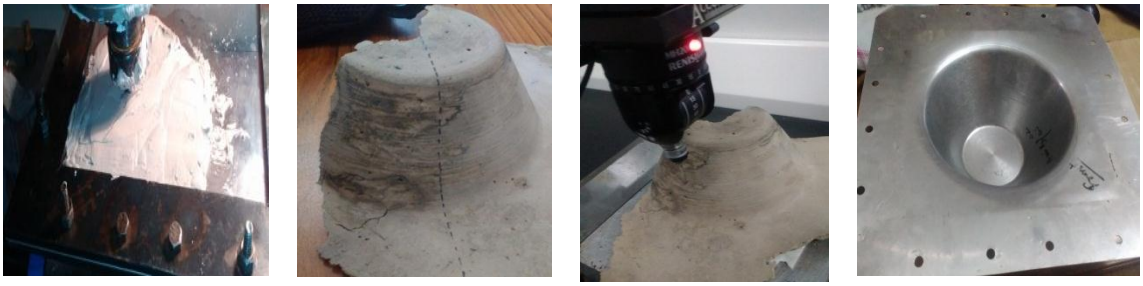

(a) (b) (c) (d)

Fig. 4.3 (a) Casting of cone on POP, (b) casted shape of cone, (c) CMM measuring of casted shape and (d) cone in unclamped position

The predictions from the plot in Fig. 4.4 for cone shape made with Δ_z = 0.5 mm is that pillow effect can be seen in this plot also. After making of component, the spring-back in the sheet is 1.5003 mm and the cone is able to achieve the desired height at the ends of the minor base. When the cone is unclamped, this spring-back increases from 1.5003 mm to 1.723 mm. The spring-back noticed in the wall is 0.4802 mm towards the center of cone.

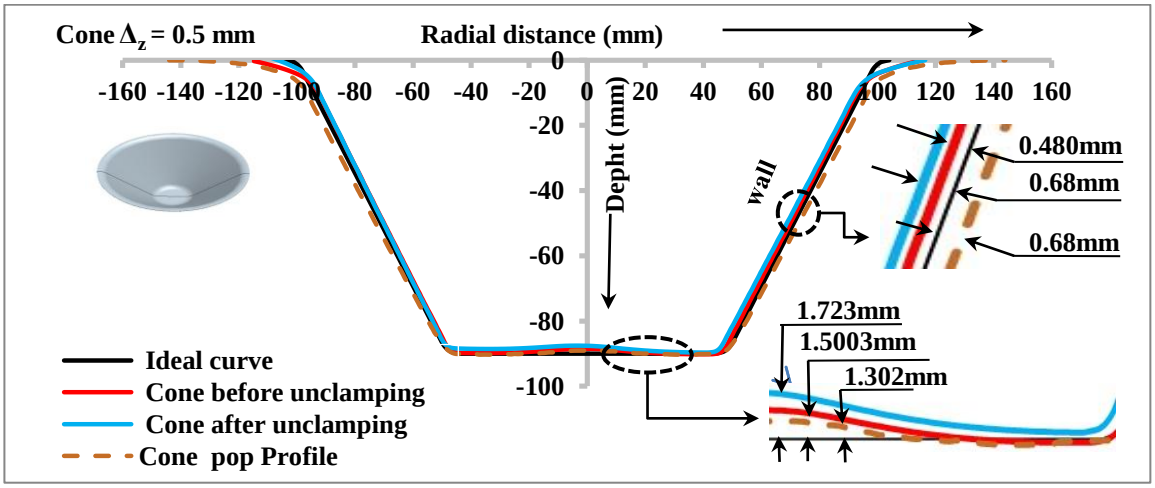

Fig. 4.4 Plot of cone with Δ_z = 0.5 mm, R_t = r_1= 4.125 mm

When the component is unclamped, the spring-back increases to 0.68 mm. On the other hand, for second type of analysis at the end of program, the spring-back analyzed at the base is 1.302 mm and in wall deviation it can be clearly seen that the walls were deviated from the actual ideal path by 0.68 mm away from the desired profile. The total spring-back in the wall after unclamping and the when the tool is in contact with base is 1.36 mm and at the base is 0.421 mm where the pillow effect is developed.

From 1st and 2nd Experiment, it can be concluded that as we increase the incremental depth from 0.25 mm to 0.5 mm, the spring-back in sheet increases due to the power needed to deform the cone is increased. Hence, residual stresses also got increased.

4.2.3 Cone with $\Delta_z = z_3$, $R_t = r_1$

In 3rd experiment under SPIF, again the component cone is formed. In this experiment, the pitch (incremental depth) is varied to its 3rd stage. This time the pitch chosen is equal to 0.75 mm, rest of all other parameters are kept constant. The cone profile at the stage of end of program is also measured again with the help of POP model by doing the reverse engineering of the model by use of CMM. Component forming process and casting of POP model steps are all same as previous one. Plot of points generated from the CMM is shown in Fig. 4.5. With the help of CMM, it becomes possible to generate point on the profile of cone at step size of 1 mm. In the experiment, again two analyses are noticed. First, for the variation in profile when the pitch is changed stepwise and second, what is the profile at end of task?

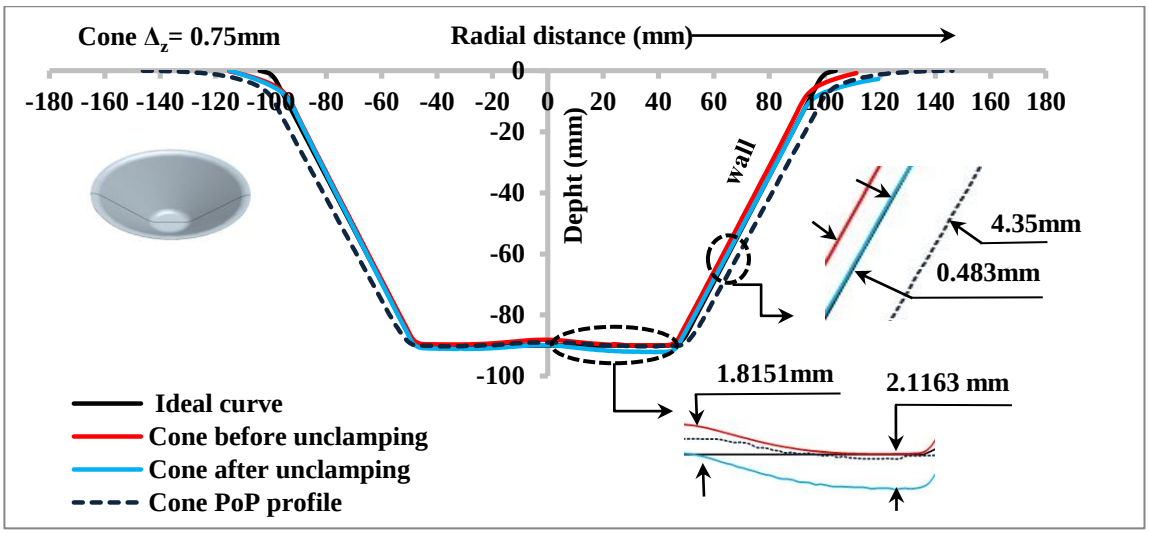

Fig. 4.5 Plot of cone with Δ_z = 0.75 mm and R_t = r_1=4.125 mm

As clear from the plot, the accuracy of component is greatly affected by the change in incremental depth. Spring-back can also be seen in plot. The maximum spring-back occur at bottom that generated pillow effect is 1.8151 mm at the center. At the edges of the minor base the profile is completely overlapping with the desired profile. The deviation of wall from the desired location is given as 0.483 mm. After the removal of blank from the flanges, the sheet accuracy is greatly affected by the spring-back. The sheet bends more in one side. Then the peak region of the bottom pillow meets the desired profile and the edges minor base bent down from the desired profile by 4.1163 mm. On the other hand, in case of casted shape of cone on POP the profile of minor base of the cone is approximately overlapping with the target shape (ideal or desired) one. But the wall of components is not matching with the desired shape. The wall is deflected from the ideal profile by 4.35 mm. The conclusion from the 1st, 2nd and 3rd plot is that as we are increasing the step down or pitch or incremental depth the spring-back is continuously increasing. More strain hardening occurs in the sheet. The shape at the end of program is more accurate when the incremental depth is smaller. As the Δ_z (pitch) increased the deformation in shape is noticed more.

4.2.4 Cone with $\Delta_z = z_2$, $R_t = r_2$

After comparing, the effect of change of incremental depth on the final accuracy of the component then the effect of change in radius of tool on the final accuracy is studied by changing the diameter of tool in three stages.

Table 4.2 Parameter variation to study effect of R_t variation on cone

Exp no.	Tool diameter R_t (mm)	Tool pitch Δ_z (mm)
2	4.125	0.5
4	5.329	0.5
6	6.349	0.5

To analyze this effect cone is made with the following input parameters:

Opening radius (R) = 100 mm, wall angle (α) = 60°, height of component (H) = 90 mm, radius of upper fillet (R_{uf}) = 7 mm, radius of lower fillet (R_{lf}) = 7 mm, radial increment (Δ_r) = 0.3 mm, incremental depth (Δ_z) = 0.5 mm, tool radius (R_t) = 5.329 mm. In this experiment, again two motives are covered. The effect of the tool radius changes on shape of component and shape at end of program is studied. It can be notice from the Fig. 4.6 that the pillow

effect occurs at the base of cone. The spring-back in the sheet when the punch is removed from the sheet is equal to 1.2187 mm. The error in profile at wall on right side of cone is of 0.5039 mm from the ideal path but on the left side it is just 0.6 mm. After unclamping the plate from the flanges, it is noticed that the error in the bottom of cone is 1.3106 mm at the center of minor base and at the edges profile is same as desired.

It can be noticed from Fig. 4.6 that at the stage of end when program ends, the profile at that time is simply overlapping with the profile after the removal of punch from bottom. At the walls, the profile at the end of program is deviated from the ideal walls by distance of 0.688 mm. It can be concluded from the Figure that, with increase in radius of tool the profile after removal of punch is overlapping with profile at end of program, spring-back in sheet got reduced.

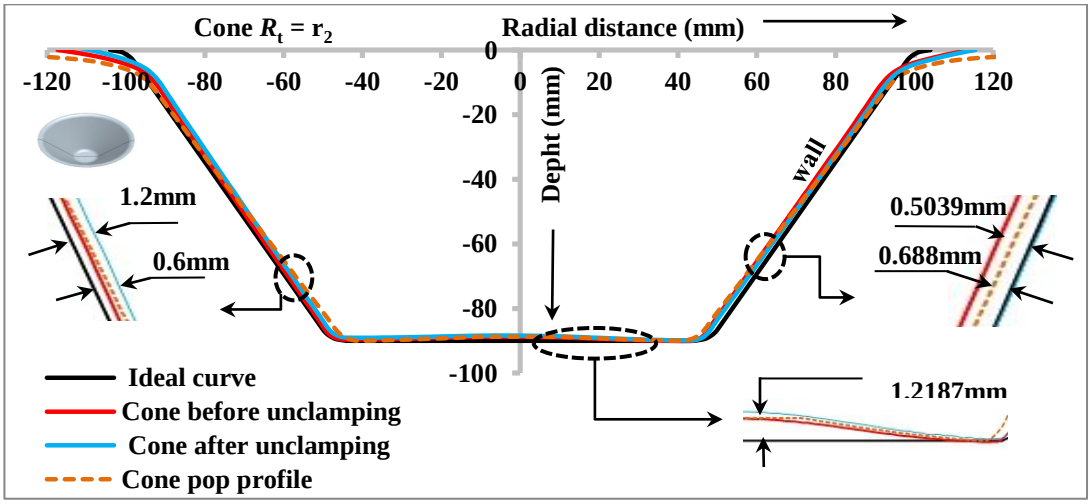

Fig. 4.6 Plot of cone with Δ_z = 0.5 mm and $R_t = r_2$ = 5.329 mm

4.2.5 Cone with $\Delta_z = z_2$, $R_t = r_3$

In the last experiment of SPIF to make the cone shaped profile, the analysis is made possible to study the effect of the change in radius of tool in its third stage. All others input parameters to obtain the cone shaped profile are kept constant. Now, radius changes from 5.326 mm to 6.349 mm. After forming the component on axis CNC milling and measuring on CMM, the plots of points to generate profile is shown in Fig. 4.7. At last, in this experiment the radius of tool is varied to its third stage. As clear from the plot the spring-back produced in this sheet of experiment is very less than all other cases. Pillow effect can be seen to very small region. The base of cone formed in same as the desired profile. And the height of component is same as the desired one. In this experiment the POP model of component at the end of program is also casted to see profile at the end of spiral path following process. At the minor base, the

spring-back is very less and in case of wall the deviation in walls from the desired one profile is of 1.1734 mm at right hand side and at left hand side of the plot the deviation is of 1.6357 mm. Then after declamping the plate from the flanges, it can notice that there is less amount of distortion at the minor base. At the walls due to bending along one edge the deviation is 1.1734 mm on right hand side of walls and of 0.4915 mm on left hand side. While measuring the casted POP model it shows the spring-back of 0.425 mm at base and 1.7028 mm in the walls.

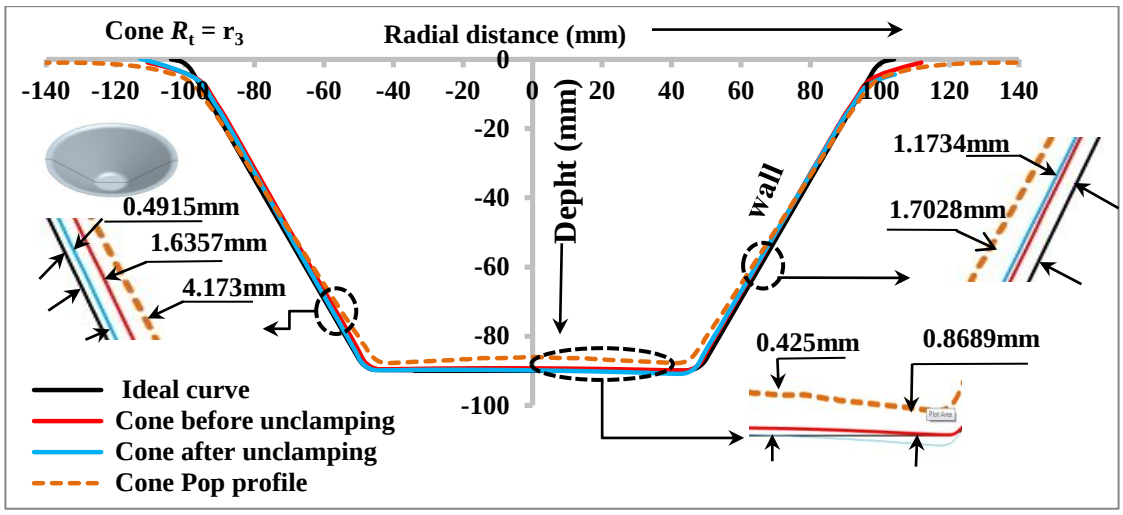

Fig. 4.7 Plot of cone with Δ_z = 0.5 mm and R_t = r_3=6.349 mm

It can be noticed from the 2nd, 4th and 5th experiment that as we increase the tool radius, the spring-back in the sheet decreases resulting in achieving the accurate shape. When the tool is in touch at base the profile at that time also started matching with the desired as we increased the radius of tool

After performing all the experiments for the cone shaped component. The same type of research analyses are performed for the funnel shaped component. Funnel shaped component has continuous varying wall angle i.e. the wall angle at the major base is selected (α_{min}) as 5° and at the minor base (α_{max}) it is selected as 60°. In between the major and the minor base the slope of wall is continuously varying from 5° to 60° after following each contour of spiral path.

4.2.6 Funnel with $\Delta_z = z_1$, $R_t = r_1$

While performing the series of experiments to study the accuracy of components made by SPIF on CNC milling machine the funnel shaped component also made. To study the effect

of change in incremental depth (tool pitch) upon component profile, the parametric variation done according to Table 4.3.

Table 4.3 Parameter variation to study effect of Δ_z variation on funnel

Exp no.	Tool diameter R_t (mm)	Tool pitch Δ_z (mm)
6	4.125	0.25
7	4.125	0.5
8	4.125	0.75

The input parameters for making first funnel are selected as opening radius (R) =100 mm, minimum wall angle (α_{min}) = 5°, maximum wall angle (α_{max}) = 60°, radius of lower fillet (R_{lf}) =7 mm, incremental depth (Δ_z) = 0.25 mm, tool radius (R_t) = 4.125 mm. In case of funnel the height of component is not considered as input. Height of funnel depends upon the maximum wall angle and the opening radius of the funnel.

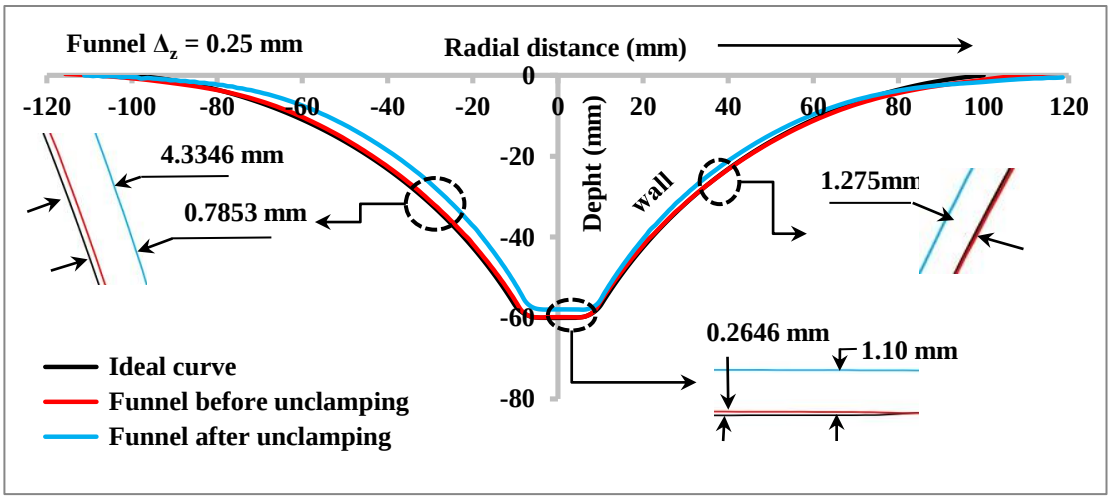

Fig. 4.8 Plot of funnel with Δz = 0.25 mm and R_t = r_1= 4.125 mm

In this series of experiments for funnel shaped component the effect of change in incremental depth and the change in radius of tool on the component profile is studied the results from the CMM is concluded in the form of plots. In Fig. 4.8 of funnel it is clearly noticeable the spring-back at bottom of after making the component in clamped position is equal to the 0.2646 mm. The wall deviation from the desired one profile is not actually visible i.e. profile at walls is overlapping with desired profile. After unclamping the funnel formed blank from the flanges spring-back in the component highly noticeable. The error at

the base profile increased from 0.2646 mm to 1.1012 mm. The walls also got deviated from the actually formed position on right hand section the error of 1.2753 mm and in the left hand side this error in the profile is 4.3346 mm.

4.2.7 Funnel with $\Delta_z = z_2$, $R_t = r_1$

Next sheet is made with increased incremental depth changed from the 0.025 mm to 0.5 mm. This experiment is able to predict the results for effect of increased Δ_z (pitch) on funnel shape. The process making funnel is same as cone. The plot generated after doing the reverse engineering of the components on CMM is shown in Fig. 4.9. With the help of this experiment we are clearing our two objectives about the results. First, Effect of change in incremental depth is noticed and second, what were the shape errors at the end of program?

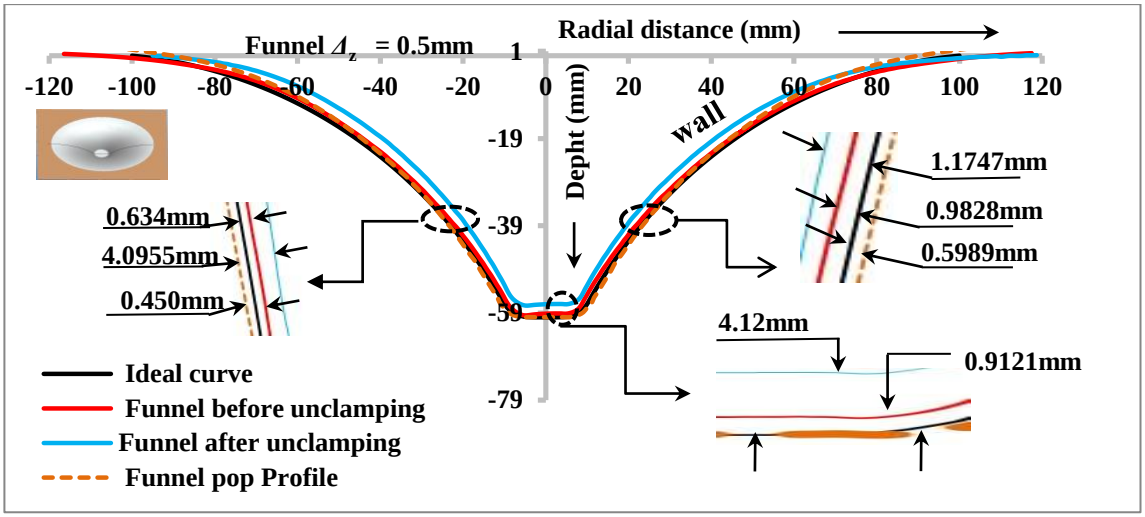

Fig. 4.9 Plot of funnel with Δ_z = 0.5 mm and $R_t = r_1$= 4.125 mm

As clear from the Fig 4.9, the distortion error at the base of component after the making of the funnel when tool is not in contact with base is measure as 0.9121 mm from the target profile. In walls the error that can be seen at some points of the profile 0.9828 mm on the right hand side walls and of 0.634 mm on the left hand side of walls. When the blank is unclamped from the flanges then the distortion occurred in the sheet due to the presences of residual stresses and strain hardening. The deviation at the base from the current (ideal) profile after unclamping is 4.12 mm. The spring-back at the walls can be seen to greater extent. The wall shifting from the ideal profile and creating the error of 1.1747 mm at the right side of funnel and 4.0955 at the left side of walls. In this test it becomes possible to measure the profile at the end of program. To see that the how profile at the end of program,

when tool is in contact with the base got distorted when the tool contact breaks. The shape of funnel at the end of program is casted in the POP as shown in Fig. 4.10. Then this casted piece is measured on CMM by doing the reverse engineering of the component. The deviation in wall at unclamped position from clamped position is of magnitude 1.084 mm.

(a) (b) (c) (d)

Fig. 4.10 (a) Casting of funnel on POP, (b) casted shape of funnel, (c) CMM measuring of casted shape and (d) funnel in unclamped position

It can be concluded from 1st and 2nd experiment that, with the increasing in pitch of tool the spring-back got increased accuracy got disturbed more. The errors in the profile of formed components with respect to ideal component are increased.

4.2.8 Funnel with $\Delta_z = z_3$, $R_t = r_1$

To compare the result for changing the pitch of tool, in this experiment the pitch of tool is varied to its third value. During this experiment the pitch of tool is increased from 0.5 mm to 0.75 mm. The plot obtained after making and measuring the component with Δ_z = 0.75 mm is shown in Fig. 4.11 which describes the results about the question of goals. From the Fig. 4.11 it is clearly visible that, after making the component when it is measured on CMM in clamped position the noticeable error at the base is 0.2 mm.

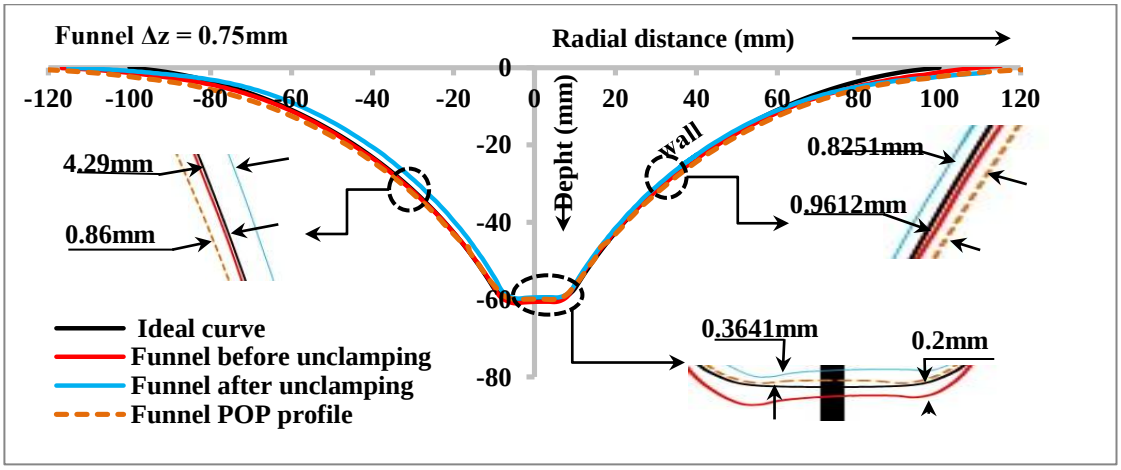

Fig. 4.11 Plot of funnel with Δ_z = 0.75 mm and $R_t = r_1$= 4.125 mm

On the other hand, at the walls the error of the magnitude is not noticeable as shape is perfectly overlapping with the desired. After unclamping the sheet from the flange sprig back occur in the component 0.3641 mm at the base and 4.29 mm at walls. This error at the walls is more than that of previous results for Δ_z = 0.5 mm. For the profile (the shape casted on POP) at the end of program it can be noticed that the base is exactly same as desired. But the wall deviated from the ideal by 0.9612 mm. The deviation of shape at the unclamped position from the profile at clamped position is of magnitude of 5.151 mm.

It can be concluded from Fig. 4.11 that as the pitch of tool is increased the spring-back in the walls also gets increased and the distortion occurred is more as compare to previous case. The increasing in pitch is distorting the component with the reason of more development of residual stresses in the sheet.

4.2.9 Funnel with $\Delta_z = z_2$, $R_t = r_2$

The variation in tool radius is also studied on the funnel shaped component bye varying the radius in three steps. Now for this experiment the tool radius is changed from the 4.125 mm to 5.329 mm. Rest all other parameters are kept constant as it in previous shaped funnel. The incremental depth chosen for varying the radius change is selected as 0.5 for all three stages of radius variation according to following Table 4.4. In this experiment, after making (forming) the funnel shape component then after measuring the profile on CMM the plot generated is shown in Fig. 4.12. After the end of program when the contact between the tool and workpiece breaks then the spring-back at the base of funnel is measured as 0.09 mm which show that base is overlapping with desired shape.

Table 4.4 Parameter variation to study effect of R_t variation on funnel

Exp no.	Tool radius R_t (mm)	Tool pitch Δ_z (mm)
7	4.125	0.5
9	5.329	0.5
10	6.349	0.5

The profile error in the walls is as 1.159 mm on the right side walls. In this experiment, the second motive to know the shape at the end of program also studied. After unclamping the component the distorted shape is measure with the help of CMM explains that the spring-back in the bottom is measure as 1.9364 mm and at the walls is 4.5273 mm on right hand side

of walls and 1.698 on the left hand side of funnel walls upon unclamping the funnel from the flanges. The POP casted model measured and defined that base is exactly same at end of program and the wall deviation of 1.52 mm is noticed.

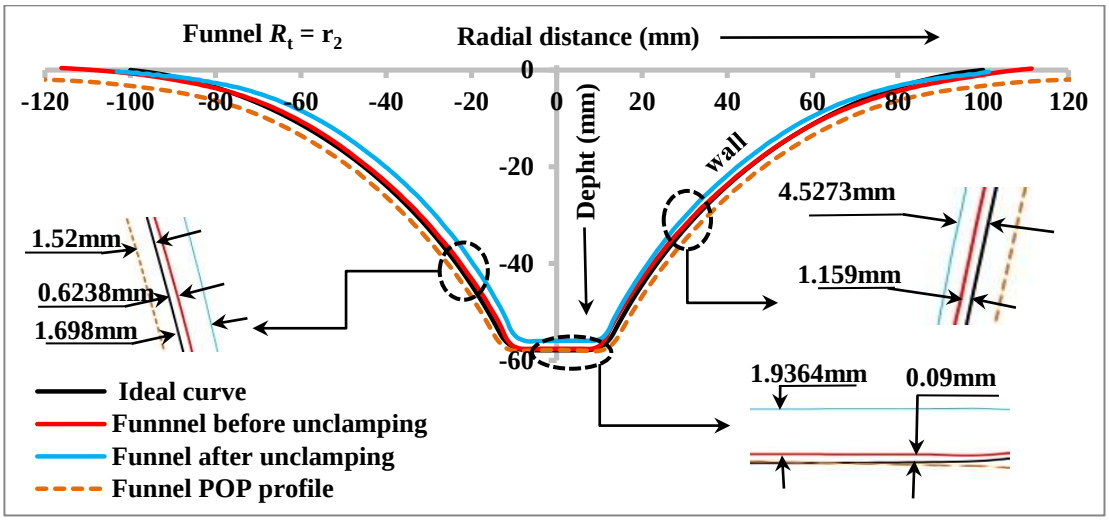

Fig. 4.12 Plot of funnel with Δ_z = 0.5 mm and $R_t = r_2$ = 5.329 mm

4.2.10 Funnel with $\Delta_z = z_2$, $R_t = r_3$

For last stage the variation of radius of tool, the radius of tool selected is 6.349 mm. After this experiment, results can be concluded for the analyzing the effect of change in radius of tool on the final accuracy of component made by SPIF. The plot generated for the comparison of profile after making and measuring of component is given in Fig. 4.13. From Fig. 4.13 it is very much clear that the profile at the end of experiment when tool is not in touch with the base, the profile is exactly desired one. The height of component achieved is same as the ideal desired height of component. The wall profile at this point is also overlapping with the desired profile. Accuracy of component got increased when the component is in clamped position. The shape of profile at the end of program also measured with the help of POP model. POP model is showing that the wall profile is exactly same as the desired at the end of the program. The base error in POP model is noticed as 0.8879 mm. After the measuring of component in clamped position, when the component is unclamped from the flanges the spring-back due to residual stress is noticed. At the base the error in the profile notices is 2.0773 mm, and the deviation occurred in the walls were of magnitude 4.46 mm.

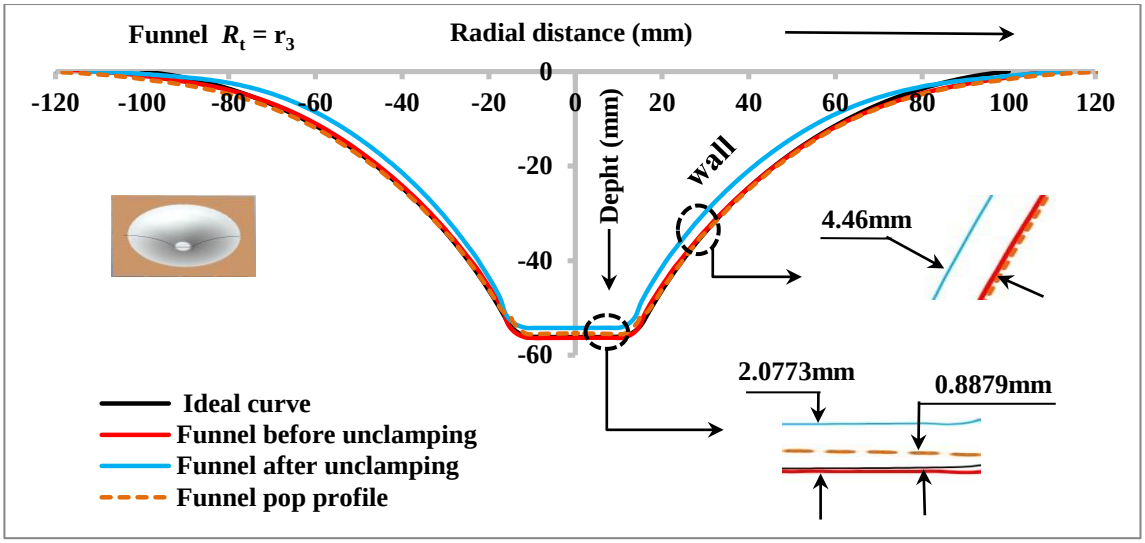

Fig. 4.13 Plot of funnel with Δ_z = 0.5 mm and $R_t = r_3$ = 6.349 mm

It can be concluded from 7th, 9th, 10th experiment that with increasing the tool radius, the friction between the workpiece and the tool increases that is affecting the accuracy. Upon increasing the tool radius the spring-back at the base decreases and in the walls it increases due to hardening of component.

4.3 Experiments to study multiple feature on single sheet

The study of change in increment depth and the change in radius of tool for funnel and Cone shaped profile showing same results. Now, the study of multiple components on single sheet is done. The motive of this study is to analyze, the effect of newly made component on the previously already made other components that, how the profile of already formed component is affected by making of new component on same sheet. This study has one more advantage on the large scale production. As ISF is slow process and currently used for only small scale production. Forming of multiple components on single sheet makes the process faster to make the ISF feasible for large scale production. Indirectly making of multiple components on single sheet reduces the setup time. The setup time is the time taken while changing the sheet for making of next component to make same type of component on small sheet again and again. In this experiment bigger sheet is chosen to make multiple components on single sheet which are having same or somehow different profile also. While making the multiple components, the effect of change in radius of tool and change in incremental depth is not studied. In this series of experimentation, only the effect of making same type of shape

parallel to other same type of shape is studied and making of different shape on single sheet is studied.

4.3.1 Four cones at four corners of sheet

In this series of making multiple components on single sheet cone is chosen to form four times at four different locations on sheet. The input parameters chosen for making the same dimensioned cone were as opening radius(R) = 45 mm, wall angle (α) = 50°, height of component (H) = 40 mm, radius of upper fillet (R_{uf}) = 7 mm, radius of lower fillet (R_{lf}) = 7 mm, radial increment (Δ_r) = 0.3 mm, incremental depth (Δ_z) = 0.5 mm, tool radius (R_t) = 4.125 mm. The pattern of making the cones on sheet is as cone 1→ cone 2→ cone 3→ cone 4. The cone 1 is formed and measured on CMM, then cone 2 formed and measuring of cone 1 and cone 2 is done to analyze the effect that how the previously made and measure profile of cone 1 is varying by the making of cone 4. Then after, cone 3 is formed and measuring of clamped sheet is again done for cone 1 , cone 2 , cone 3 , in the measurement it is seen that how the making of cone 3 is effecting the previously made cone 1 and cone 4. Then at last, the cone 4 is formed and measurement of the all the cones is performed. In this measurement it is noticed that, how the making of cone 4 is affecting the profile of cone 1, cone 2 and cone 4. After making and measuring of all the cones the sheet is then unclamped from the clamped fixture. After unclamping the sheet it is seen that whole sheet got distorted due to residual stresses in the sheet. The unclamped sheet is measured again for all cones. All the cones are measured in unclamped position of sheet. In this series of making and measuring of cones, the cone 1 is measured for 5 times, the cone 2 is measured for four times, cone 3 for three times , cone four for 2 times. After measuring all the cones in clamped and unclamped position the profile of these cones is compared with the actual desired or ideal profile in the form of plots and discussion is done on this plot to obtain the results.

For cone 1, the plot generated after doing all the measurements of cone 1 is as shown in Fig. 4.14. The sheet for making four cones divided in four parts. The cone 1 is formed at the lower left corner in the sheet. The black color continuous line [——] represents ideal profile. The blue dotted line [— —] represents cone 1 profile when no other cone is formed on sheet only single cone is present on sheet. The red color dotted line [— —] represents the cone 1 profile after making cone 4. The blue color continuous line [——] denotes the cone 1 profile after making cone 3. The line in green color dotted [— —] represents the profile of cone 1

after making cone 4. The sky blue color continuous line [——] represents the profile of cone 1 after it is unclamped.

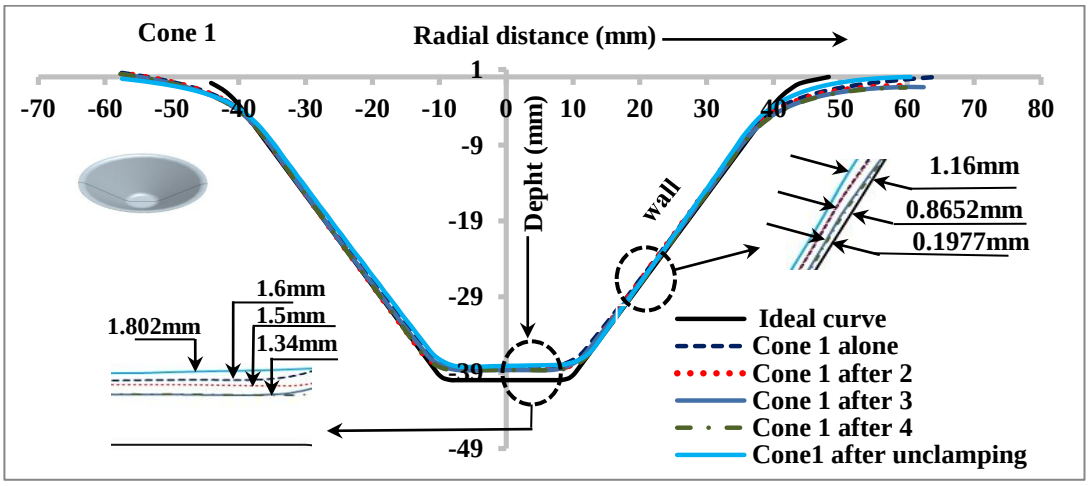

Fig. 4.14 Deviation of cone 1 in clamped and unclamped position

When the cone 1 is measure first time along x-axis after making and comparing with ideal it is noticed that the spring-back (Error between ideal and actual profile) at the base is equal to the 1.6 mm and the walls deviated from ideal by 0.8652 mm towards the center on cone. After making cone 2 then cone 1 is again measured and plots after the measurement explains that spring-back at the base reduced to 1.5 mm and at the wall spring-back remained same. After making cone 3 the spring at bottom of cone 1.34 mm and at the walls it become 0.1977 mm. Accuracy of cone is increasing. At last point after making the cone 4 the spring-back at the bottom remained same of 1.34 mm the wall error is same ass of 0.1977 mm. After making all measurement in clamped position when the cone one is unclamped the spring-back occurred due to the residual stress greatly affected the part accuracy. The spring-back at bottom changed from 1.34 to 1.78 mm and the wall deviation changed from the 0.1977 mm to 1.16 mm.

For cone 2, the error measured and plotted as CMM output after measuring the cone in clamped and unclamped position as shown in plot given in Fig. 4.15. The line representation will remain same as in case of cone 1 plot. This cone is measure for four times. The cone 2 is formed at the lower right corner of the sheet. The plot of cone 2 clearly displaying that the when the cone 2 is formed first time and measured for just after forming the spring-back at the base is noticed 1.278 mm and at the wall the spring-back is noticed as 0.3407 mm.

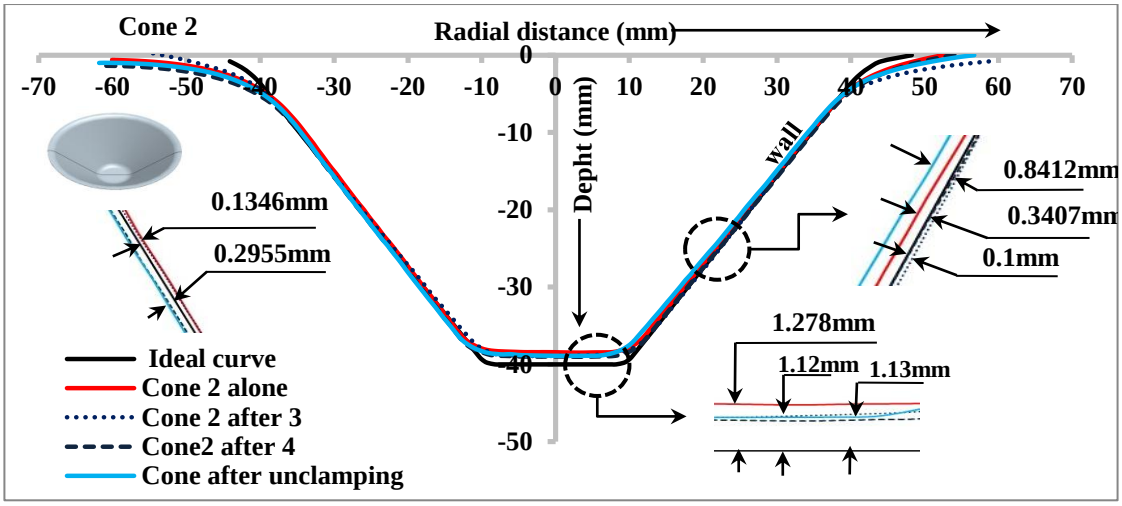

Fig. 4.15 Deviation of cone 2 in clamped and unclamped position

After making cone 3 and cone 4 the spring-back at the bottom remained same of 1.12 mm at the walls it is perfectly matching with desired profile. After unclamping the sheet from the fixture distortion occurred at the base and walls were 1.12 mm at the base and 0.8412 mm at the walls. Final height achieved is 38.87 mm the difference in spring-back at the bottom is reducing just because of bending of sheet due to continuous action of cyclic load to make part. While increasing the number of component on sheet the wall is bending toward the ideal desired profile due to the bending of sheet and as we unclamped the part from the flange the wall error again occur.

For cone 3, the inaccuracies occurred in the profile of cone 3 after making of cone 4 are shown in Fig. 4.16. The cone 3 is measure thrice to obtain results. The spring-back occurs in this cone at the bottom after the making of cone 3 is of magnitude 0.8342 mm and at the wall the error in profile is 0.13 mm. After unclamping the plate (blank) from the flanges the error in height at the base is noticed as 1.3951 mm on the other hand in the walls the wall error is of magnitude 1.20 mm. The error at the walls from clamped position to unclamped position is of magnitude 1.3087 mm. Again this plot justify that the accuracy is improving while making parts in sheet due to bending of sheet but total height of obtained after making component remaining approximately same. The cone 3 is formed at the upper left corner of the sheet

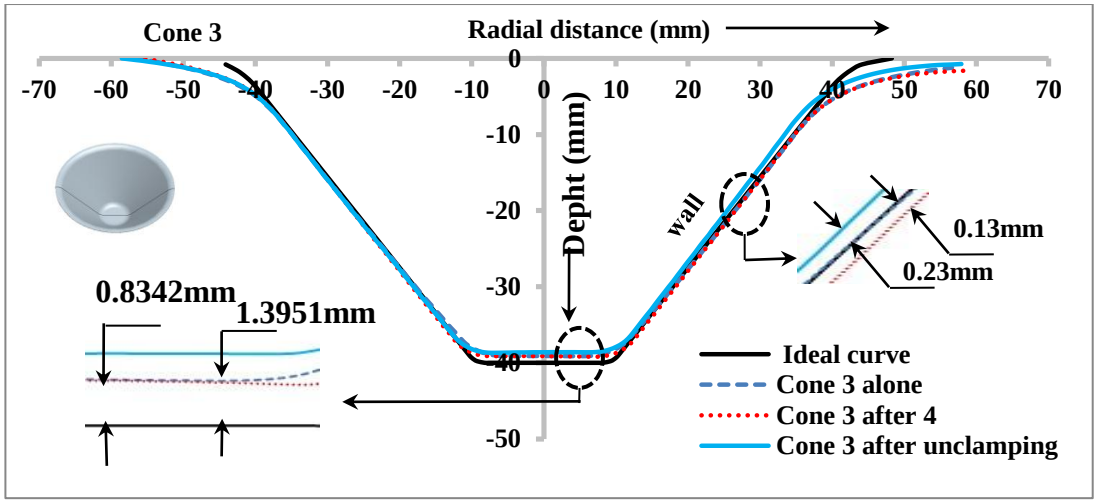

Fig. 4.16 Deviation of cone 3 in clamped and unclamped position

The cone 4 is formed at upper right corner of the sheet. The plot generated to measure the inaccuracy in the profile of cone 4 is shown in Fig. 4.17. This Cone is measured only for two times. One after making the cone in clamped position and second is in unclamped position just after making of part. From the plot above it is clearly visible that after making the Cone four alone. The spring-back at the base of magnitude 1.026 mm and the wall is perfectly overlapping with the desired one profile. When the plate got unclamped the profile at the bottom remained same with the error of 0.5907 mm on the same wall error can be 0.6058 mm.

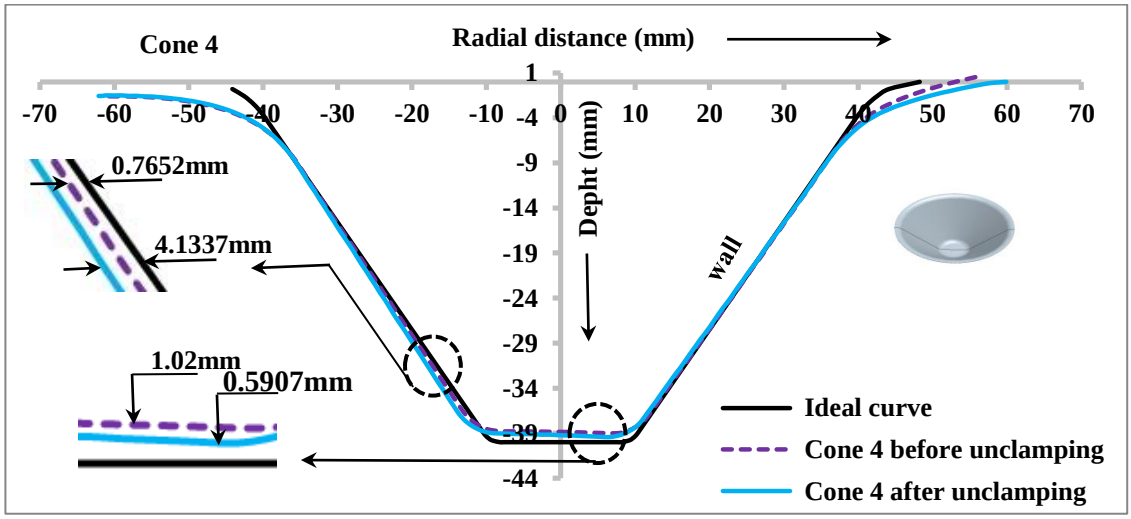

Fig. 4.17 Deviation of cone 4 in clamped and unclamped position

After making all the cones, the sheet in clamped and in unclamped condition is shown in Fig. 4.18.

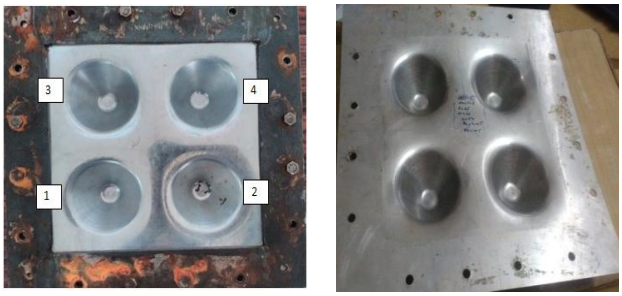

(a) (b)

Fig. 4.18 View of formed sheet (a) clamped position and (b) unclamped position

It can be concluded from the 1st, 2nd, 3rd, 4th cone that in clamped position as the no. of component on single sheet the accuracy of component is also increasing. Spring-back got decreases as the number of component got increased. Because of the strain hardening of sheet got increased. As the no of component is increased the wall accuracy is increasing because of bending of sheet is taking place. But in unclamped position spring-back of sheet is increasing due to the symmetric loading of sheet which creates distributed residual stresses in the sheet. Bending of sheet occurs at the top position of sheet.

4.3.2 Two cups and two funnel on diagonals of sheet

After analyzing the effect of making multiple component of same profile on the single sheet, now the study of making two different type of component on single sheet can be done. In this experiment funnel and Cone shaped component is made on single sheet. There are 2 Cones and two funnels on the sheet. The inputs parameters for the cone is as opening radius (R) =45 mm, wall angle (α) = 50°, height of component (H) = 40 mm, radius of upper fillet (R_{uf}) = 7 mm, radius of lower fillet (R_{lf}) = 7 mm, radial increment (Δ_r) = 0.3 mm, incremental depth (Δ_z) = 0.5 mm, tool radius (R_t) = 4.125 mm. Both the cones are having same input profile. On the other hand, the input parameters for two funnel shaped component is as opening radius (R)= 55 mm, minimum wall angle (α_{min}) = 5°, maximum wall angle (α_{max}) = 60°, radius of lower fillet (R_{lf})=7 mm, incremental depth (Δ_z)= 0.3 mm, tool radius (R_t) = 4.125 mm. In case of funnel, the height of funnel is not considered as input. Height of funnel depends upon the maximum wall angle and the opening radius of the funnel.

The pattern of making the funnel and cones on sheet is as funnel 1→ cone 1→ cone 2→ funnel 4. The funnel 1 is formed and measured on CMM, then cone 1 formed and measuring

of funnel 1 and cone 1 is done to analyze the effect that how the profile of funnel 1 is varying by the making of cone 1. Then after, cone 2 is formed and measuring of clamped sheet is again done for funnel 1 , cone 1 , cone 2 , in this measurement it is seen that how the making of cone 2 is effecting the previously made funnel 1 and cone 1. Then at last, the funnel 2 is formed and measurement of the all the components are performed. In this measurement it is noticed that how the making of funnel 2 is affecting the profile of funnel 1, cone 1, and cone 4. After making and measuring of both cones and funnels the sheet is then unclamped from the clamped fixture and again measure to compare accuracy in unclamped state.

For funnel 1: The plot generated for funnel 1 after making and measuring and unclamping to compare the accuracy of funnel after the making of other component is shown in Fig. 4.19. The funnel 1 is measured for 5 times to compare the overall accuracy of funnel at each stage. After making the funnel 1 on the lower left corner of the sheet then it is measured for first time on CMM in clamped position. The spring-back at base of cone is measure as 1.58 mm and the walls deviated from the desired profile is its 1.7581 mm. After making the cone 1 the profile spring-back at the base is 1.4325 mm and at the walls it is same as previous deviated from desired. Then when the cone 2 and funnel 2 got formed the spring-back the base remained same of 1.393 mm from ideal one.

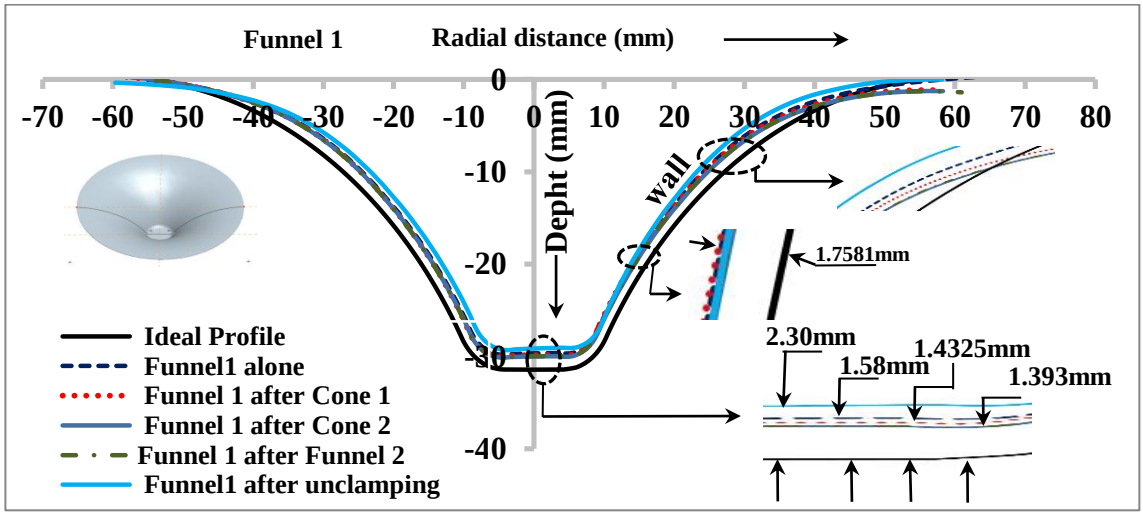

Fig. 4.19 Deviation of funnel 1 in clamped and unclamped position

The profile of wall near the major base in lowering down after each component got formed due to bending of sheet. After that sheet is when unclamped and measured, the plot at the unclamped position defines the spring-back at the base of magnitude 4.30 mm. The error at the walls of funnel shaped component is approximating same as previous one.

For cone 1: To study the effect of shape next cone 1 is formed at the lower right corner. This Cone is measured for four times. The plot generated after forming the cone and making all measurements as shown in Fig. 4.20. The plot of cone 1 is clearly outlining that the when the cone 1 is formed first time and measured for just after forming. The spring-back at the base is noticed 1.3505 mm and at the wall the spring-back is noticed as 0.7658 mm. After making Cone 2 and funnel 2 the spring-back at the bottom 1.3435 mm at the walls it is 0.8065 mm from desired profile. After unclamping the sheet from the fixture the distortion occurred at the base and walls is 0.8665 mm at the walls and 1.6211 mm at the base.

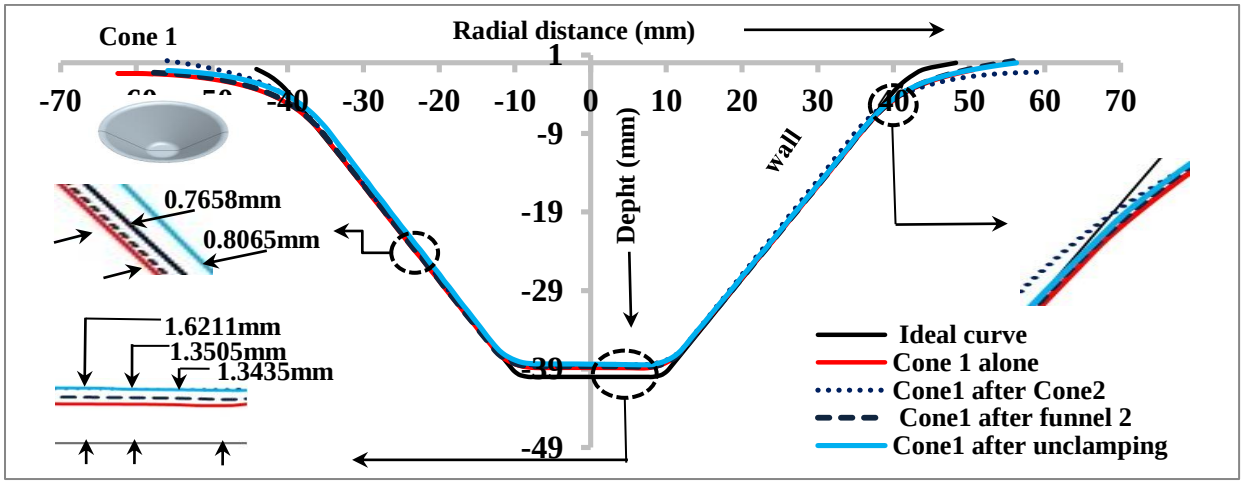

Fig. 4.20 Deviation of cone 1 in clamped and unclamped position

For cone 2: The cone 2 is formed on the upper left of the sheet to study one other variation effect. The plot of points measured by CMM for its three time measurement of cone is given below in Fig. 4.21. In this plot of cone 2 the error generated in profile of Cone 2 after making and measuring states that the spring-back at the base (minor base) of 1.6986 mm an in the walls the error is 0.1643 mm. After the funnel 2 on upper right corner the deviation in the profile of cone 2 is spring-back got reduced to 0.9076 mm. The wall profile is perfectly overlapping with the desired profile. When the sheet is unclamped the error in profile due to residual stresses becomes 0.5011 mm and wall deviated from the desired path by amount of 0.1022 mm.

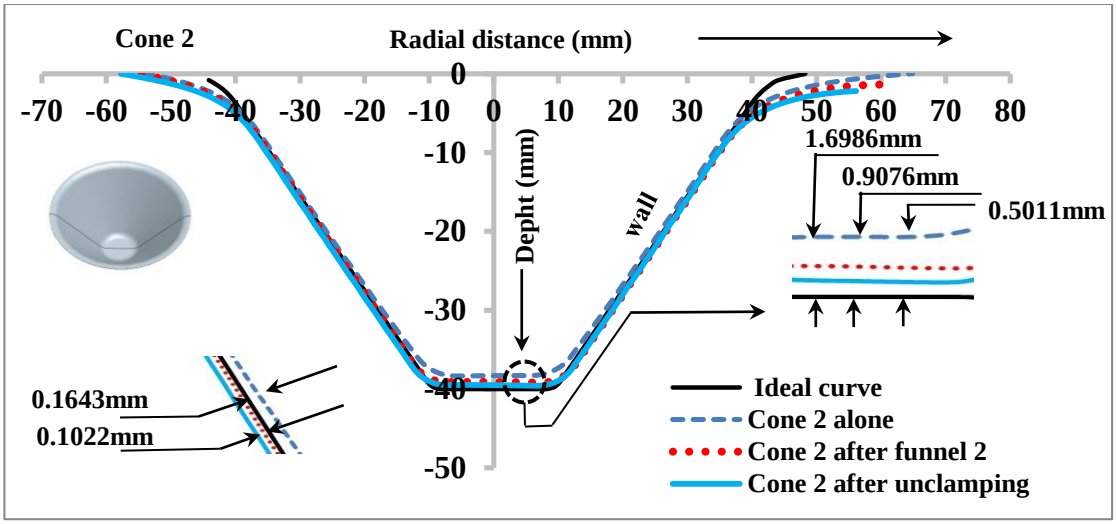

Fig. 4.21 Deviation of cone 2 in clamped and unclamped position

For funnel 2: After making one funnel and two Cones on the same sheet, the funnel 2 is formed at the upper right corner of sheet. CMM output from funnel two is plotted as shown in Fig. 4.22. The funnel 2 after it is made showing the spring-back of 1.196 mm at the base and of 1.277 mm at the walls. After measuring in clamped position then the sheet is unclamped the profile in unclamped position says that the spring-back at base remained same of 1.96 mm and of 1.931 mm at walls on left hand side of cone.

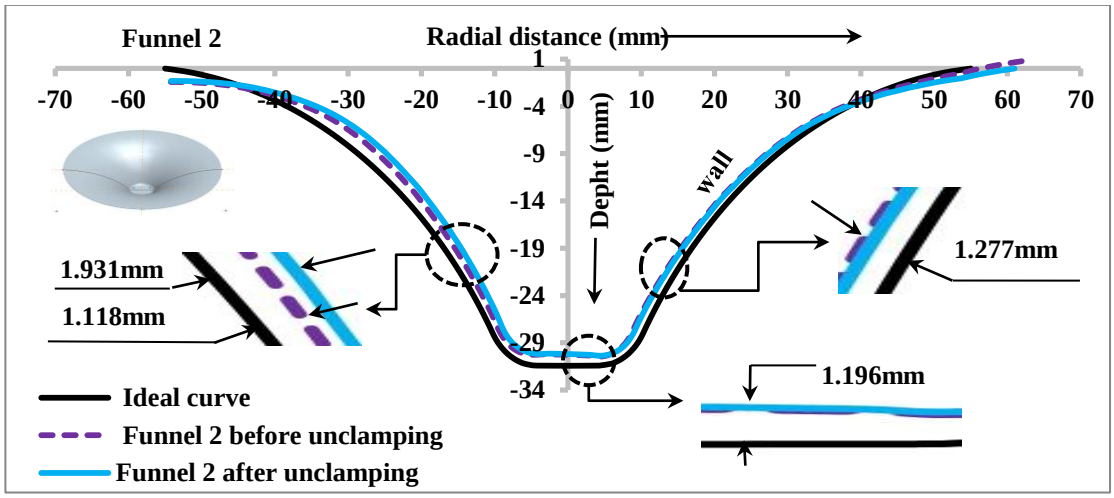

Fig. 4.22 Deviation of funnel 2 in clamped and unclamped position

It can be concluded from 1st, 2nd, 3rd and 4th plots that, accuracy is improving ass no of component increase. Spring-back in sheet got decreased. The bending of sheet takes place at

the top. Spring-back in unclamped position is more than that of clamped position. Profile got distorted on unclamping the part. The sheet upon unclamping is shown in Fig. 4.23.

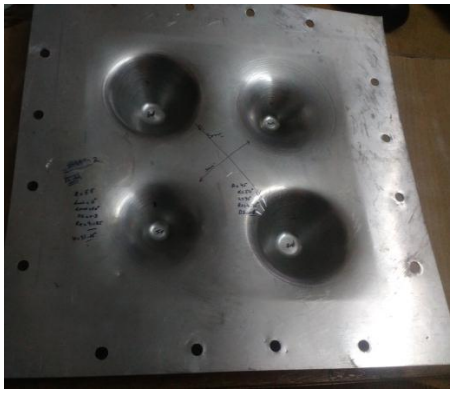

Fig. 4.23 View of sheet upon unclamping the sheet from the flanges

4.3.3 One cone and one funnel on diagonal

After comparing the effect of making components at four corners of sheet now the components only made at the diagonal of the sheet. In this experiment one funnel shaped and one small cone shaped component made. In this experiment shape of profile at the end of program also studied. On lower left diagonal funnel is formed. Upper right diagonal the cone is formed as shown in Fig. 4.24.

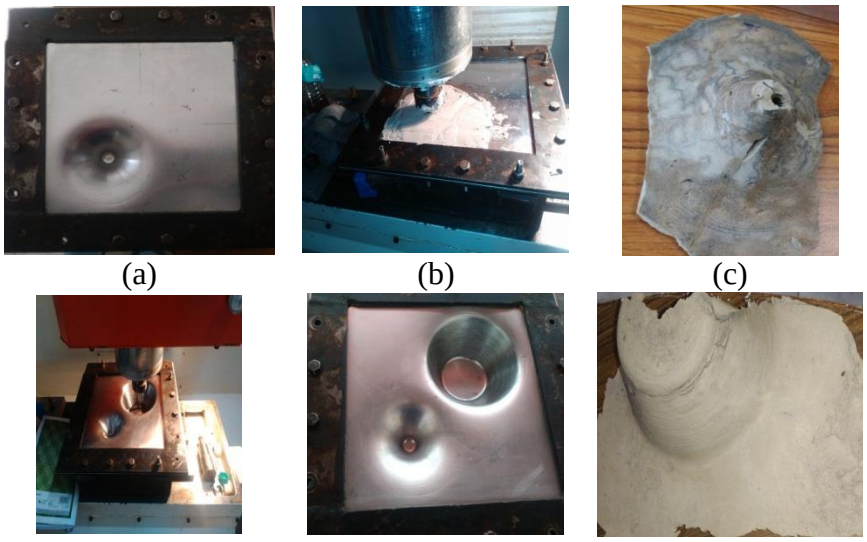

(a) (b) (c)

(d) (e) (f)

Fig. 4.24 Process chain for making whole sheet (a) sheet after forming funnel, (b) POP casting of funnel, (c) casted POP for measuring, (d) forming of cone, (e) sheet after forming cone and (f) POP casting of cone

The inputs parameters for the cone is as opening radius (R) = 65 mm, wall angle (α) = 60°, height of component (H) = 55 mm, radius of upper fillet (R_{uf}) = 7 mm, radius of lower fillet (R_{lf}) = 7 mm, radial increment (Δ_r) = 0.3 mm, incremental depth (Δ_z) = 0.5 mm, tool

radius (R_t) = 4.125 mm. On the other hand, the input parameters for funnel shaped component is as opening radius (R) = 65 mm, minimum wall angle (α_{min}) = 5°, maximum wall angle (α_{max}) = 60°, radius of lower fillet (R_{lf}) = 7 mm, incremental depth (Δ_z) = 0.3 mm, tool radius (R_t) = 4.125 mm. In case of funnel the height of funnel is not considered as input because height of funnel depends upon the maximum wall angle and the opening radius of the funnel. The process chain of making both the components on single sheet is shown in Fig. 4.22. After making the funnel 1, it is measured on CMM and the plot generated after measuring funnel is shown in Fig. 4.25.

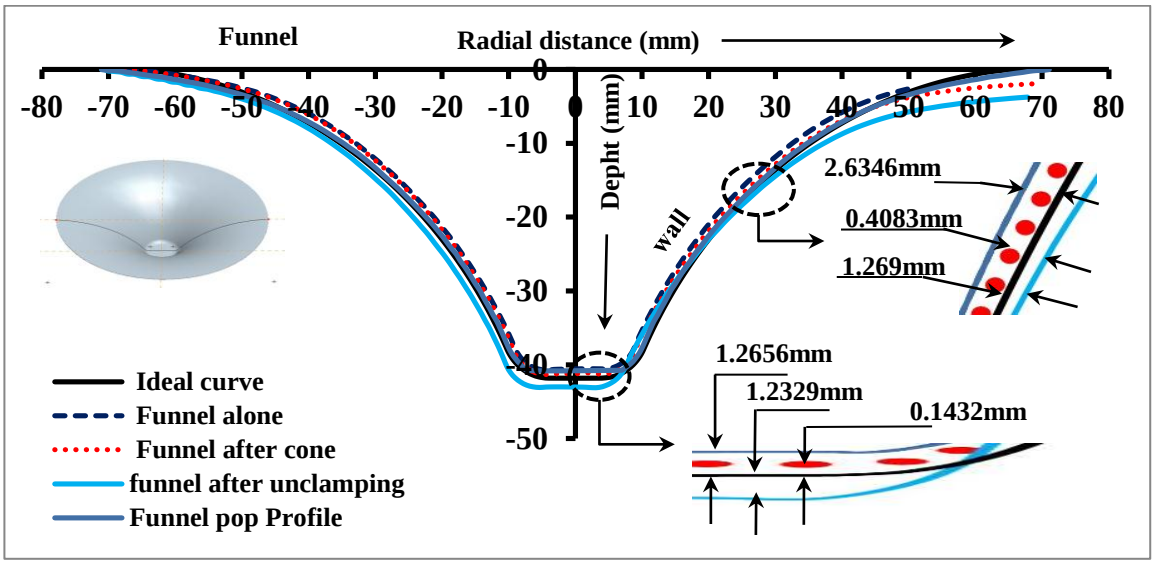

Fig. 4.25 Deviation of funnel 1 in clamped and unclamped position

For funnel 1: It is clear from the Fig. 4.25 that the spring-back occurred just after the forming and detaching the tool from the base is of magnitude 1.2656 mm and at walls it becomes 4.6346 mm. After, the making of cone when again the funnel is measured it is noticed that spring-back at base reduced to 0.1432 mm and at walls it reduced to 0.4083 mm. At the time of end of program the profile is exactly matching at base at walls the error of 2.6346 is noticed. After unclamping the sheet there is huge distortion and bending occurred in the sheet. Due to this bending of sheet the spring-back at base become 1.2336 mm the change of shape from last clamped position to unclamped position is 1.3761 mm at the wall error is of magnitude 1.269 mm from the desired position.

For cone 1: After making funnel now the cone is formed a measured in clamped and unclamped position. The plot generated after plotting the points of CMM output is shown in Fig. 4.26. From the plot it is very much clear that the pillow effect formed at the minor base.

Height of the component is continuously varying from center to edges of the base. Minimum height achieved at peak of pillow. The spring-back at this position is measured as 1.028 mm and at the edges of the minor base the spring-back noticed were as 0.2712 mm. Error at the walls is notice of magnitude 1.0154 mm .The shape of POP model of cone at the end of program is exactly overlapping with the desired shape of Cone.

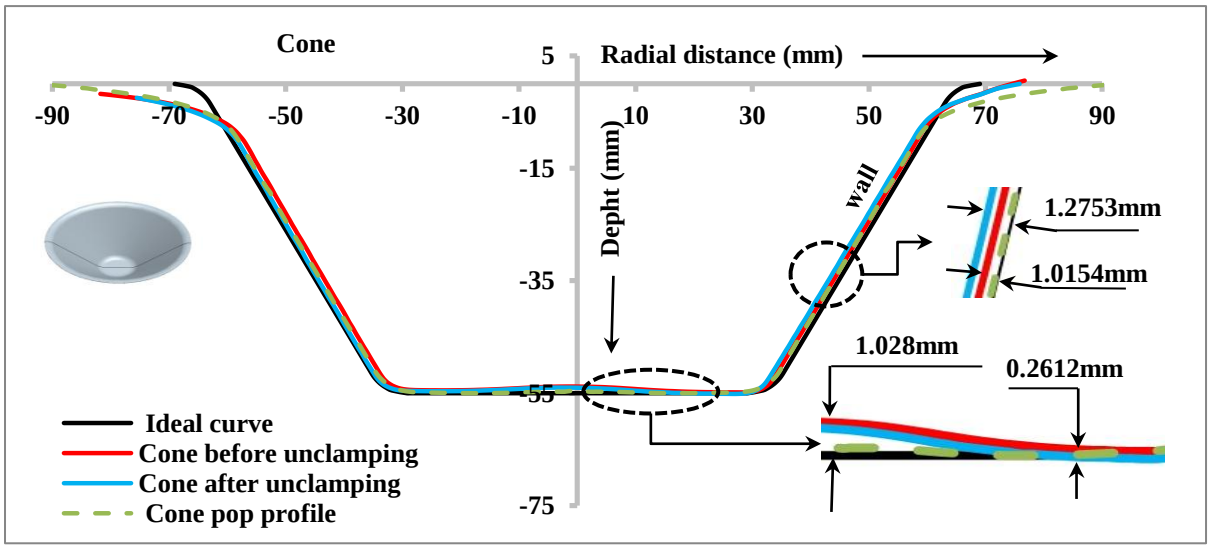

Fig. 4.26 Deviation of cone 1 in clamped and unclamped position

After unclamping the Cone from flanges the shape is slightly distorted. Spring-back at base remained same but at the wall, the spring-back becomes 1.2753 mm. it can be concluded from this experiment that, bending of sheet occurs due to making of other components. And Accuracy got improved. There is a change in the profile as the tool is detached from the base with respect to the profile at the end of program when the tool is in contact with sheet at the end of profile.

4.4 Experiments to study multi stage incremental forming

The multistage incremental forming is done to improve the accuracy of component. The components which have higher wall angle and which are impossible to form in single stage are formed in multistage technique. The forming of component with higher wall angle causes fracture in component by tearing of sheet. Multi stage forming having such an advantage over the single stage forming that, it is able to form the component having the wall angle equal to the 90° which is not possible to form in single stage forming with any type of material. In this present experiment of the multistage forming the thickness variation is the basic concern of study that, how the thickness of component varies at every stage of forming. To study this

analysis the component is formed in four stages to check the thickness variation at different height as shown in Table 4.5

Table 4.5 Different stages during component forming is stopped with thickness variation

Stage of variation	Height at which component forming stopped
1st	03.75 mm
2nd	10.00 mm
3rd	20.00 mm
4th	30.00 mm

In first stage, the component is formed up to only the end of upper fillet. After forming the component, is measure with the help of the CMM. Then another Formed type of component is cone with full depth of 30 mm. The inputs parameters for the cone is as opening radius (R) = 37.5 mm, wall angle (α) = 60°, height of component (H) = 30 mm, radius of upper fillet (R_{uf}) = 7.5 mm, radius of lower fillet (R_{lf}) = 7.5 mm, incremental depth (Δ_z) = 0.5 mm, tool radius (R_t) = 5.329 mm. In this experiment, the workable space of sheet is reduced to 125 mm × 125 mm. The workspace available 240 mm × 240 mm is reduced to 125 mm × 125 mm with the help of two acrylic sheets one above aluminum sheet and one below aluminum sheet as shown in Fig. 4.27.

(a) (b) (c)

Fig. 4.27 (a) Acrylic sheet used for reduction of area, (b) aluminum sheet between two acrylic sheets and (c) setup after fixing acrylic sheet on CNC Table

The measurement up to upper fillet region defines that how the profile error up to upper fillet region is variation with respect to the ideal profile. The plot generated after comparing the profile with ideal profile up to fillet height is shown in Fig. 4.28.

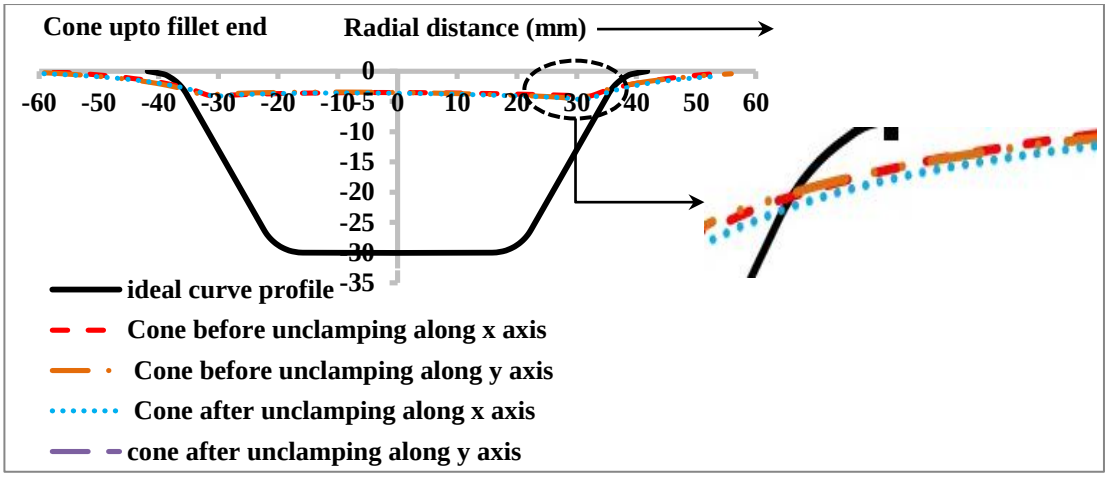

Fig. 4.28 Deviation in the upper fillet region from ideal profile when the component is formed upto only fillet height

From Fig. 4.28 it very much clears that, the error between the ideal and formed curve is caused due to bending of sheet takes places in upper fillet region. The black color line shows the ideal profile [——] and the other lines show the profile of component upto upper fillet region. This component is measured along x and y axes both in clamped and in unclamped position and show the approximately same errors from the ideal profile. The formed component is shown in Fig. 4.29.

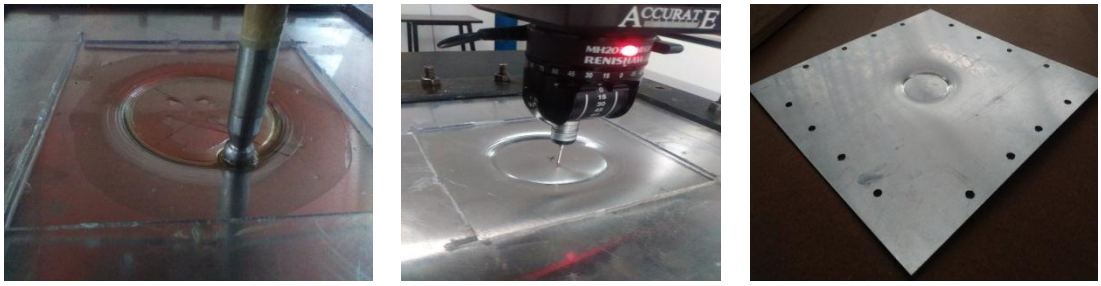

(a) (b) (c)

Fig. 4.29 (a) Forming upto fillet end, (b) measuring in clamped position and (c) sheet after unclamping for first stage

After, measuring the component in clamped and in unclamped position the thickness of unclamped part is measured. The component is cut out in half from its center line with the help of hand cutter. Thickness of sheet is measure with the help of digital vernier calliper having least count of 0.02 mm.

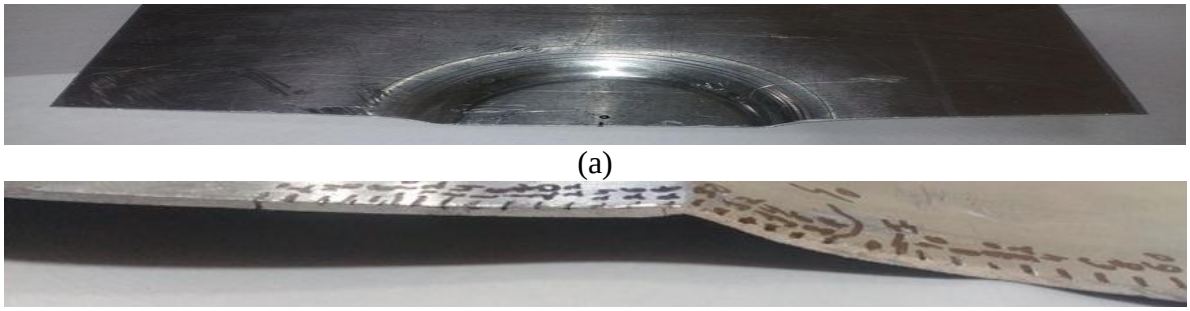

(a)

(b)

Fig. 4.30 (a) Sheet cut from center of component and (b) varying thickness for stage first

*For second stage***,** after measuring the thickness, again component is formed upto the height of 10 mm and thickness measurement is done. All the input parameters remained same for this component. The formed component is shown the Fig. 4.31.

(a) (b) (c)

Fig. 4.31 (a) Forming of component, (b) measuring of component and (c) unclamped view of component for stage second

After, measuring the component in clamped and in unclamped position the plot generated for showing the error near the upper fillet region is shown in the plot as shown in Fig. 4.32. From the Fig. 4.32, it is very much clear that when the component is stopped at height of 10 mm the wall error at that time is equal to the 3.02422 mm. and bending of sheet at upper fillet region is of magnitude 2.045 mm.

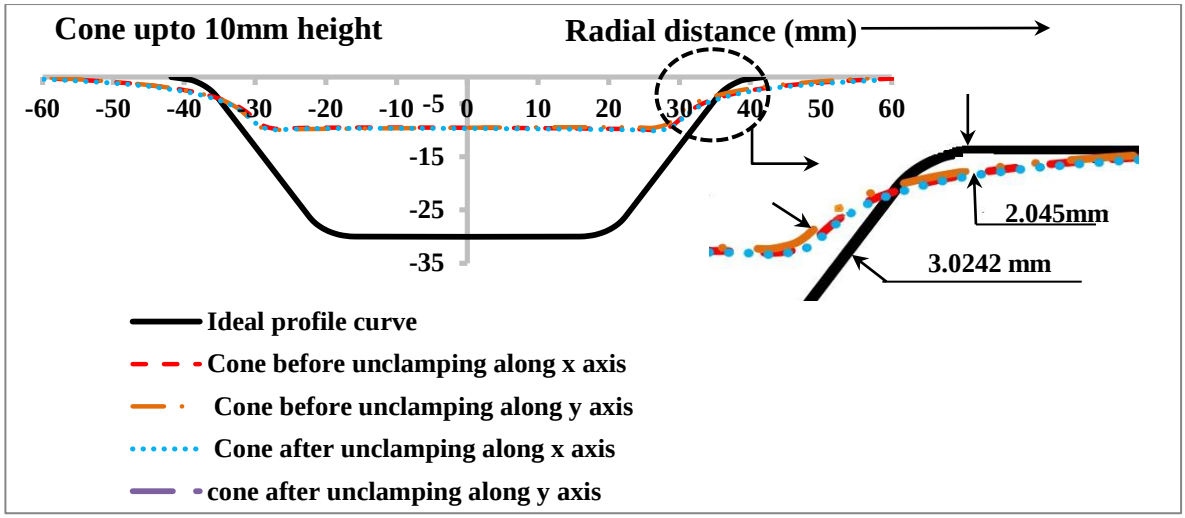

Fig 4.32 Deviation of profile at upper fillet region for component height of 10 mm

After measuring the component in clamped and unclamped position the thickness of component is measured by cutting the component from its half as shown in Fig. 4.33.

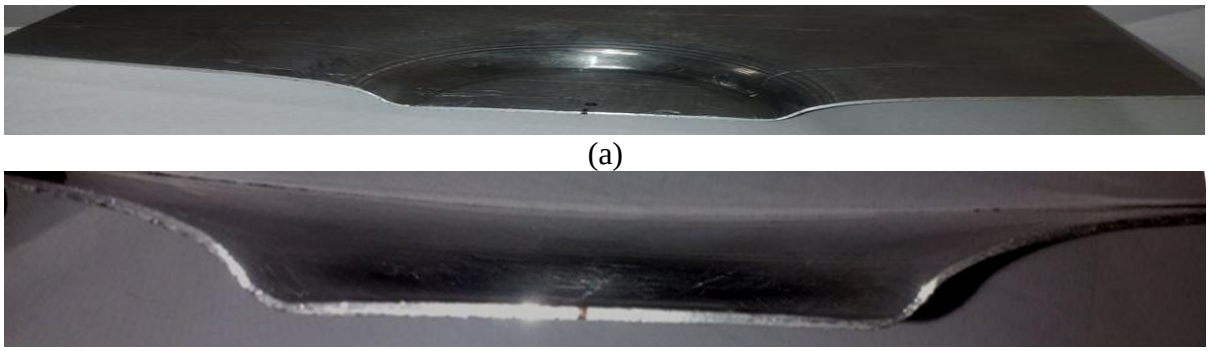

(a)

(b)

Fig. 4.33 (a) Half section view of component and (b) close view showing thickness variation for stage second

For third stage, this time the component is formed upto height if 20 mm and then again measured in clamped and in unclamped position. The plot generated after comparing the profile with the ideal profile is shown in the Fig. 4.34.

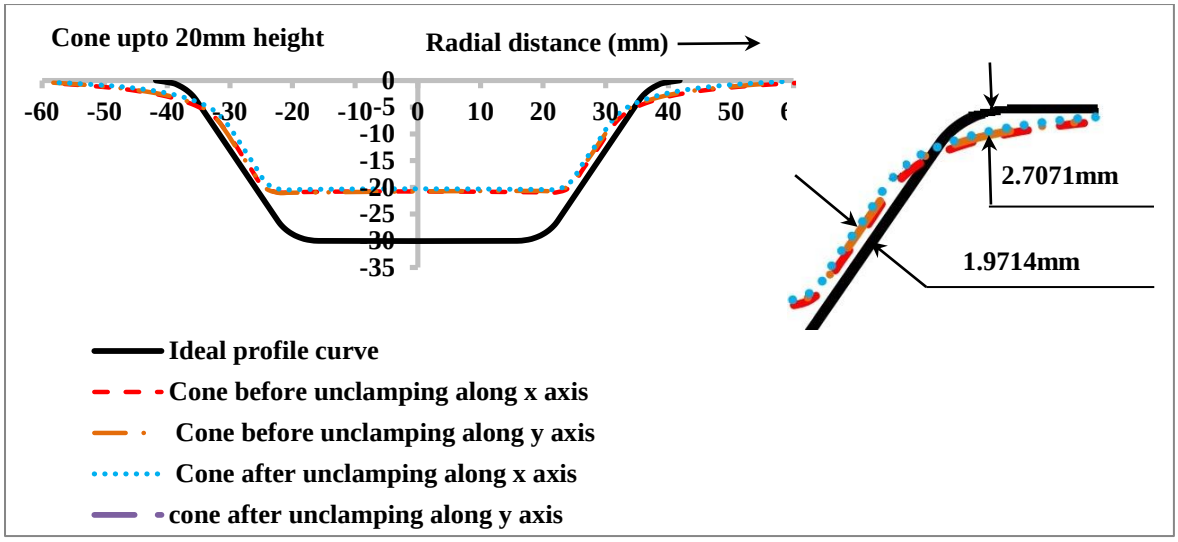

Fig. 4.34 Deviation of profile near upper fillet and walls for third stage of component

The Fig 4.35 is shows that the various step of forming the component upto height of 20 mm. it is very much clear from the Figure that the wall deviation from the ideal profile is 1.9714 mm and the bending of sheet takes place in upper region is of magnitude 2.7071 mm.

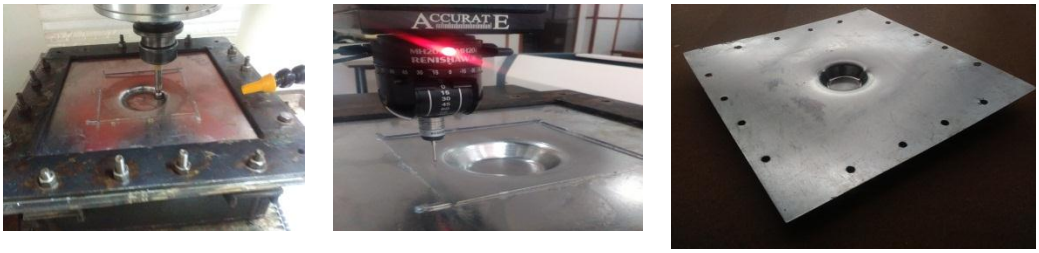

(a) (b) (c)

Fig. 4.35 (a) Forming of component, (b) measuring of component and (c) unclamped view of component at third stage

After the measurement of cone in clamped and in unclamped position, the sheet is cut from half to have thickness measurement. The thickness measure for the height of 20 mm in its third stage is shown in Fig. 4.36.

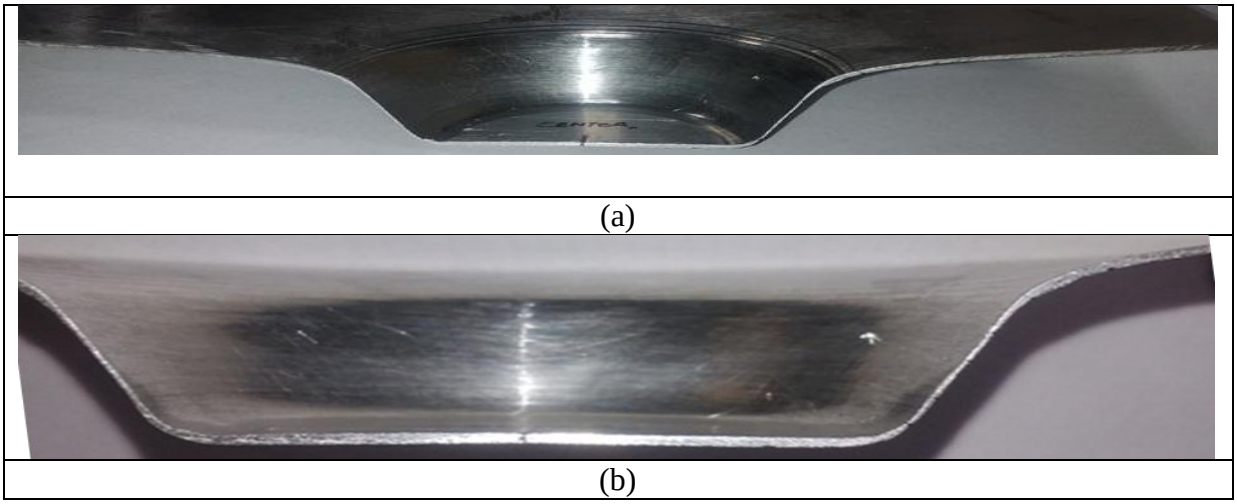

(a)

(b)

Fig. 4.36 (a) Half section view of component and (b) close view showing thickness variation for third stage

*For fourth and final stage***,** the component is formed and measured to the full depth. The plot generated after the comparison of formed profile and ideal profile is shown in Fig. 4.37. it is clearly shown in Figure that the wall deviation in the u base region is 2.3468 mm and the wall deviation is 1.4827 mm. In this experiment the profile of component at the end of program is also measured with the help of CMM.

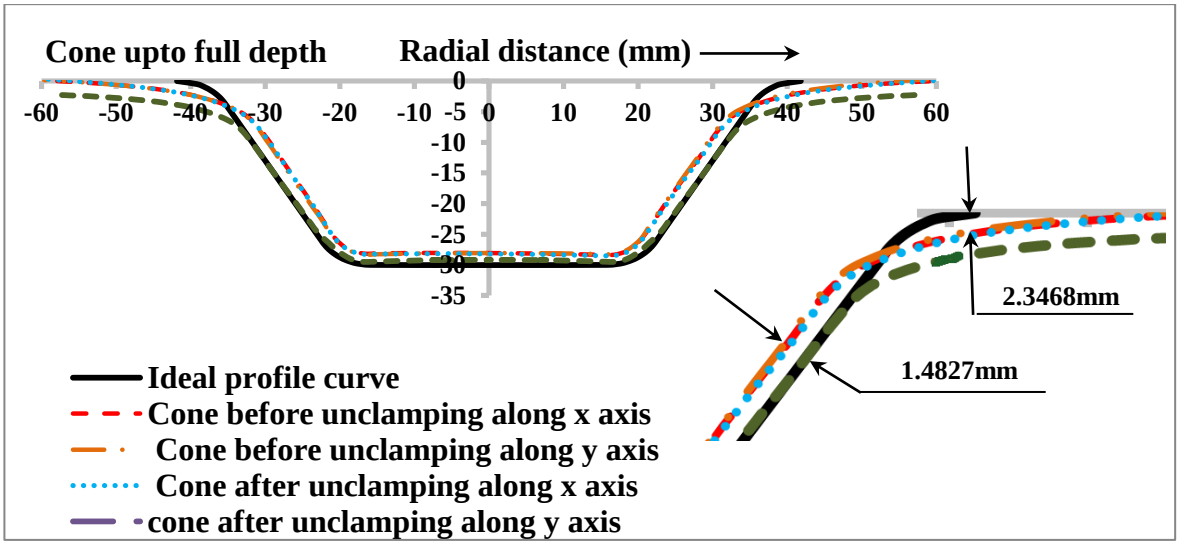

Fig. 4.37 Deviation of profile near upper fillet and wall for fourth stage of component

The process of forming the component and the measurement of component is shown in Fig. 4.38. After forming the component the POP profile is generated to measure the error between the profiles at end of program with the ideal profile.

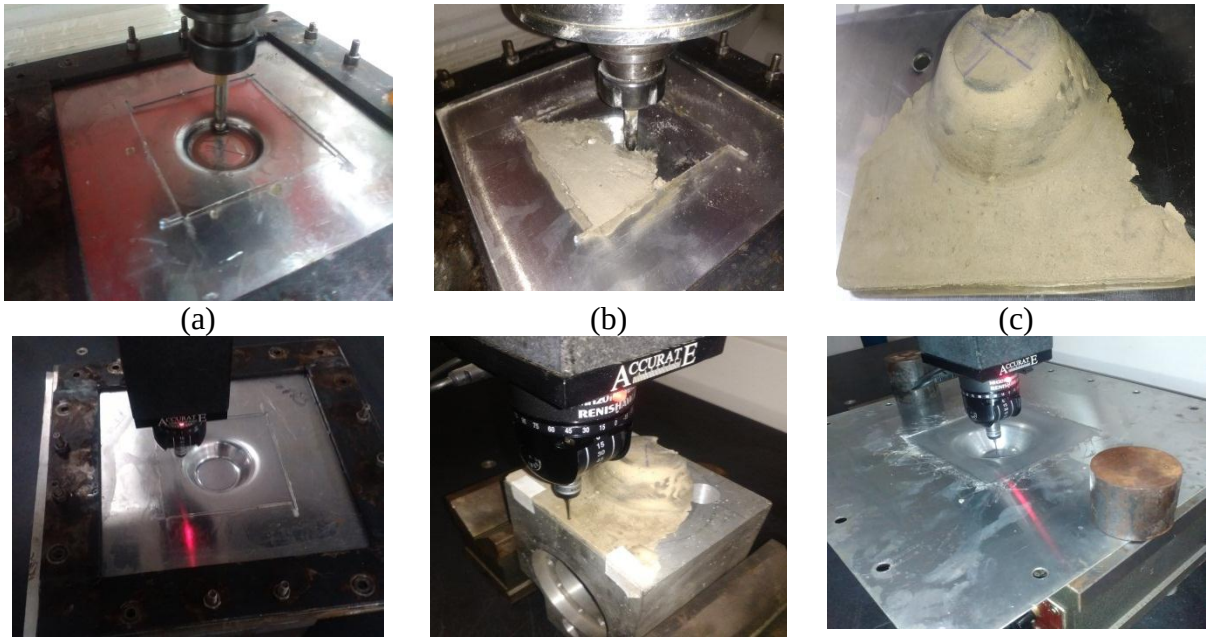

Fig. 4.38 (a) Forming of component, (b) casting POP profile at end of program, (c) casted profile, (d) measuring component in clamped position, (e) measuring of POP profile and (f) measuring of component in unclamped position

The thickness of component is measure after measuring the component in clamped and in unclamped position. The component is cut from its middle and the perfectly formed sectional thickness is measured with the help of vernier calliper. The thickness measuring process is shown in the Fig. 4.39. It is very much clear from the Figure that, the thickness at wall is region is very less as compare to the other portions of the component. In the upper fillet region and in the lower fillet region the thickness is varying as the slope of component is changing. The base of components has constant thickness. The minimum thickness is achieved is at the starting of lower fillet region which show that there are more chances of breakage the lower fillet region.

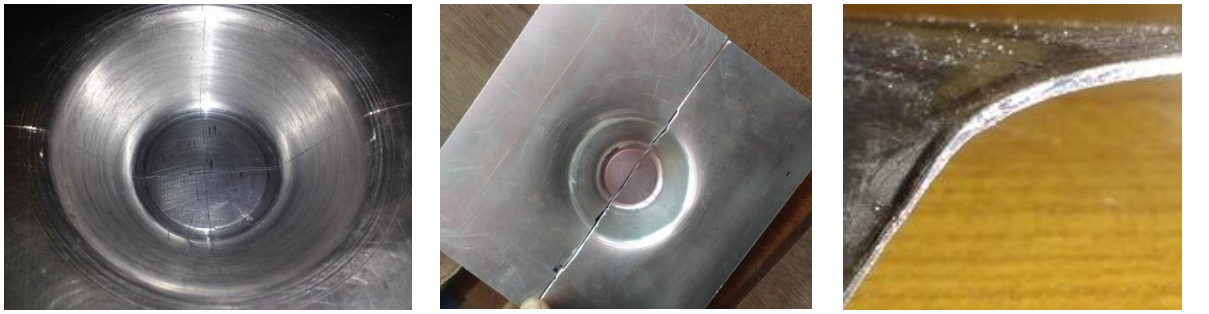

(a) (b) (c)

(d)

(e)

Fig. 4.39 (a) Formed cone, (b) component cut from middle, (c)thickness variation in upper fillet region, (d) thickness variation in lower fillet and base of component and (e) variation of thickness of whole cone

After, measuring the thickness of all the at all the stages the plot is generted between the radius and the thickness at each stage. The x-axis of plot represents the radius and y-axis of plot represents the thicnkness. The pitch of change in radius for measuring the thickness is taken as 2 mm. Combine thicness plot generated is shown in the Fig. 4.40. The minimun value of thickness achieved in 1^{st} stage is = 0.79 mm. In case of 2^{nd} stage the minimum value achieved is = 0.64mm,in case of third stage the minimal thickness achieved is = 0.43 mm. In the last fpirth stage the minimal value of thickness achieved is equal to the = 0.39 mm. So, it is clear from the plot that as, the depth of compnent is increasing the thickness of sheet is reducing. Full depth component has achived minum value of thickness.

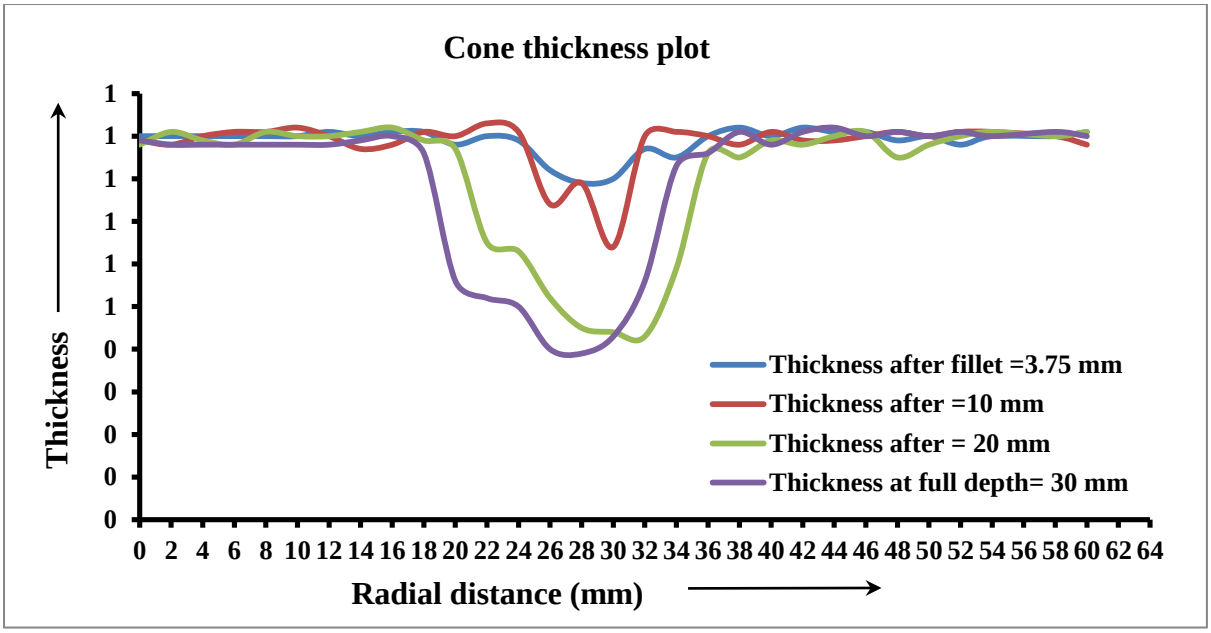

Fig. 4.40 Thickness variation of component along radius at three stage of height achieved for H = 3.75 mm, 10 mm, 20 mm, 30 mm

4.5 Validation experimental result with the theoretical result using bond graph

The detail diagram of beam discretization is shown in Fig. 4.41. This diagram shows all the reticules at each part of component throughout the beam span.

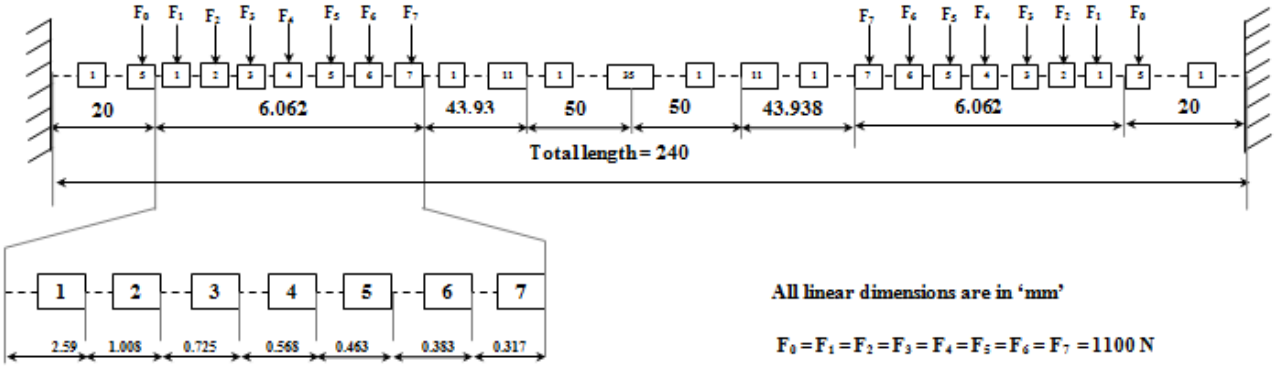

Fig 4.41 Detail view of discretization of whole length of beam

The length of each seven reticules in the loading region is calculated by simple geometrical calculation of profile with known value of changing slope in upper fillet region. The parametric variation of load and correspond deflection is shown in Table 4.6. From literature [32] it is known that Young's modulus (E) of material continuously increases as the load on the position of load changes. The parametric variation and corresponding deflection simulated using bond graph model is given in Table 4.6.

Table 4.6 Parameter variations in upper fillet region and correspond deflection

Young's Modulus(E) (N/mm^2)	Thickness of sheet (mm)	Load applied (N)	Length of reticule (mm)	Load applied in upper fillet at reticule (R)	Deflection calculated (mm)
072.48568	0.902	1100	25.000	Left end of R_1	0.532353
102.69700	0.902	1100	02.598	Right end of R_1	0.503055
114.22710	0.902	1100	01.008	Right end of R_2	0.590634
122.19130	0.902	1100	00.725	Right end of R_3	0.516136
128.67400	0.902	1100	00.568	Right end of R_4	0.520018
134.42880	0.902	1100	00.463	Right end of R_5	0.522642
139.86540	0.902	1100	00.383	Right end of R_6	0.523898
145.30300	0.902	1100	00.317	Right end of R_7	0.529680
Total deflection					4.238419 mm

The thickness of sheet kept constant as 0.902 mm and the load applied taken as 1100 N are considered from the literature [28]. The deflection calculated with the help of bond graph model is 4.284 mm and is considerably lying in the range of experimental spring-back range. This proves the validation of process SPIF with the help of bond graph approach.

Chapter 5 Conclusions

5.1 Conclusions

After performing all the experiments under the topic of single point incremental forming, the conclusions generated for the motive to complete objectives of this thesis work is discussed in this chapter. Four types of objectives were covered in this work.

- During the study of effect of parameter variations on the accuracy of component formed by single point incremental forming, incremental depth and radius of tool is varied in three stages. It is noticed that for both type of component shapes i.e. cone and funnel with the increase in incremental depth, the spring-back of component increases. Due to more generation of residual stresses in the component, the error between the formed profile and generated profile increases i.e. the accuracy of components decreases. On the other hand, as the radius of tool is increased the spring-back in the sheet decreases i.e. accuracy increases.
- In case of studying the multiple components on a single sheet for making the process feasible for large scale production, it is noticed that in clamped position as the no. of component on single sheet increases, the accuracy of component also increases. Spring-back decreases as the number of component is increased. As the no. of component is increased, the wall accuracy increases because of bending of sheet takes place. But in unclamped position, spring-back of sheet increases due to the symmetric loading of sheet and this creates distributed residual stresses in the sheet. Bending of sheet occurs at the top position of the sheet.
- During forming the component in multistage, it is noticed that the thickness at wall region is very less as compared to the other portions of the component. In the upper fillet region and in the lower fillet region, the thickness varies as the slope of component changes. The base components have constant thickness. The minimum thickness is achieved at the starting of lower fillet region and this shows that there are more chances of breakage at the lower fillet region. As the component height increases, the sheet thickness after forming component is reduced.
- For the validation of SPIF process with the help of bond graph approach, it is assumed that the sheet is clamped at the edges i.e. it is a clamped beam. The deflection calculated from the bond graph model is successfully relating the spring-

back of sheet. Experimental results and theoretical results from bond graph model are very close to each other and are within the acceptable ranges.

5.2 Scope for future work

The scope of SPIF in future work is very much vast and more work can be done in this field. While performing all the experiment to study the objectives of this thesis, it is concluded that accuracy of components is greatly affected by the parameter variation. The stability of process is also an issue parallel to the accuracy of component. On repeating the same experiments with same input parameters, it is seen from the literature that every time stability of results get disturbed i.e. every time accuracy of component do not remain constant. More method can be developed to enhance the accuracy of component. Accuracy of asymmetrical and complex shapes can be studied in topic of multiple features on single plate. New algorithms can be developed to study the crack formation and the causes the failure of sheet. FEM simulation of multiple features on single plate can be done to validate the results of multi forming. The bond graph modeling can be done for multistage incremental forming. Bond graph modeling can also be used to relate with the FEM simulation results.

References

1 Drishtikona I. Sheet Metal Stamping in Automotive Industry.2012. https://drishtikona.files.wordpress.com/ 2012/08/ch5.pdf

2 Leszak E. Apparatus and process for incremental dieless forming. *Patent US 3342051A 1967*.

3 Kitazawa K. Incremental Sheet Metal Stretch-Expanding with CNC Machine Tools. In: *Proceedings of the Fourth ICTP Beijing* 1993: 42–46.

4 Kitazawa K, Wakabayashi A, Murata K, and Yaejima K. Metal-flow phenomena in Computerized numerically controlled incremental stretch-expanding of aluminium sheets. *Keikinzoku Journal of Japan Institute of Light Metals* 1992; 46: 65–70.

5 Yang TJ, and Kim DY. Improvement of formability for the incremental sheet forming process. *International Journal of Mechanical Sciences* 2000; 42: 1271–1286.

6 Jeswiet J. Incremental single point forming. *Trans. of North American Manufacturing Research Institute* 2001; 29: 75–79.

7 Hirt G, Junk S, and Bambach M. Modelling and Experimental Evaluation of the Incremental CNC Sheet Metal Forming Process. In: *7th International Conference on Computational Plasticity,* Barcelona, 2007:76–88

8 Hirtl G, Ames J, Bambachl M, and Kopp R. Forming strategies and process modelling for CNC incremental sheet forming. *CIRP Annals-Manufacturing Technology* 2004; 53: 203–206.

9 Ambrogio Y, Fratini L, Muzzupappa M, Costantino I, De Napoli L, and Filice L. Influence of some relevant process parameters on the dimensional accuracy in incremental forming: a numerical and experimental investigation. *Journal of Materials Processing Technology* 2004; 49: 501–507.

10 Ambrogio G, Filice L, and Micari F. Some relevant correlations between process parameters and process performance in incremental forming of metal sheets. In: *Proceedings of the VI ESAFORM Conference* 2003; 175–178.

11 Jeswiet J, Micari F, Hirt G, Bramley A, Duflou J,and Allwood J. Asymmetric Single Point Incremental Forming of Sheet Metal. *CIRP Annals Manufacturing Technology* 2005; 54: 623–649.

12 Kobayashi S, Hall IK, and Thomsen EG. A Theory of Shear Spinning of Cones. *Trans ASME series B Journal of Engineering for Industry* 1961; 83: 485–495.

13 Jeswiet J, Duflou J, and Szekeres A. Forces in Single Point and Two point Incremental Forming. *Journal Advanced Materials Research* 2005; 8: 449–456.

14 Cerro I, Maidagan E, Arana J, Rivero A, and Rodrıguez. Theoretical and experimental analysis of the dieless incremental sheet forming process. *Journal of Materials Processing Technology* 2006; 177: 404–408.

15 Ambrogio G, Cozza V, Filice L, and Micari F (2007). An analytical model for improving precision in single point incremental forming. *Journal of Materials Processing Technology* 2007; 191: 92–95.

16 Ambrogio G, Filice L, Ingarao G, and Manco L. Measuring of Geometrical Precision of Some parts Obtained by Asymmetric Incremental Forming Process After Trimming. *Proceeding of AIP Conference*, Portugal 2007: 431–436.

17 Reddy BL, Rao BC, Reddy, and Reddy P V R. A Review on Springback in Metal Forming. *International Journal of Engineering Research & Technology (IJERT)* 2014; 3: 2278–2281.

18 Micari F, Ambrogio G, and Filice L. Shape and dimensional accuracy in single point incremental forming: state of the art and future trends. *Journal of Materials Processing Technology* 2007; 191: 390–395.

19 Durante et al. The influence of tool rotation on an incremental forming process. *Journal of Materials Processing Technology* 2009; 209: 4621–4626.

20 Silva MB, Skjoedt M, Bay N, and Martins, P. Formability in multistage single point incremental forming. *7th Euromech Solid Mechanics Conference, At Lisboa*, Portugal 2009:67–68.

21 Behera Ak, Verbert J, Lauwers B, and Duflou, J. Tool path compensation strategies for single point incremental sheet forming using multivariate adaptive regression spline. *Computer-Aided Desig* 2013; 45:575–590.

22 Green D, Bramley A, and Leach AN. A new incremental sheet forming process for small batch and prototype parts. *IEEE Conference in Verlag Meisenbach Bamberg*, Germany 2001; 95–102.

23 Cozza V, Filice L, Micari F, and Ambrogio G. An analytical model for improving precision in single point incremental forming. *Journal of Materials Processing Technology* 2007; 191: 92–95.

24 Tunckol Y, Aerens R, and Duflou JR. Force Analysis for Single Point Incremental Forming. *Conference in Sheet Metal* 2007; 543–550.

25 Hirt G et al. Tools and Equipment used in Incremental Forming. In: *1st Incremental Forming Workshop,* University of Saarbrucken *2007*:25–29

26 Micari F. Some remarks on material formability in single point incremental forming of sheet metal. In: *8th International Conference on Technology of Plasticity, Verona* 2005: 537–538.

27 Silvaa M, Skjoedtb M, Martins PAF, and Bay N. Revisiting the fundamentals of single point incremental forming by means of membrane analysis. *International Journal of Machine Tools & Manufacture* 2008; 48: 73–83.

28 Bhattacharya A, Reddy NV, and Cao J. Formability and surface finish studies in single point incremental forming. *Proceedings of the ASME International Manufacturing Science and Engineering Conference* 2011:621–627.

29 Timoshenko S, and Woinowsky-Krieger S. *Theory of plates and shells*. McGraw–Hill New York 1959.

30 Asghar J, Lingam R, Shibin E, and Reddy NV. Tool path design for enhancement of accuracy in single-point incremental forming. *Journal of Engineering Manufacture IMechE* 2014; 228: 1027–1035.

31 Bhattacharya A, Bera TK, and Thakur A. On cutter deflection profile errors in end milling: Modeling and Experimental Validation. *Materials and Manufacturing Processes* 2015; 30: 1042–1050.

32 Mukherjee A, Karmakar R, and Samantaray AK. *Bond Graph in Modelling, Simulation and fault Identification*. FL: CRC Press, 2006.

33 Kumar S, Kumar Sunil, and Singh CD. Modeling and Simulation of Underwater Flexible Manipulator as Raleigh Beam Using Bond Graph. *International Journal of Mechanical, Aerospace, Industrial, Mechatronic and Manufacturing Engineering* 2015; 9: 8–14.

34 Pathak PM, Kumar A, and Sukavanam N. Bond Graph Modeling of Planar Two Links Flexible Space Robot. In: *13th National Conference on Mechanisms and Machines (NaCoMM07),IISc*, Bangalore, India. 2007:12-13.

INFORMATION

Author:

Dharminder singh

ME - Thapar University,Patiala,2016
B-Tech- Amritsar College of Engineering and Technology, Amritsar, 2014
Email: Dschahal94@gmail.com or Dschahal95@yahoo.com
Website: https://www.facebook.com/Dharmindr.singh.chahal
Mob: +91 98554 35889, +91 94746 17025

Supervisors:

Dr. Tarun Kumar Bera
(PhD-IIT Kharagpur, Post Doc-CNRS, France)
Associate Professor
Mechanical Engineering Department
Thapar University, Patiala
Punjab, India, PIN- 147 004
email: tarunkumarbera@gmail.com, tkbera@thapar.edu
Mob: +91 98554 35889, +91 94746 17025

Dr. Anirban Bhattacharya
(PhD-IIT Kanpur)
Assistant Professor
Department of Mechanical Engineering
(Block - III, 3rd Floor)
Indian Institute of Technology Patna
Patna - 801103, India
Phone (O): 0612-3028117
Cell: +91-9781603965
email: abhatta@iitp.ac.in,